Francesco Giovanni Celiberto^a

^aUniversidad de Alcalá (UAH), Departamento de Física y Matemáticas, Campus Universitario, Alcalá de Henares, E-28805, Madrid, Spain

ARTICLE INFO

Keywords: Bottom flavor Hi-Lumi LHC Precision studies QCD resummation Natural stability

Abstract

We study the inclusive production of hadrons with bottom flavor at the LHC and its luminosity upgrade. We describe the collinear fragmentation of singly b-flavored hadrons, B mesons and Λ_b baryons, via the KKSS07 determination of fragmentation functions, while for charmed B mesons, $B_c(^1S_0)$ and $B_c(^3S_1)$ particles, we employ the novel ZCFW22 set, built on the basis of stateof-the-art nonrelativistic QCD inputs. We use the JETHAD multimodular working environment to analyze rapidity and transverse-momentum distributions for observables sensitive to the associated emission of two hadrons or a hadron-plus-jet system. Our reference formalism is the NLL/NLO+ hybrid collinear and high-energy factorization, where the standard collinear description is improved by the inclusions of energy logarithms resummed up to the next-toleading approximation and beyond. We provide corroborating evidence that b-flavor emissions act as fair stabilizers of the high-energy resummation, thus serving as valuable tools for precision studies of high-energy QCD. As a bonus, we highlight that the predicted production-rate hierarchy between noncharmed b-hadrons and charmed $B_c(^1S_0)$ mesons is in line with recent LHCb estimates. This serves as simultaneous benchmark both for the hybrid factorization and for the single-parton fragmentation mechanism based on initial-scale inputs calculated via the nonrelativistic QCD effective theory.

Contents

1	Opening remarks		2
2	Bottom flavor production within NLL/NLO+ hybrid factorization		4
	2.1 High-energy resummation at work		5
	2.2 NLL-resummed differential cross section		6
	2.3 Collinear inputs	1	10
	2.4 Natural stabilization of the NLL series	. 1	10
3	Hi-Lumi LHC distributions		13
	3.1 Uncertainty estimation	1	13
	3.2 Kinematic constraints on final-state ranges		
	3.3 Rapidity-interval distributions		
	3.4 Doubly-differential transverse-momentum distributions		
4	Summary and Outlooks	2	20

francesco.celiberto@uah.es
ORCID(s): 0000-0003-3299-2203

1. Opening remarks

Exploring the heavy-flavor domain stands as a frontier research field whereby addressing unresolved quests of particle physics. Here, possible experimental evidences of the associated production of heavy quarks and Beyond-the-Standard-Model (BSM) particles are milestones in the search for long-awaited signals of New Physics. Still they can play a crucial role in precision studies of strong interactions, the values of charm- and bottom-quark masses making perturbative Quantum ChromoDynamics (QCD) applicable.

Special emphasis deserves the hadroproduction of the bottom quark, which represents the heaviest quark species that can fragment and generate hadrons. A rigorous description of $(b\bar{b})$ pair production by the hands of collinear factorization and within the Next-to-Leading Order (NLO) perturbative accuracy was formalized at the end of the eighties [1–4], while detailed analyses on differential distributions at Next-to-NLO (NNLO) have been undertaken only recently [5, 6]. A key actor here is the bottom mass, m_b . It genuinely marks the transition point between two distinct factorization schemes.

For *b*-flavored particles emitted with low transverse momentum, so that $m_b \gtrsim |\vec{q}|$, a suitable description is found in the so-called Fixed Flavor Number Scheme (FFNS, see Ref. [7] for insight). It exclusively incorporates collinear Parton Distribution Functions (PDFs) and/or Fragmentation Functions (FFs) of light partons (light-flavored quarks and the gluon). To be precise, here we refer to a scheme with a number of active flavors $n_f = n_l$, with n_l being the number of light flavors. Additionally, in the FFNS, heavy quarks manifest solely in the final state and their masses must not be set to zero. This is a required condition not to face perturbative-convergence issues due to the rise of power corrections of the form $|\vec{q}|/m_b$.

Conversely, when the transverse momentum is large, $m_b \ll |\vec{q}|$, contributions scaling with $\ln(|\vec{q}|/m_b)$ progressively grow and demand for an all-order logarithmic resummation of collinear logarithms of the factorization scale over the mass of the heavy quark(s) [8, 9]. In that case, the Zero-Mass Variable-Flavor Number Scheme (ZM-VFNS, or simply VFNS) emerges as the most suitable framework whereby combining fixed-order radiative corrections with the resummation [9–14]. Within the VFNS, all quark flavors are treated as massless particles and participate to the Dokshitzer-Gribov-Lipatov-Altarelli-Parisi (DGLAP) evolution. The flavor number increases by one every time a heavy-quark threshold is crossed.

An elegant matching between the FFNS scheme and the VFNS one is realized by means of the so-called General-Mass Variable-Flavor Number Scheme (GM-VFNS). It embodies calculations involving both massive quarks at lower scales and massless quarks at higher scales, while the heavy-quark masses serve as control parameters for the transition between the two descriptions. Several implementations of the GM-VFNS have been proposed so far [15–19]. For an exhaustive exploration of these studies, we direct the reader to Refs. [10, 12, 20].

While the use of a GM-VFNS undoubtedly improves the description of both the kinematic limits, it still suffers from some ambiguities. On one hand, it systematically misses power corrections rising from initial-state quarks, which might be quenched, however, by the smallness of heavy-flavor PDFs. On the other hand, it does not behave as desired in the intermediate region, $m_b \sim |\vec{q}|$, since the difference between the pure ZM-VFNS contribution and its massless limit does not automatically vanish and it must be suppressed by hand (see Ref. [16] for a detailed discussion).

A simplest solution comes instead from the use of a ZM-VFNS with a suitable choice of the Heavy-Flavor Matching Point (HFMP), namely the transition scale starting from which the massive flavor is treated as if it were massless. As extensively shown in Ref. [21], numerically accurate predictions can be achieved with HFMP(s) ranging from five to 10 times the mass of the heavy quark(s). The main benefits of this choice are: the possibility of keeping the size of missing power corrections steadily below $4 \div 1\%$, a fully preserved resummation accuracy, and an improved continuity in predictions for observables.

Notably, bottom-flavored emissions are useful not only to study direct-production channels, but also to access the top sector. For this reason, mechanisms governing b-quark fragmentation are believed to play an important role within the top-physics domain. The production of b-particles at hadron colliders in NNLO QCD and its application to $(t\bar{t})$ events with leptonic decays were extensively investigated in Refs. [22, 23]. The same approach finds application in precision studies of electroweak interactions, particularly in the analysis of photon radiation originating from massive charged fermions, like via $(b\bar{b})$ decays from a Higgs boson [24]. Refs. [25–27] investigate the role of the bottom quark in the associated production of lepton pairs. The semi-inclusive emission of a Higgs boson decaying into b-quarks

¹We remark that also a scheme with $n_f = n_l + 1$ would still be a FFNS, provided that the (first) heavy-quark species is considered light.

accompanied by a weak vector within NNLO QCD was considered in Ref. [28]. Ref. [29] examines electroweak emissions from heavy fermions in W^{\pm} boson production processes with Monte Carlo techniques.

The total cross section for the production of a Higgs boson or a Z boson in bottom fusion and via the FONLL [30, 31] matching procedure² was computed in Refs. [32, 33] and [34], respectively. The associated production of an electroweak boson with b-quarks was investigated in Refs. [35, 36]. Effects of collinear logarithms and finite bottom-mass powers in $(b\bar{b}H)$ tags were addressed in Refs. [37, 38]. Refs. [39, 40] contain a detailed study on the inclusion of the resummation of soft logarithms at NNLO in the perturbative component of the bottom fragmentation function. Matching issues arising from the the noncommutativity of the light-mass limit and soft-emission one were recently highlighted [41]. Analyses on heavy-quark fragmentation in lepton collisions at NNLO plus logarithmic corrections were presented in Refs. [42, 43]. QCD corrections to the hadroproduction of $(t\bar{t}b\bar{b})$ systems were considered in Refs. [44–48].

Studies on bottom-flavored jets and hadrons at high energies can be found in Refs. [49–52]. Ref. [53] investigates kinematic correlations of lepton pairs from semi-leptonic decays of B mesons. Multiple parton interactions in double B^+ productions at the LHC were considered in Ref [54]. The VFNS collinear fragmentation to B-mesons was first studied at NLO in Ref. [55]. The obtained FFs came out from a fitting procedure on LEP1 data. A subsequent fit to data from LEP1 and SLAC-SLC was made [56]. The resulted FF parametrization was then employed in the computation of NLO cross section for the inclusive hadroproduction of B mesons within the GM-VFNS. There, b-quark finite-mass effects were also assessed [57].

Predictions for the semi-inclusive emission of singly b-flavored particles, encompassing B mesons and Λ_b baryons which we collectively denote as \mathcal{H}_b hadrons, were recently compared with LHCb and CMS data [58]. That analysis relied upon the assumption that a single set of functions could aptly describe the VFNS fragmentation all species of \mathcal{H}_b particles. Consequently, FFs for any singly bottomed hadron species might be derived from the general ones by just multiplying it by an energy-independent branching fragmentation fraction.

However, analyses conducted by the Heavy Flavor Averaging Group (HFAG) highlighted a departure from the universality assumption regarding the branching fraction, particularly in the case of Λ_b tags, as evidenced by data from LEP and Tevatron [59]. On the contrary, the universality seems to be valid of B-meson emissions. A recent examination of semi-inclusive Λ_b rates at LHCb and CMS emphasized the need to go beyond the branching-fraction description when the observed transverse momentum enlarges [60]. Therefore, for the time being the use of the FF determination of Ref. [56, 58] is safe provided that only B mesons or both B mesons and A_b baryons are inclusively considered, but it is not valid for A_b baryons only. Forthcoming data with diminished experimental uncertainties will contribute to a better understanding of this aspect.

Particular relevance in accessing the heavy-flavor sector deserves the case of mesons with both the charm and the bottom quark in their leading Fock level: $|c\bar{b}\rangle$ for positive-charged particles, $|\bar{c}b\rangle$ for negative ones. Because of the presence of two heavy quarks, these charmed B mesons can be thought of as generalized quarkonium states. However, contrarily to charmonia and bottomonia, they cannot annihilate into gluons. Thus, they are quite stable and exhibit narrow decay widths (for novel determinations of the B_c lifetime, see Refs. [61–63]). Being top quarks extremely short-lived and not able to hadronize, charmed B mesons actually represent the final frontier of meson spectroscopy (see, e.g. Ref. [64]). The CDF Collaboration at Tevatron observed the $B_c \equiv B_c(^1S_0)$ particle for the first time in 1998 [65]. The $B_c^* \equiv B_c(^3S_1)$ resonance was detected by ATLAS only in 2014 [66].

The simultaneous presence of a charm and a bottom quark in their leading Fock level makes charmed B mesons excellent testing grounds to shed light on the core nature of strong and weak interactions. Analyses on direct emissions as well as on indirect productions from electroweak decays stand as gold-plated channels whereby testing $B_c^{(*)}$ formation mechanisms as well as unraveling peculiar features of their decay products. As an example, they are useful to investigate rare Higgs decays [67–69].

Data analyzed by LHCb have shown that B_c meson production rates are three orders of magnitudes lower than \mathcal{H}_b states, at most [70, 71]. This explains why charmed B-meson channels are generally excluded from fits of b-hadron fragmentation parameters, thus making our knowledge of their formation mechanism quite scarce. For this reason, any attempt at catching the core fragmentation dynamics of $B_c^{(*)}$ particles still needs to rely upon model-dependent studies and/or effective approaches.

²See Ref. [16] for a FONLL application to Deep Inelastic Scattering (DIS) structure functions.

An intriguing opportunity to access the production mechanism of charmed B mesons comes from an effective theory, known as NonRelativistic QCD (NRQCD) [72–74]. Originally developed to explain issues in the description of charmonium and bottomonium production, the NRQCD framework builds on the assumption that, to the observed bound state, all the possible Fock states contribute through a linear combination. All these contributions are ordered in a double expansion in powers of the strong coupling, α_s , and the nonrelativistic relative velocity between two constituent heavy quarks, v.

The question whether a NRQCD-inspired description is valid for the perturbative component of the collinear fragmentation of a single parton to the detected $B_c^{(*)}$ meson, or it should be rather adopted for the *short-distance* production of a charm-plus-bottom system directly in the hard subprocess, strictly depends on the transverse momenta at play. Indeed, while the short-distance mechanism suitably describes the production of the two constituent heavy quarks at low transverse momentum, namely when they feature a relative transverse separation of order $1/|\vec{q}|$, when $|\vec{q}|$ grows the fragmentation of a single parton, followed by its inclusive hadronization into the physical state, starts to prevail. Phenomenological efforts to unravel the transition region between the two regimes were originally made in the context of charmonia [75–79]. The main outcome was that the (gluon) fragmentation contribution starts to dominate when $|\vec{q}| \gtrsim 10 \div 15$ GeV. An analogous threshold was then set also for charmed *B*-mesons [80], whereas more recent analyses [81] pointed out how this lower bound might be larger.

Although NRQCD can model the initial-scale input of the $B_c^{(*)}$ fragmentation, the other key ingredient for a proper collinear description is the DGLAP evolution. Thus, by starting from NLO NRQCD calculations of heavy quarks [82] and gluon [83] fragmentation channels, first sets of VFNS-compatible, DGLAP-evolving FFs for $B_c(^1S_0)$ and $B_c(^3S_1)$ mesons were derived in Ref. [84]. They were named ZCFW22 NLO functions. A similar strategy was applied to obtain the ZCW19⁺ NLO FFs for vector quarkonia [85, 86].

In this article we will study the inclusive emission, at the LHC ad its luminosity upgrade, of a \mathcal{H}_b hadron or a $\mathcal{B}_c^{(*)}$ meson accompanied by another b-particle or by a light-flavored jet, as a testing ground for the manifestation of imprints of high-energy QCD dynamics. We will make use of the hybrid collinear and high-energy factorization framework [85, 87–91], as implemented in the JETHAD code [86, 88, 91] to analyze rapidity-interval and double transverse-momentum differential rates for observables sensitive to the QCD resummation of high-energy logarithms within the next-to-leading approximation and beyond.

We will hunt for stabilizing effects of our distributions under radiative corrections and energy-scale variations, discovering that they are present and allow for a consistent description of these observables at LHC energies and at the natural scales provided by process kinematics. We will come out with a bonus result, namely that the aforementioned production-rate hierarchy between charmed $B_c(^1S_0)$ mesons and noncharmed b-hadrons is in fair agreement with recent LHCb findings [70, 71]. This will serve as simultaneous benchmark both for our resummed calculations and for the single-parton fragmentation mechanism from NRQCD.

For completeness, we mention Refs. [92–94], where another hybrid-factorization approach, designed for single forward detections, was presented. Then, Refs. [95, 96] investigate small-x resummed inclusive or differential Higgs and heavy-quark LHC rates from the Hell method [97–99]. The latter builds on the basis of the Altarelli–Ball–Forte (ABF) approach [100–105], whose purpose is connecting collinear factorization and small-x resummation. It makes use of high-energy factorization theorems [106–111].

The structure of this article reads as follows. Section 2 gives introductory remarks and technical details on NLL/NLO⁽⁺⁾ hybrid collinear and high-energy factorization applied to *b*-flavor production. Section 3 contains phenomenological analyses on our high-energy distributions. Section 4 summarizes results and provides outlooks.

2. Bottom flavor production within NLL/NLO+ hybrid factorization

The first part of this Section (2.1) consists in a brief summary of recent phenomenological progresses concerning the QCD semi-hard regime. Then (2.2) the NLL/NLO⁺ hybrid collinear and high-energy is explained and adapted to the study of inclusive double b-hadron and b-hadron plus light-jet final states at the Hi-Lumi LHC. The third part (2.3) provides us with details on collinear ingredient. Finally in (2.4) the *natural stability* [112] of b-flavor sensitive distributions is discussed.

2.1. High-energy resummation at work

The theoretical description of hadron collisions at high energies relies upon the well-defined *collinear factorization*, where long-distance and short-distance dynamics are decoupled. This remarkable features permits to factorize the nonperturbartive hadronic content from the perturbatively calculable information on parton scatterings. Nevertheless, there exist particular kinematic limits where the purely collinear description is spoiled by the emergence of large logarithmic corrections. Their impact on cross sections can be enough sizable to offset the narrowness of the QCD running coupling, α_s , thus harming the perturbative series convergence. In such cases the collinear factorization must be improved via the inclusion to all orders of one or more logarithmic *resummations*.

The kinematic sector matter of our analysis is the *semi-hard* regime (see Refs. [113, 114] for novel applications), where the energy scale hierarchy $\sqrt{s} \gg \{Q_i\} \gg \Lambda_{\rm QCD}$ is strongly valid. Here, \sqrt{s} stands for the center-of-mass energy, $\{Q_i\}$ represents one or a set of reaction-related hard scales, and $\Lambda_{\rm QCD}$ is the QCD hadronization scale. Whereas the second inequality simply states that perturbative QCD can be employed in our calculations, the first one heralds the fact that we have accessed the QCD $Regge\ limit$. Here, large $\ln(s/Q_i^2)$ type logarithms enter the perturbative series with a power increasing with the order of α_s . Thus, any pure fixed-order perturbative techniques are not anymore applicable. As anticipated, they need to be enhanced by considering the all-order resummation of terms proportional to energy logarithms.

The Balitsky–Fadin–Kuraev–Lipatov (BFKL) approach [115–117] is the well-established tool to resum terms proportional to $(\alpha_s \ln s)^n$, namely the ones constituting the Leading Logarithmic (LL) approximation, and also factors proportional to $\alpha_s (\alpha_s \ln s)^n$, namely the ones specific of the Next-to-Leading Logarithmic (NLL) approximation. Following the BFKL factorization method, any high-energy amplitude can be rewritten as a transverse-momentum convolution of a universal Green's function with two singly off-shell *emission functions* (also known as *impact factors*) describing the subprocess that leads, in the corresponding fragmentation region, to the emission of a forward or backward final-state particle from the stemming hadron. The Green's function evolves according to the BFKL integral equation, whose kernel has been calculated within the NLO fixed-order accuracy. Recent studies have been done to calculate its NNLO correction [118–122] (see also Ref. [123]).

While the BFKL kernel is known at NLO, only a few emission functions have been computed within the same accuracy, such as: (*i*) the ones for collinear incoming partons [124, 125], which are the common basis for (*ii*) forward light hadron [126] and jet [127–129] emissions, and (*iii*) the emission function for forward Higgs in the large top-mass range [130, 131]. Conversely, emission functions for forward Drell–Yan [132–135], heavy-quark pair [136–138], and J/ψ states at small transverse momentum in the short-distance case [139] are currently known at LO only. Those impact factors served as key ingredients for phenomenological advancements in our knowledge of high-energy QCD through the study of semi-inclusive final states characterized by the detection of a forward particle always accompanied by a backward one. Here is an incomplete list: production of two jets at the LHC with large transverse momenta and strongly separated in rapidity (Mueller–Navelet reaction [140], for relevant applications see Refs. [87, 129, 141–149]), promptly complemented by the investigation of the double light hadron channel [150, 151], multi-jet states [152–156], hadron plus jet [88, 157–161], Higgs plus jet [89], heavy-light two-jet [90], forward Drell–Yan plus jet [162], and hadron with heavy flavor [84, 85, 112, 138, 139, 163–167] hadroproductions.

Notably, single forward production processes gives us a direct channel to the gluon content of the proton at small-x by means of the Unintegrated Gluon Distribution (UGD), whose evolution is driven by the BFKL kernel. Exploratory, model-dependent studies of the UGD have been carried out via the exclusive ρ - and ϕ -meson electroproduction at HERA [168–175] and the EIC [176–180] and the exclusive photoproduction of vector quarkonia [181–183]. Moreover, the information on the gluon content at small-x embodied in the UGD was the starting point to improve the collinear-factorization picture in the context of prime extractions of small-x resummed PDFs [184–186], as well as to determine small-x enhanced unpolarized and polarized gluon TMD distributions [187–197]. Work done in Ref. [198] sheds light on the connection existing between TMD and BFKL dynamics, whereas Refs. [199, 200] investigate the link between the UGD and color-dipole cross sections.

A crucial problem rising from the BFKL description of Mueller–Navelet rapidity distributions and azimuthalangle correlations is the weight of the NLL part, which is of the same order, but of opposite sign than the pure LL case. This is at the origin of strong instabilities observed in the resummed series that become manifest when factorization and renormalization scales are varied around their natural values. Therefore, Muller–Navelet observables assume unphysical values when the jet rapidity separation becomes sufficiently large. In the same way, azimuthal

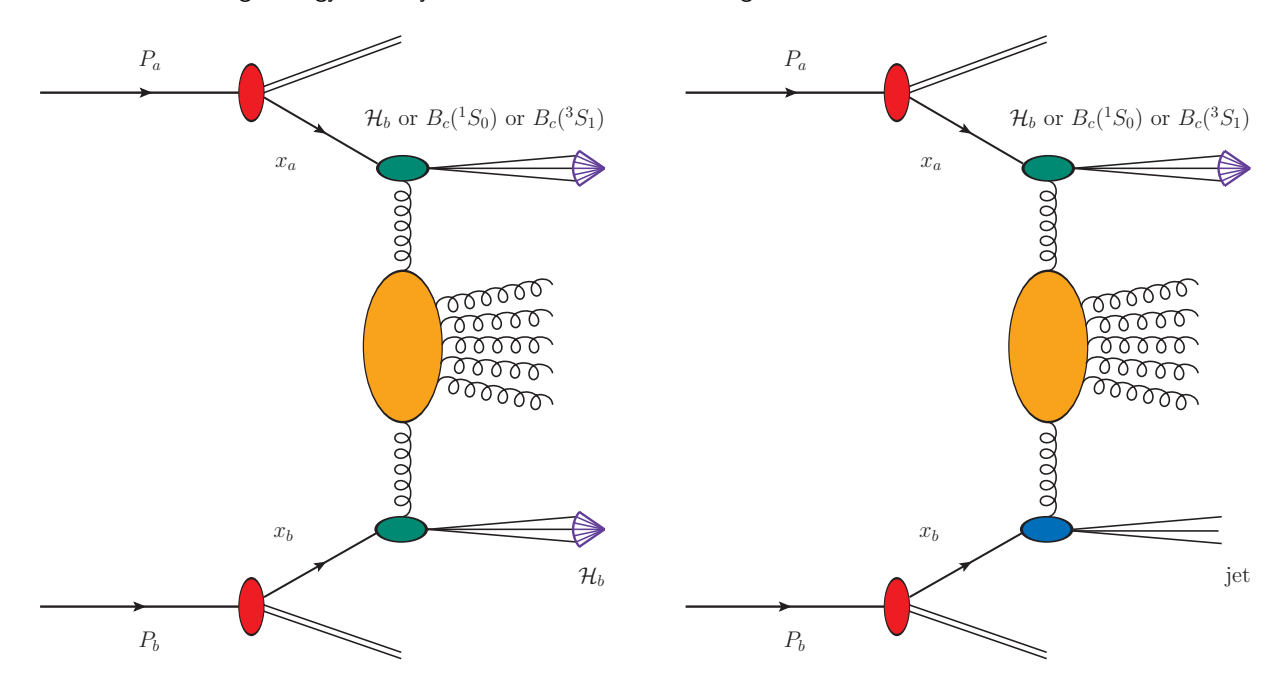


Figure 1: Hybrid collinear and high-energy factorization for double-hadron detection (left) and hadron-plus-jet inclusive hadroproduction (right). Collinear parton densities are represented by red ovals. The green (blue) blob depicts the off-shell hard factor embodied in the hadron (jet) emission function, while indigo arrows depicts the emission of *b*-flavored hadrons. The Green's function is described by the orange blob. The diagram was created with JaxoDraw 2.0 [211].

correlations exhibit an unphysical behavior both at small and at large rapidity distances. Different solutions have been tried to cure this problem. In particular, the Brodsky–Lepage–Mackenzie (BLM) prescription [201, 202] as specifically built for semi-hard reactions [203] slightly dampens those instabilities on azimuthal correlations and thus averagely ameliorates the agreement with data. However, BLM is almost ineffectual on light di-hadron or hadron plus jet semi-hard distributions. The main reason is that the optimal values for renormalization scales prescribed by BLM are much higher than the process natural scales [88, 113, 157]. Thus, total cross sections suffer from a large loss of statistics.

Fair signals of a stabilization of the high-energy resummation under NLL corrections and energy-scale variations recently emerged from semi-hard reactions whose final states show the signature of Higgs bosons [89, 204–209]. Then, a fair stabilizing trend came out from the study of Λ_c hyperons at the LHC [164], and also from analogous observables sensitive to B mesons and Λ_b baryons [165]. In those works it was proven that the stabilizing effect is encoded in the peculiar pattern of VFNS collinear FFs portraying the production of these singly heavy-flavored particles at high transverse momentum. Similar results were observed when vector quarkonia [85, 86], charmed B mesons [84], or heavy-light tetraquarks [210] are emitted in semi-hard configurations. All these results gave us corroborating evidence that the found *natural stabilization* of BFKL emerges as an *intrinsic* property genuinely correlated with final states sensitive to heavy flavor [112].

2.2. NLL-resummed differential cross section

We will study the two kinds of processes depicted in Fig. 1

$$p(P_a) + p(P_b) \rightarrow \mathcal{B}_1(q_1, y_1, \phi_1) + \mathcal{X} + \mathcal{B}_2(q_2, y_2, \phi_2),$$

$$p(P_a) + p(P_b) \rightarrow \mathcal{B}(q_1, y_1, \phi_1) + \mathcal{X} + \text{jet}(q_2, y_2, \phi_2),$$
(1)

where $p(P_{a,b})$ is an initial-state proton possessing four-momentum $P_{a,b}$, from which a parton with longitudinal-momentum fraction $x_{a,b}$ is struck. Then, $\mathcal{B}_{(1,2)}(q_{1,2},y_{1,2})$ stands for a singly bottom-flavored hadron $\mathcal{H}_b \equiv \{B+\Lambda_b\}$, or a charmed-bottomed meson $B_c(^1S_0) \equiv B_c$, or its resonance $B_c(^3S_1) \equiv B_c^*$, emitted with four-momentum $q_{1,2}$, rapidity $y_{1,2}$ and azimuthal angle $\phi_{1,2}$, and a light-favored jet is possibly tagged with four-momentum q_2 , rapidity y_2

and azimuthal angle ϕ_2 . Furthermore, \mathcal{X} represents an inclusively radiated gluon system. The large final state transverse momenta, $|\vec{q}_{1,2}|$, together with the high rapidity interval, $\Delta Y \equiv y_1 - y_2$, are required ingredients to make the final state be both semi-hard and diffractive. In addition, transverse momenta of the observed particles need to be large enough to make the VFNS fragmentation approach be valid.

Stemming protons' four-momenta can be written as Sudakov vectors with the conditions $P_a^2 = P_b^2 = 0$ and $2(P_a \cdot P_b) = s$, so that final-state four-momenta are cast via the following decomposition

$$q_{1,2} = x_{1,2} P_{a,b} - \frac{q_{1,2\perp}^2}{x_{1,2} s} P_{b,a} + q_{1,2\perp} , \quad q_{1,2\perp}^2 = -\vec{q}_{1,2}^2 . \tag{2}$$

The outgoing-object longitudinal-momentum fractions are labeled as $x_{1,2}$. They are connected with the respective rapidities and to ΔY via

$$y_{1,2} = \pm \frac{1}{2} \ln \frac{s \, x_{1,2}^2}{\vec{q}_{1,2}^2} \,, \qquad dy_{1,2} = \pm \frac{dx_{1,2}}{x_{1,2}} \,, \qquad \Delta Y = \ln \frac{s \, x_1 x_2}{|\vec{q}_1| |\vec{q}_2|} \,.$$
 (3)

According to the pure collinear factorization, one would write the LO cross section for our processes (Eq. (1)) as a one-dimensional convolution among the partonic-subprocess factor, proton PDFs, and *b*-hadron FFs. Considering the double hadron case as depicted in the left diagram of Fig. 1, we have

$$\frac{\mathrm{d}\sigma_{[p+p\to B+B]}^{\mathrm{LO}}}{\mathrm{d}x_{1}\mathrm{d}x_{2}\mathrm{d}^{2}\vec{q}_{1}\mathrm{d}^{2}\vec{q}_{2}} = \sum_{i,j=-5}^{5} \int_{0}^{1} \mathrm{d}x_{i} \int_{0}^{1} \mathrm{d}x_{j} f_{i}(x_{i},\mu_{F})f_{j}(x_{j},\mu_{F}) \\
\times \int_{x_{1}}^{1} \frac{\mathrm{d}\xi_{1}}{\xi_{1}} \int_{x_{2}}^{1} \frac{\mathrm{d}\xi_{2}}{\xi_{2}} D_{i}^{B_{1}} \left(\frac{x_{1}}{\xi_{1}},\mu_{F}\right) D_{j}^{B_{2}} \left(\frac{x_{2}}{\xi_{2}},\mu_{F}\right) \frac{\mathrm{d}\hat{\sigma}_{ij}}{\mathrm{d}x_{i}\mathrm{d}x_{j}\mathrm{d}\xi_{1}\mathrm{d}\xi_{2}\mathrm{d}^{2}\vec{q}_{1}\mathrm{d}^{2}\vec{q}_{2}}, \tag{4}$$

with the *i* and *j* indices running over parton species, $f_{i,j}(x_{1,2}, \mu_F)$ being the proton PDFs, $D_{i,j}^{B_{1,2}}(x_{1,2}/\xi_{1,2} \equiv z_{1,2}, \mu_F)$ denoting *b*-hadron FFs, $x_{1,2}$ and $\xi_{1,2}$ respectively standing for incoming- and fragmenting-partons' longitudinal fractions, and $d\hat{\sigma}_{ij}$ representing the partonic cross section. Analogously, we write the following collinear-convolution formula for the *b*-hadron plus light-jet case depicted in the right diagram of Fig. 1

$$\frac{\mathrm{d}\sigma^{\mathrm{LO}}_{[p+p\to B+\mathrm{jet}]}}{\mathrm{d}x_{1}\mathrm{d}x_{2}\mathrm{d}^{2}\vec{q}_{1}\mathrm{d}^{2}\vec{q}_{2}} = \sum_{i=-5}^{5} \int_{0}^{1} \mathrm{d}x_{i} \int_{0}^{1} \mathrm{d}x_{j} \, f_{i}(x_{i},\mu_{F}) f_{j}(x_{j},\mu_{F}) \int_{x_{1}}^{1} \frac{\mathrm{d}\xi}{\xi} D_{i}^{B} \left(\frac{x_{1}}{\xi},\mu_{F}\right) \frac{\mathrm{d}\hat{\sigma}_{ij}}{\mathrm{d}x_{1}\mathrm{d}x_{2}\mathrm{d}\xi \, \mathrm{d}^{2}\vec{q}_{1}\mathrm{d}^{2}\vec{q}_{2}} \,. \tag{5}$$

At variance with the collinear framework, to write the expression for the high-energy resummed cross section in the hybrid factorization, one first makes use of BFKL and then completes the picture by adding collinear PDFs and FFs. We suitably rewrite the differential cross section as a Fourier expansion in terms of azimuthal coefficients

$$\frac{d\sigma^{\text{NLL/NLO}^{+}}}{dy_{1}dy_{2}d\vec{q}_{1}d\vec{q}_{2}d\phi_{1}d\phi_{2}} = \frac{1}{2\pi^{2}} \left[\frac{1}{2} C_{0}^{\text{NLL/NLO}^{+}} + \sum_{n=1}^{+\infty} C_{n}^{\text{NLL/NLO}^{+}} \cos(n(\pi - \Phi)) \right], \tag{6}$$

with $\Phi \equiv \phi_1 - \phi_2$. The $C_n^{\text{NLL/NLO}^+}$ coefficients are calculated within the BFKL formalism at a full NLL accuracy. Making use of the $\overline{\text{MS}}$ renormalization scheme [212], we obtain [213]

$$C_{n}^{\text{NLL/NLO}^{+}} = \int_{0}^{2\pi} d\phi_{1} \int_{0}^{2\pi} d\phi_{2} \frac{d\sigma^{\text{NLL/NLO}^{+}}}{dy_{1}dy_{2} d|\vec{q}_{1}| d|\vec{q}_{2}|d\phi_{1}d\phi_{2}} \cos(n(\pi - \Phi))$$

$$= \frac{e^{\Delta Y}}{s} \int_{-\infty}^{+\infty} dv \, e^{\Delta Y \bar{\alpha}_{s}(\mu_{R})\chi^{\text{NLO}}(n,v)}$$

$$\times \alpha_{s}^{2}(\mu_{R}) \left\{ \mathcal{E}_{1}^{\text{NLO}}(n,v,|\vec{q}_{1}|,x_{1}) \left[\mathcal{E}_{2}^{\text{NLO}}(n,v,|\vec{q}_{2}|,x_{2}) \right]^{*} + \bar{\alpha}_{s}^{2}(\mu_{R}) \Delta Y \frac{\beta_{0}}{4N_{c}} \chi(n,v) \mathcal{F}(v) \right\} ,$$
(7)

where $\bar{\alpha}_s(\mu_R) \equiv \alpha_s(\mu_R) N_c/\pi$ with N_c the color number, $\beta_0 = 11 N_c/3 - 2n_f/3$ is the first coefficient of the QCD β -function with n_f the flavor number. A two-loop running-coupling choice with $\alpha_s(M_Z) = 0.118$ and with dynamic thresholds for the flavor number n_f is made. The kernel entering the exponent of Eq. (7) encompasses the resummation of LL and NLL terms. Its analytic expression is

$$\chi^{\text{NLO}}(n,\nu) = \chi(n,\nu) + \bar{\alpha}_{s}\hat{\chi}(n,\nu) , \qquad (8)$$

where

$$\chi(n,\nu) = -2\gamma_{\rm E} - 2\operatorname{Re}\left\{\psi\left(\frac{n}{2} + \frac{1}{2} + i\nu\right)\right\} \tag{9}$$

stand for the LO kernel eigenvalues, γ_E is the Euler-Mascheroni constant, and $\psi(z) \equiv \Gamma'(z)/\Gamma(z)$ the Gamma-function logarithmic derivative. The $\hat{\chi}(n, \nu)$ function in Eq. (8) represents the NLO kernel correction in the Mellin space

$$\hat{\chi}(n,\nu) = \bar{\chi}(n,\nu) + \frac{\beta_0}{8N_c}\chi(n,\nu) \left(\frac{10}{3} + \ln\frac{\mu_R^4}{m_{1\perp}^2 m_{2\perp}^2} - \chi(n,\nu)\right), \tag{10}$$

where $m_{1,2\perp}$ are the transverse masses of the two outgoing states. For a *b*-hadron one has $m_{B\perp} = \sqrt{m_B^2 + |\vec{q}_B|^2}$, with $m_B \equiv m_{H_b} \equiv m_{\Lambda_c} = 5.62$ GeV or $m_B \equiv m_{B_c^{(*)}} = 6.275$ GeV. Conversely, the transverse mass of a light-flavored jets can be safely set to transverse momentum, say $m_{\mathcal{J}\perp} \equiv |\vec{q}_{\mathcal{J}}|$. The NLO $\bar{\chi}(n, \nu)$ function was computed in Ref. [214]

$$\bar{\chi}(n,\nu) = -\frac{1}{4} \left\{ \frac{\pi^2 - 4}{3} \chi(n,\nu) - 6\zeta(3) - \frac{\mathrm{d}^2 \chi}{\mathrm{d}\nu^2} + 2\Xi(n,\nu) + 2\Xi(n,-\nu) \right\}$$
 (11)

$$+ \frac{\pi^2 \sinh(\pi v)}{2 v \cosh^2(\pi v)} \left[\left(3 + \left(1 + \frac{n_f}{N_c^3} \right) \frac{11 + 12 v^2}{16(1 + v^2)} \right) \delta_{n0} - \left(1 + \frac{n_f}{N_c^3} \right) \frac{1 + 4 v^2}{32(1 + v^2)} \delta_{n2} \right] \right\} .$$

The $\Xi(n, v)$ function reads

$$\Xi(n,v) = -\int_0^1 dx \, \frac{x^{-1/2+iv+n/2}}{1+x} \left\{ \frac{1}{2} \left(\psi' \left(\frac{n+1}{2} \right) - \zeta(2) \right) + \text{Li}_2(x) + \text{Li}_2(-x) \right.$$

$$+ \ln x \left[\psi(n+1) - \psi(1) + \ln(1+x) + \sum_{k=1}^\infty \frac{(-x)^k}{k+n} \right] + \sum_{k=1}^\infty \frac{x^k}{(k+n)^2} \left[1 - (-1)^k \right] \right\}$$

$$= \sum_{k=0}^\infty \frac{(-1)^{k+1}}{k + (n+1)/2 + iv} \left\{ \psi'(k+n+1) - \psi'(k+1) \right\}$$
(12)

$$+ \; (-1)^{k+1} \left[\rho(k+n+1) + \rho(k+1) \right] - \frac{\psi(k+n+1) - \psi(k+1)}{k + (n+1)/2 + i \nu} \; \bigg\} \;\; ,$$

with

$$\rho(z) = \frac{1}{4} \left[\psi'\left(\frac{z+1}{2}\right) - \psi'\left(\frac{z}{2}\right) \right] , \tag{13}$$

and

$$\operatorname{Li}_{2}(z) = -\int_{0}^{z} \mathrm{d}\zeta \, \frac{\ln(1-\zeta)}{\zeta} \ . \tag{14}$$

The two quantities

$$\mathcal{E}_{1,2}^{\text{NLO}}(n, \nu, |\vec{q}_{1,2}|, x_{1,2}) = \mathcal{E}_{1,2}(n, \nu, |\vec{q}_{1,2}|, x_{1,2}) + \alpha_s(\mu_R) \,\hat{\mathcal{E}}_{1,2}(n, \nu, |\vec{q}_{1,2}|, x_{1,2}) \tag{15}$$

stand for the emission functions of the forward b-hadron and the light jet. At LO one has

$$\mathcal{E}_{\mathcal{B}}(n,\nu,|\vec{q}_{\mathcal{B}}|,x_{\mathcal{B}}) = 2\sqrt{\frac{C_F}{C_A}}|\vec{q}_{\mathcal{B}}|^{2i\nu-1} \int_{x_{\mathcal{B}}}^{1} \frac{\mathrm{d}\xi}{\xi} \left(\frac{\xi}{x_{\mathcal{B}}}\right)^{2i\nu-1} \left[\frac{C_A}{C_F} f_g(\xi) D_g^{\mathcal{B}} \left(\frac{x_{\mathcal{B}}}{\xi}\right) + \sum_{i=q,\bar{q}} f_i(\xi) D_i^{\mathcal{B}} \left(\frac{x_{\mathcal{B}}}{\xi}\right)\right]$$
(16)

and

$$\mathcal{E}_{\mathcal{J}}(n, \nu, |\vec{q}_{\mathcal{J}}|, x_{\mathcal{J}}) = 2\sqrt{\frac{C_F}{C_A}}|\vec{q}_{\mathcal{J}}|^{2i\nu-1} \left(\frac{C_A}{C_F} f_g(x_{\mathcal{J}}) + \sum_{j=q,\bar{q}} f_j(x_{\mathcal{J}})\right), \tag{17}$$

with $C_F \equiv (N_c^2 - 1)/(2N_c)$ and $C_A \equiv N_c$ being the Casimir factors for a gluon emission from a quark and a gluon, respectively. The $\mathcal{F}(\nu)$ function at the end of the last row of Eq. (7) embodies the logarithmic derivative of LO emission functions

$$\mathcal{F}(\nu) = \ln\left(|\vec{q}_1||\vec{q}_2|\right) + \frac{i}{2} \frac{\mathrm{d}}{\mathrm{d}\nu} \ln\frac{\mathcal{E}_1}{\mathcal{E}_2^*} \,. \tag{18}$$

What is left in Eq. (7) are the NLO corrections to $\mathcal{E}_{\mathcal{B},\mathcal{J}}$ functions, $\hat{\mathcal{E}}_{1,2}$. The NLO correction to the \mathcal{B} hadron at large transverse momentum was computed in Ref. [126] and is provided in the Appendix A. Our choice for the jet NLO emission function builds on analyses described in Refs. [126, 128]. It relies upon a jet algorithm obtained in the "small-cone" limitand with a cone-type distance [129, 215, 216], where the radius is set to r = 0.5 (see the Appendix B).

A proper "resummation versus fixed-order" study should rely upon comparing NLL predictions from our highenergy approach with NLO calculations in pure collinear factorization. Unfortunately, a numerical technology aimed at computing NLO distributions for two-particle reactions in hadron collisions is still missing. Thus, for the sake of comparison with reference fixed-order results, one can truncate the expansion of the azimuthal coefficients of Eq. (7) up to the $\mathcal{O}(\alpha_s^3)$ order. In this way, one obtains an effective high-energy fixed-order (HE-NLO⁺) expression that collects the leading-power asymptotic signal present in a pure NLO calculation, whereas terms proportional by inverse powers of the partonic center-of-mass energy are neglected. The $\overline{\text{MS}}$ expressions for HE-NLO⁺ azimuthal coefficients reads

$$C_n^{\text{HE-NLO}^+} = \frac{e^{\Delta Y}}{s} \int_{-\infty}^{+\infty} dv \, \alpha_s^2(\mu_R) \left[1 + \bar{\alpha}_s(\mu_R) \Delta Y \chi(n, \nu) \right] \, \mathcal{E}_1^{\text{NLO}}(n, \nu, |\mathbf{\kappa}_1|, x_1) \left[\mathcal{E}_2^{\text{NLO}}(n, \nu, |\mathbf{\kappa}_2|, x_2) \right]^* \,, \tag{19}$$

with the exponentiated kernel expanded and truncated at $\mathcal{O}(\alpha_s)$.

We will also compare our NLL results with the pure LL background. The latter is obtained by discarding NLO corrections of both the kernel and the emission functions

$$C_n^{\text{LL/LO}} = \frac{e^{\Delta Y}}{s} \int_{-\infty}^{+\infty} d\nu \, e^{\Delta Y \bar{\alpha}_s(\mu_R)\chi(n,\nu)} \, \alpha_s^2(\mu_R) \, \mathcal{E}_1(n,\nu,|\vec{q}_1|,x_1) \left[\mathcal{E}_2(n,\nu,|\vec{q}_2|,x_2) \right]^*. \tag{20}$$

Eqs. (7) to (20) shed light on the structure of our hybrid factorization. According to BFKL, the cross section is high-energy factorized as a convolution between the Green's function and two singly off-shell emission functions. The latters embody collinear inputs, namely collinear convolutions between incoming protons' PDFs and outgoing hadrons' FFs. The NLL/NLO⁺ label tells us that the resummation of energy logarithms is performed within a full NLL accuracy and within NLO perturbative order. The '+' superscript in Eqs. (7) and (19) highlights that some Next-to-NLL (NNLL) extra terms come from the cross product between NLO corrections of the two emission functions. Finally, factorization (μ_F) and renormalization (μ_R) scales are set to the *natural* scales suggested by kinematics. In particular, we fix $\mu_F = \mu_R = \mu_N \equiv m_{1\perp} + m_{2\perp}$.

Our guiding line here is to consider, as a *natural* scale, any energy scale with the same order of magnitude of the typical energy of the emitted particle. Since, in our case, two objects are emitted, there are in principle to scales (one for each fragmentation region). Natural values for them are $m_{1\perp}$ and $m_{2\perp}$, respectively. For the sake of comparing our observables with future, possible predictions coming from other approaches, it is convenient to make a simple choice, namely to have just one scale. As a bonus, choosing the sum of $m_{1\perp}$ and $m_{2\perp}$ turns out to match the settings of many other numeric codes aimed at precision QCD phenomenology (see, *e.g.*, Refs. [217–219]).

2.3. Collinear inputs

As for collinear PDFs, we make use of the NNPDF40_nlo_as_01180 NLO set [220, 221] as implemented in LHAPDF v6.5.4 [222]. It was obtained on the basis of global fits by means of the well-defined *replica* methodology originally proposed in Ref. [223] in the context of a neural-network approach (we refer to Ref. [224] for an in-depth analysis on ambiguities about *correlations* among different PDF sets).

Parton fragmentation to singly-bottomed $\mathcal{H}_b \equiv \{B + \Lambda_b\}$ hadrons is depicted via the KKSS07 NLO FF determination, which was originally obtained by fitting data on inclusive productions of noncharmed B mesons in lepton annihilation [56]. Here, the threshold for bottom- and antibottom-quark evolution is set to 4.5 GeV and its initial-scale parametrization reads as a power-like function with three parameters [225]. Light partons and the charm quarks are perturbatively generated with DGLAP, while their FFs are zero below the threshold for the bottom. The current KKSS07 set [58] for \mathcal{H}_b particles was constructed from the original noncharmed B-meson ones by switching off the branching fraction for the $b \to B^\pm$ subprocess, which was assumed to be $f_u = f_d = 0.397$ [56]. Such a choice is justified by the assumption that a unique function can be employed in the description of noncharmed B-meson fragmentation or of an inclusive sum of B and A_b channels, but not for the A_b -baryon case alone.

Our strategy for charmed B-meson fragmentation is more involved. It was presented for the first time in our recent study focused on accessing the high-energy spectrum of QCD via the hadroproduction of these doubly heavy-flavored states [84]. It takes inspiration from a first determination of VFNS, DGLAP-evolving FFs for vector quarkonia [85, 86]. The starting point is the NLO calculation, within the NRQCD effective theory, of initial-scale inputs for charm, bottom quark [82] and gluon [83] fragmentation channels to $B_c(^1S_0) \equiv B_c$ and $B_c(^3S_1) \equiv B_c^*$ mesons (see Refs. [226, 227] for similar calculations). To generate DGLAP-evolved sets for our charmed B mesons we need to plug the NRQCD inputs into a numeric evolution code. Among them, we cite: QCD-PEGASUS [228], HOPPET [229], QCDNUM [230], APFEL (++) [231–233], and EKO [234, 235]. Contrariwise to PDFs, which obey a space-like evolution equation, FFs must be time-like evolved [236, 237]. In Ref. [84] we employed APFEL++ to generate novel and phenomenology-ready LHAPDF FF grids, which we named ZCFW22 NLO determinations.

For the sake of comparison, we employ the NNFF10_KAsum_nlo set [238] (see Ref. [239] for advancements) to describe charged-kaon fragmentation at NLO.

2.4. Natural stabilization of the NLL series

Here we provide details on the stabilizing mechanism emerging from the VFNS collinear fragmentation of b-hadrons. The linking dynamics between heavy-flavor FFs and the observed stability of semi-inclusive distributions calculated within the hybrid collinear and high-energy factorization at NLL/NLO⁽⁺⁾ was first unveiled through a study of semi-hard emissions of heavy-light hadrons, namely: D particles [240–248], Λ_c baryons [241, 249, 250], and \mathcal{H}_b states [55–58, 60, 251–254]. This striking property came out for the first time from an analysis of semi-inclusive detections of Λ_c [91, 164], $D^{*\pm}$ [166, 167], and \mathcal{H}_b [91, 165] hadrons in forward directions of rapidity at the LHC. Such a remarkable result was then corroborated by similar investigations on vector quarkonia [85, 255] and $B_c^{(*)}$ mesons [84], whose formation mechanism was modeled on the basis of single-parton NRQCD fragmentation [82, 83, 226, 227, 256–261]. A further evidence came recently out in the context of heavy-light tetraquarks [210, 262] described via a Suzuki–Nejad–Amiri–Ji initial-scale fragmentation input [263–266] (see Refs. [267, 268] for further details). A less pronounced stabilization pattern was also observed in the case of strange-quark flavored, cascade $\Xi^-/\bar{\Xi}^+$ baryon tags [161].

Panels in Fig. 2 contain the factorization-scale dependence of KKSS07 [56, 58] and ZCFW22 [84] NLO functions respectively describing the collinear fragmentation of \mathcal{H}_b hadrons (right upper plot) and $B_c^{(*)}$ mesons (lower plots). For comparison, the left upper plot carries analogous information of light-quark flavored species, namely charged kaons, described by the NNFF1.0 [238] NLO collinear-FF determination. For the sake of simplicity, we show values of our FF sets just for one value of the final-state hadron longitudinal-momentum fraction, z. In particular, we choose a value of z that roughly matches the mean value at which FFs are typically probed standard semi-hard configurations (see Section 3.2). Thus we have $z = 0.475 \simeq \langle z \rangle$. As expected, the b channel of KKSS07 and ZCFW22 functions heavily prevails over the other flavors. Particular attention deserves, however, the behavior the gluon FF, which clearly decreases with μ_F for kaons but smoothly increases for all the three b-flavored species, up to reach a plateau. More quantitative information on the FFs of Fig. 2 would come from an analysis on the associated uncertainties. However, apart the kaon NNFF1.0 determination, the other ones do not carry such information. KKSS07 functions

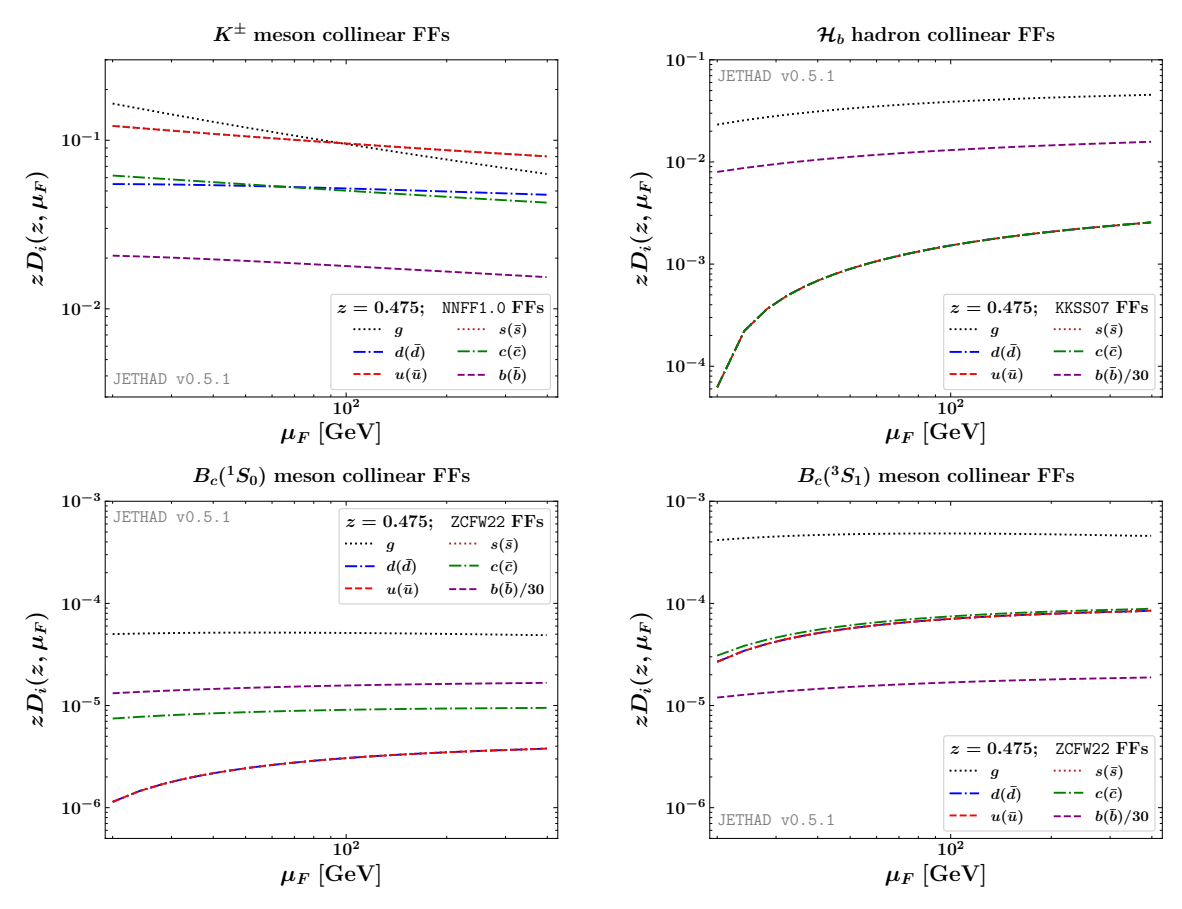


Figure 2: Factorization-scale dependence of NNFF1.0 [238], KKSS07 [56, 58], and ZCFW22 [84] NLO FFs respectively describing: kaon (upper left panel), \mathcal{H}_b hadron (upper right panel), and charmed B meson (lower panels) detections, for $\langle z \rangle \simeq 0.475$.

describing noncharmed *b*-hadron fragmentation were extracted without any uncertainty estimate, whereas the inclusion of uncertainties for the two ZCFW22 sets, possibly connected with perturbative scale-variation effects, is planned as a future extension of this work.

As extensively shown in Refs. [84, 85, 112, 164, 165, 210], the gluon collinear FF plays a crucial role. De facto, it has a strong stabilization power on our NLL/NLO⁺ observables. Its behavior with μ_E fairly controls the stability of the high-energy logarithmic series of our distributions. In the semi-hard regime proton PDFs are typically probed at $10^{-4} \lesssim x \lesssim 10^{-2}$, where the gluon PDF heavily dominates over quark ones. Given that the gluon FF diagonally multiplies with the gluon PDF in the LO hadron emission function (see Eq. (16)), its impact on the cross section is magnified. This effect is not quenched at NLO, where $\{qg\}$ and $\{gq\}$ nondiagonal channels are opened [164] (see the Appendix A). On one side, α_s decreases with μ_R both in the Green's function and in the emission functions (see Section 2.2). At the same time, however, the gluon PDF increases as μ_F enlarges. When that density multiplies a gluon FF which also increases with μ_F , as it happens for b-hadrons, the two effects balance each other. This leads to the stabilizing trend of heavy-flavor distributions under energy-scale variations. If instead the gluon FF falls down with μ_F , as it happens for light-flavored species, such charged kaons, the stabilizing pattern is lost. This harms any chance of making precision tests of semi-hard observables at the natural energies given by kinematics [88]. The emergence of the natural stability [112] in presence of both singly and doubly heavy flavored hadron species provides us with clear evidence that this striking feature is an *intrinsic* property of heavy-flavor detections, which becomes manifest whenever a heavy hadron emitted, independently of the choice made for the initial-scale input of the corresponding collinear fragmentation.

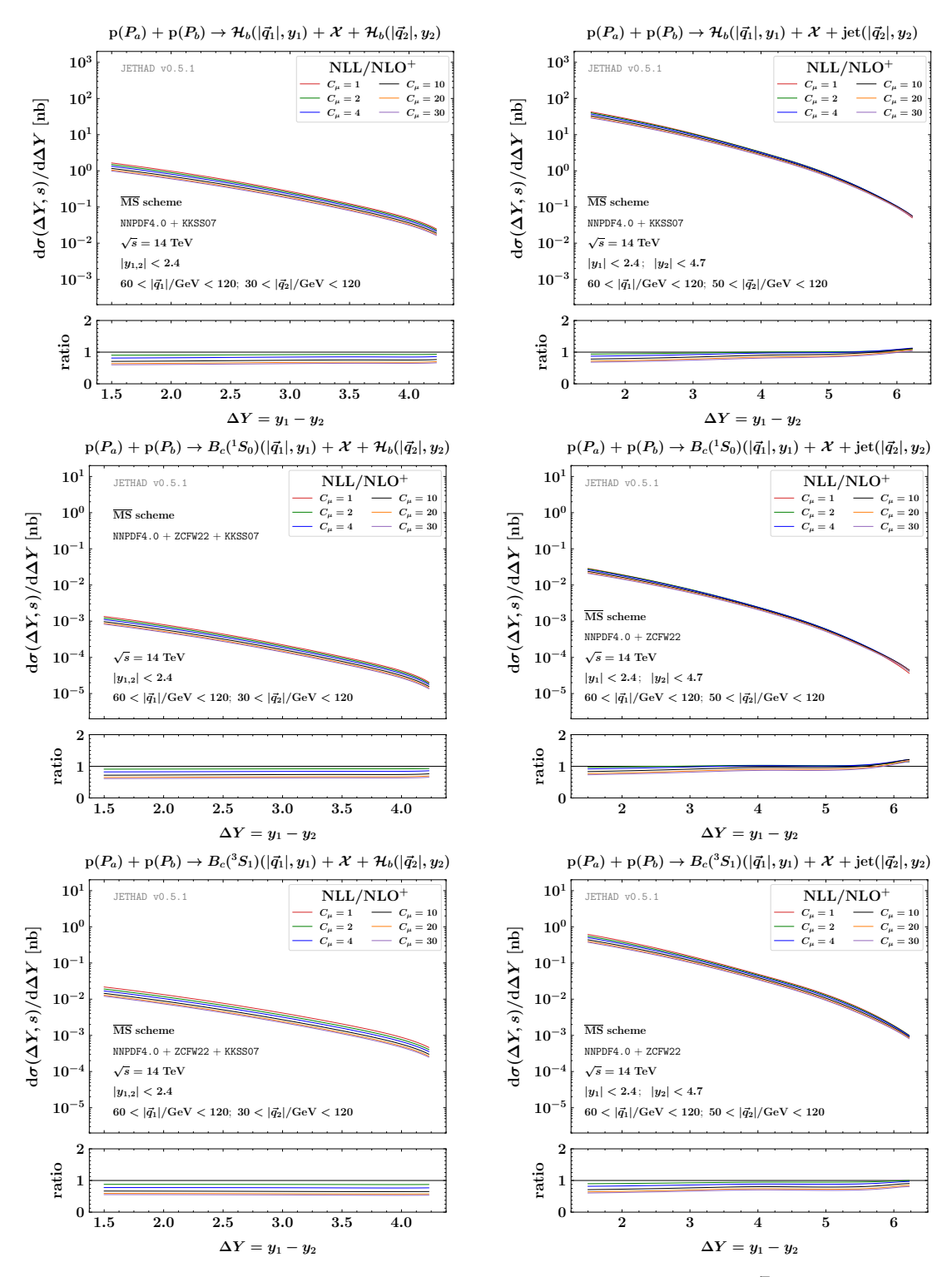


Figure 3: ΔY -rate of the double-hadron (left) and the hadron-plus-jet (right) channel at $\sqrt{s}=14$ TeV and within the NLL/NLO⁺ accuracy. Renormalization and factorization scales are progressively varied in the $1 < C_u < 30$ range.

3. Hi-Lumi LHC distributions

We performed our numeric computations via the JETHAD v0.5.1 interface [86, 88, 91], a PYTHON+FORTRAN multimodular working environment aimed at the calculation, management, and processing of high-energy distributions obtained from different theoretical approaches. In particular, rapidity and transverse-momentum differential cross sections were calculated by means of JETHAD FORTRAN 2008 core modules, whereas its PYTHON 3.0 analyzer was used to elaborate results. Section 3.1 gives details on our procedure to gauge the size of uncertainties for our resummed observables. Final-state kinematic cuts are presented in Section 3.2. Then, Section 3.3 carries a discussion of our NLL/NLO+ predictions.

3.1. Uncertainty estimation

A widely-used methodology to quantify the weight of Missing Higher-Order Uncertainties (MHOUs) relies upon assessing how much our observables are sensitive to variations of factorization and renormalization scales around their natural values. It is well-known that the effect MHOUs gives perhaps the major contribution to the overall uncertainty [91]. For this reason, we will gauge the size of simultaneously varying μ_F and μ_R around $\mu_N/2$ and $2\mu_N$. The C_μ parameter in panels of figures of Sections 3.3 and 3.4 is just the $C_\mu \equiv \mu_F/\mu_N = \mu_R/\mu_N$ ratio. This will represent our standard procedure to estimate the size of MHOUs. Then, for the sake of comparison with other approaches, where energy scales are allowed to assume values much larger than the natural ones (see, e.g., the BLM method [201–203]), we will also present an accessory, extended MHOU scan, with the C_{μ} parameter ranging from 1 to 30. Another possibly relevant uncertainty is encoded in proton PDFs. Quite recent analyses on high-energy production rates have shown, however, that selecting distinct PDF parametrizations as well as distinct members inside the same set produces a very small effect [88, 91, 157, 165]. Therefore, we will calculate our observables by considering only the central member of the NNPDF4.0 parametrization. Then, other potential uncertainties could come from a collinear improvement of the NLO kernel (see Refs. [269–271] and reference therein), which consists in including renormalization-group (RG) terms to make the BFKL equation compatible with the DGLAP one in the collinear limit, or from changing the renormalization scheme. The first case was deeply addressed in Ref. [91]. As a result, the impact of collinear-improvement techniques on rapidity-differential rates is fairly contained inside error bands produced by MHOUs, and it is even smaller in the case of when other differential observables. The same article provides us with an overestimation of the effect of passing from \overline{MS} [212] to MOM [272, 273] renormalization scheme. MOM results for rapidity distributions are systematically higher than MS ones, but still contained into MHOU bands. We stress, however, that a proper MOM analysis should be based on MOM-evolved PDFs and FFs, not available so far.

We will produce uncertainty bands for our distributions by combining MHOUs with the numeric error generated by the multidimensional integration (see Section 3.2). The latter will be constantly kept below 1% by the JETHAD integration subinterfaces.

3.2. Kinematic constraints on final-state ranges

We will consider two main observables: (i) the rapidity-interval distribution, namely the cross section differential in the rapidity separation, $\Delta Y = y_1 - y_2$, between the two produced particles, and (ii) the doubly-differential transverse-momentum distribution.

The first observable genuinely corresponds the C_0 azimuthal-angle coefficient, defined in Section 2.2, integrated over final-state transverse momenta and rapidities and taken at fixed values of ΔY

$$\frac{\mathrm{d}\sigma(\Delta Y;s)}{\mathrm{d}\Delta Y} = \int_{|\vec{q}_{2}|^{\min}}^{|\vec{q}_{2}|^{\max}} \mathrm{d}|\vec{q}_{1}| \int_{|\vec{q}_{2}|^{\min}}^{|\vec{q}_{2}|^{\max}} \mathrm{d}|\vec{q}_{2}| \int_{\max{(y_{1}^{\min},\Delta Y + y_{2}^{\min})}}^{\min{(y_{1}^{\max},\Delta Y + y_{2}^{\max})}} \mathrm{d}y_{1} \ C_{0}^{[\mathrm{order}]} \left(|\vec{q}_{1}|,|\vec{q}_{2}|,y_{1},y_{2};s\right) \Big|_{y_{2} = y_{1} - \Delta Y} \ , \ (21)$$

where the '[order]' label for C_0 inclusively refers to: NLL/NLO⁺, HE-NLO⁺, or LL/LO. Here we made use of a $\delta(\Delta Y - y_1 + y_2)$ function to remove the integration over one of the two rapidities, say y_2 . Transverse momenta of the forward b-hadron and the backward one stay in the ranges $60 < |\vec{q}_1|/\text{GeV} < 120$ and $30 < |\vec{q}_2|/\text{GeV} < 120$, respectively. These cuts fairly meet the criteria of applicability of a VFNS-based fragmentation approach, in which energy scales must be sufficiently higher than thresholds for the DGLAP evolution of heavy-quark species. Then, light jets are tagged in transverse-momentum ranges lightly different but compatible with current and forthcoming studies at the LHC [274], say $50 < |\vec{q}_2|/\text{GeV} < 60$. The use of such asymmetric transverse-momentum ranges

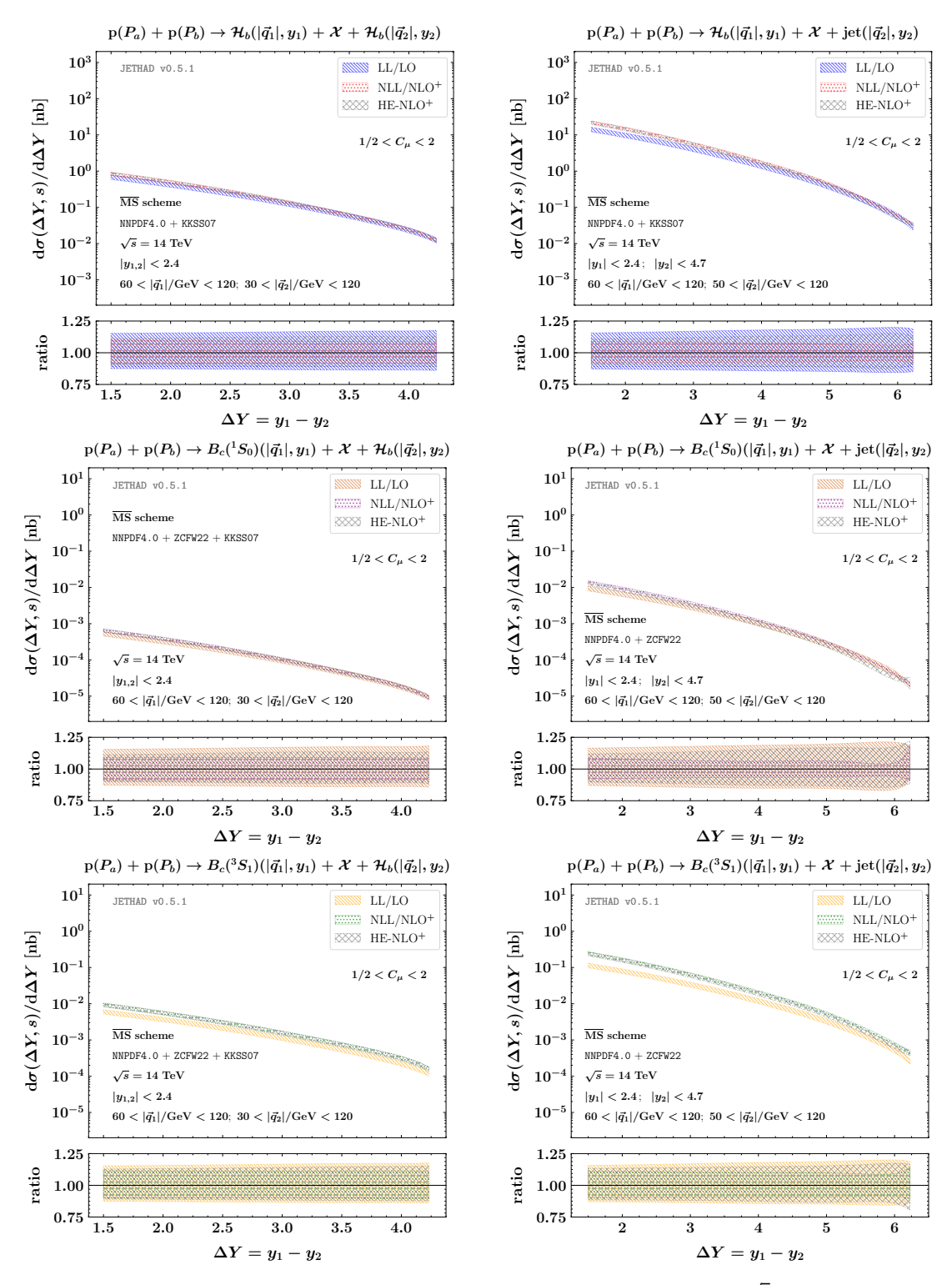


Figure 4: ΔY -rate of the double-hadron (left) and the hadron-plus-jet (right) channel at $\sqrt{s}=14$ TeV and within the NLL/NLO⁺ accuracy. Shaded bands exhibit the combined effect of renormalization- and factorization-scale variation in the $1/2 < C_{\mu} < 2$ range.

eases disentangling the pure high-energy dynamics from the fixed-order signal [88, 144, 145]. It also dampens large Sudakov logarithms due to almost back-to-back configurations which would require the employment of another resummation [275–280]. Finally, it quenches instabilities connected to radiative corrections [281, 282] as well as violations of the energy-momentum conservation relation [283]. As for the rapidity ranges, we select typical cuts of current LHC studies, where hadrons are detected only in the barrel calorimeter [284], say from –2.4 to 2.4, whereas the jet can be also tagged in endcaps' regions [274], say from –4.7 to 4.7.

The second observable is given by the C_0 azimuthal-angle coefficient, integrated over rapidities while ΔY is kept fixed, but this time being differential in the transverse momenta of the two outgoing objects

$$\frac{d\sigma(|\vec{q}_1|,|\vec{q}_2|,\Delta Y;s)}{d|\vec{q}_1|d|\vec{q}_2|d\Delta Y} = \int_{\max(y_1^{\min},\Delta Y + y_2^{\max})}^{\min(y_1^{\max},\Delta Y + y_2^{\max})} dy_1 \ C_0^{[order]} \left(|\vec{q}_1|,|\vec{q}_2|,y_1,y_2;s\right) \Big|_{y_2 = y_1 - \Delta Y} \ . \tag{22}$$

Here we consider the previously mentioned kinematic cuts for rapidities, whereas the two transverse momenta can run from 10 to 100 GeV. This observable was recently proposed, in the context of singly bottom-flavored hadrons [165] and cascade Ξ baryons [161], as a favorable testing ground whereby unraveling the interplay among distinct resummations.

3.3. Rapidity-interval distributions

In Fig. 3 we present rapidity-interval distributions for our reference processes, calculated within NLL/NLO⁺ hybrid factorization and taken at $\sqrt{s} = 14$ TeV. Left plots refer to double-hadron channels, while right plots are for the hadron-jet ones. Final states with \mathcal{H}_b hadrons, $B_c(^1S_0)$ mesons, or $B_c(^3S_1)$ resonances are considered in upper, central, and lower plots, respectively. More in particular, any forward b-flavored hadron is always accompanied by a singly bottomed hadron \mathcal{H}_b (left plots) or by a light-flavored jet (right plots). This is to avoid the presence of two identified charmed B mesons in the final state, which would lead to a substantial lowering in statistics. We will adopt this choice also in the next Section (3.4). The minimum values of our distributions are the ones obtained at the maximum values of ΔY . They are uniformly larger than 10^{-2} nb when only \mathcal{H}_b hadrons (and light jets) are produced, and larger than 10^{-5} nb in the two $B_c^{(*)}$ cases. This represents a very promising statistics that can be easily accessed via dedicated experimental studies at the forthcoming Hi-Lumi upgrade of the LHC. The decreasing trend with ΔY of our NLL-resummed distributions is a general feature shared by all the semi-hard hadroproduction final states investigated so far. It comes out as the interplay between two competing effects. Indeed, although the high-energy dynamics encoded in the partonic hard factor would make the cross section grow with energy, collinear PDFs and FFs fall off very fast with ΔY , since this kinematically translates to longitudinal-momentum fractions very close to one. The net result is a dampening effect with ΔY of hadronic distributions.

The core analysis shown in Fig. 3 is a study of our rapidity-interval differential distributions under a progressive variation of factorization and renormalization scales in an broad window, controlled by the C_{μ} parameter introduced in Section 3.1, which ranges from 1 to 30. This strategy actually represents an extended MHOU scan with respect to the traditional one, $1/2 < C_{\mu} < 2$. Ancillary panels drawn right below primary ones show reduced distributions, namely the ones divided by their central values calculated at $C_{\mu} = 1$. Remarkably, NLL/NLO⁺ results for all the six considered final states feature quite a weak sensitivity on C_{μ} variation in the whole spectrum of ΔY matter of our investigation. This supports the important message that a strong stabilization mechanism is encoded both in the KKSS07 functions extracted from global data on B mesons and Λ_b baryons, as well as in the novel ZCFW22 FFs built on the basis of NRQCD initial-scale inputs for $B_c(^1S_0)$ and $B_c(^3S_1)$ generalized-quarkonium states and then evolved via DGLAP in a VFNS scheme. Results contained in plots of Fig. 3 bring to light the emergence of the *natural stability* [112] from semi-inclusive b-flavor emissions at high energies.

As a complement, in Fig. 4 we show results for the same ΔY -distributions, calculated within the NLL/NLO⁺ accuracy and compared with HE-NLO⁺ and LL/LO corresponding ones. Left (right) plots are for hadron-plus-hadron (hadron-plus-jet) observables. Upper, central, and lower plots respectively correspond to \mathcal{H}_b , B_c , and B_c^* sensitive final states. This time, shaded bands are built by combining the uncertainty of the multidimensional integration, numerically performed by the JETHAD integrators, with the one coming from a traditional MHOU scan, namely with the C_μ parameter running from 1/2 to two. As done before, lower ancillary panels exhibit reduced distributions, *i.e.* divided by central values calculated when $C_\mu = 1$. The global outcome is a strong stability under higher-order corrections. This is confirmed by the fact that NLL/NLO⁺ uncertainty bands are generally narrower and partially nested inside corresponding LL/LO ones, in particular in the large- ΔY regime, where the impact of high-energy logarithms is

expected to be large. Their overlap is slightly weaker for hadron-plus-jet cases (right plots). This is not unexpected, since the emission of just one *b*-hadron rather then two reduces the stabilizing power by one half.

As discussed in previous works (see, e.g. Section 3 of Ref. [84]), shaded bands for fixed-order HE-NLO⁺ results are almost completely nested in resummed NLL/NLO⁺ ones. Future analyses on more exclusive observables, such as angularity distributions will shed light on a clearer disentanglement between our resummation and the fixed-order signal. Finally, as a bonus result, we confirm the estimate, provided by the LHCb Collaboration [70, 71], on the production-rate hierarchy between singly-bottomed hadrons and charmed B mesons. Production rates of the latters seems not to exceed 0.1% of the \mathcal{H}_b ones, at most. To compare our predictions with these numbers, we can consider the hadron-plus-jet channel (right diagram of Fig. 1) at LL/LO, whose differential cross section is linear in the b-hadron FFs (see Eq. (16)). The inspection of right plots of Fig. 4 in clearly in line with LHCb estimates for charmed B-meson sates.³ The hierarchy remains de facto unaltered both at NLL/NLO⁺ and at HE-NLO⁺. Remarkably, this fact not only represents a reliability test for our hybrid factorization, but it also definitely corroborates the validity of the single-parton fragmentation mechanism from NRQCD, at least for the $B_c(^1S_0)$ case.

3.4. Doubly-differential transverse-momentum distributions

Rapidity-interval distributions represent golden channels to unveil the onset of high-energy dynamics at hadron colliders. At the same time, pursuing the goal of exploring kinematic corners where other resummations are also at work, we need more differential observables in the transverse momentum. From one side, high transverse momenta or large imbalances between them heighten the size of DGLAP-type logarithms as well as soft, *threshold* ones [285–304]. These logarithms, which are of a different nature with respect the high-energy ones, must also be resummed.

Combining threshold and high-energy logarithms is a cumbersome task. A first double resummation was obtained in the context of the inclusive Higgs hadroproduction from gluon-gluon fusion [95]. The key ingredient there was the possibility of decoupling the two dynamics in the Mellin space, so that the small-x (high-energy) resummation and the large-x (threshold) one respectively "control" the small-N and large-N tail of the the Mellin projection of the cross section [305, 306]. In this way, the two kinds of logarithms can be separately resummed. In our case, however, the semi-inclusive emission of two objects (see Fig. 1) genuinely leads to rapidity-differential observables, for which a theoretical framework to properly perform such a double resummation is still missing.

From the other side, low transverse momenta translate into large Sudakov logarithms which are also missed by our hybrid factorization. Furthermore, effects connected to the well-known *diffusion pattern* rise [307–309]. The most natural way to catch these logarithms to all orders builds on the Transverse-Momentum (TM) resummation formalism [310–317].

Inclusive emissions of two-particle final states in proton collisions, such as photon [318–321], Higgs [322] and W^{\pm} boson [323] pairs, as well as boson plus jet [324, 325] and Z plus photon [326] systems, were proposed as favorable channels whereby testing the TM resummation. TM third-order fiducial rates for Drell-Yan and Higgs tags were respectively investigated in Refs. [327–330] and [328, 331–333]. Ref. [324] presents a pioneering joint resummation of TM logarithms rising from the emission of two states. There, the simultaneous measurement of transverse momenta of the Higgs boson and the leading jet was analyzed up to the NNLL accuracy by means of the RADISH numeric technology [331]. Ref. [334] deals with a study of TM distributions for the fully leptonic (W^+W^-) tag at the LHC.

Heavy-flavor distributions bring to a further complication. Indeed, when the transverse momentum of a heavy hadron diminishes, its transverse mass comes closer and closer to heavy-quark masses serving as DGLAP thresholds, even crossing then when energy scales are moved below their natural values (as an example, this happens when the C_{μ} parameter introduced in Section 3.1 is set to 1/2). In this case, the validity of a pure VFNS approach becomes questionable.

In this Section we consider cross sections at fixed values of ΔY and differential in the transverse momenta of both the final-state objects. In the kinematic sectors matter of our investigations energy logarithms arising from the semi-hard scale hierarchy are large. At the same time, however, also TM logarithms are potentially sizable. Therefore, we propose this study without claiming to catch the core features of these observables thanks to our hybrid-factorization framework, but rather to set the stage for futures analyses aimed at shedding light on the formal and phenomenological

³This strictly holds for $B_c \equiv B_c(^1S_0)$ mesons, while statistics for $B_c(^3S_1)$ ones a bit larger. We stress, however, that being the $B_c(^3S_1)$ particle a resonance of the $B_c(^1S_0)$ state, a more accurate description of its dynamical production mechanism might go beyond our treatment. Indeed, it could rely upon more intricate effects, such as spin correlations as well as higher-order, relativistic corrections within the same NRQCD formalism.

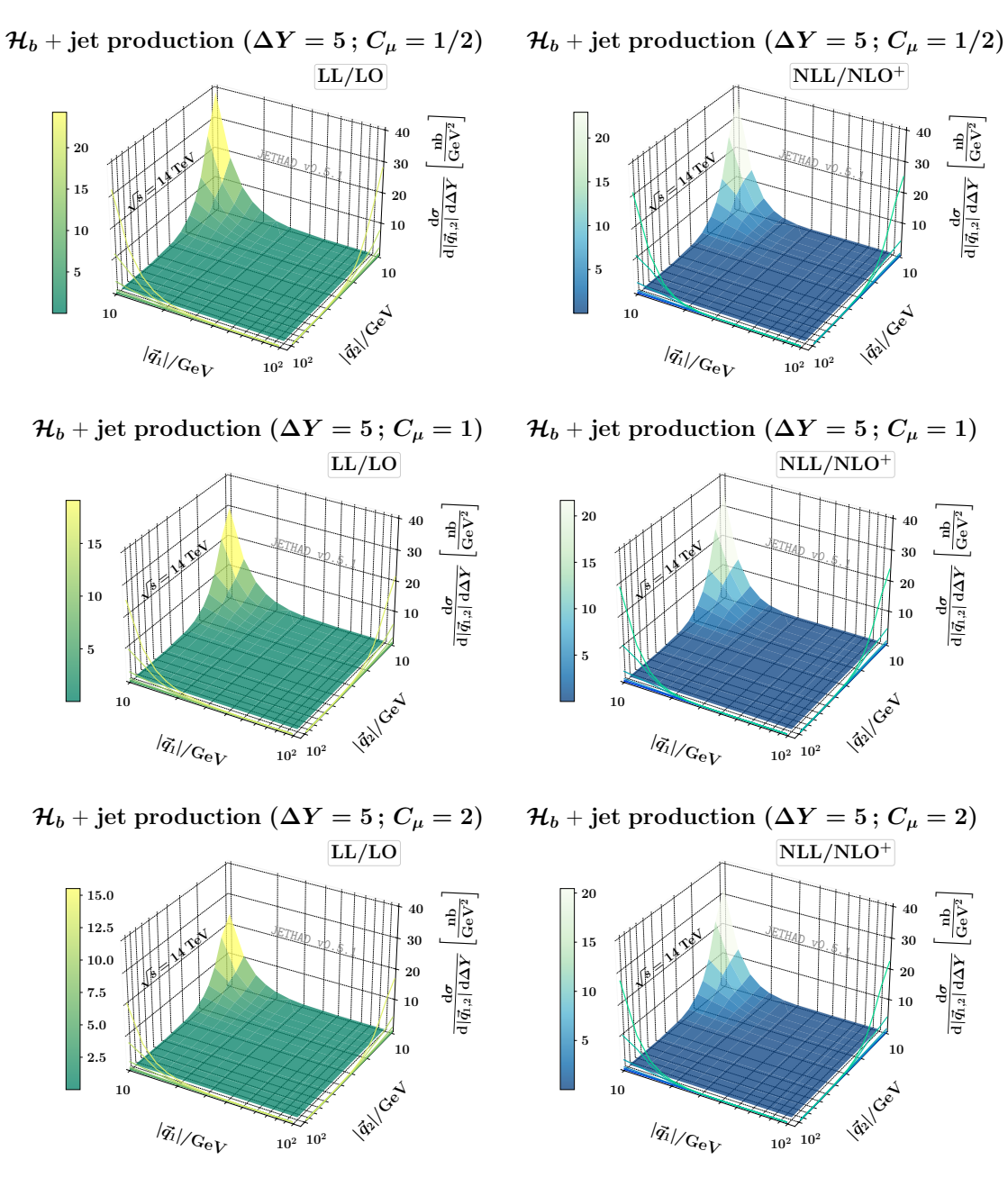


Figure 5: Doubly-differential transverse-momentum distribution for the \mathcal{H}_b -plus-jet production at $\Delta Y=5$, $\sqrt{s}=14$ TeV, and within the LL/LO (left) and NLL/NLO⁺ (right) accuracy. The C_μ scale parameter goes from 1/2 (top) to 2 (bottom).

connection among distinct resummation mechanisms. Figures presented here are for doubly differential transverse-momentum distributions at $\Delta Y = 5$. For the sake of simplicity, we present the hadron-plus-jet channel only (right diagram of Fig. 1). Predictions for singly bottomed hadrons, $B_c(^1S_0)$ mesons, and their $B_c(^3S_1)$ resonances are shown in surface 3D plots of Figs. 5, 6, and 7, respectively.

The common trend is a sharp falloff pattern when the two transverse momenta, $|\vec{q}_1|$ and $|\vec{q}_2|$, increase or when their mutual distance grows. LL/LO cross sections (left plots) are much more sensitive to MHOU studies done through energy-scale variations than NLL/NLO⁺ ones. They generally lower with C_μ (from upper to lower plots). NLL/NLO⁺

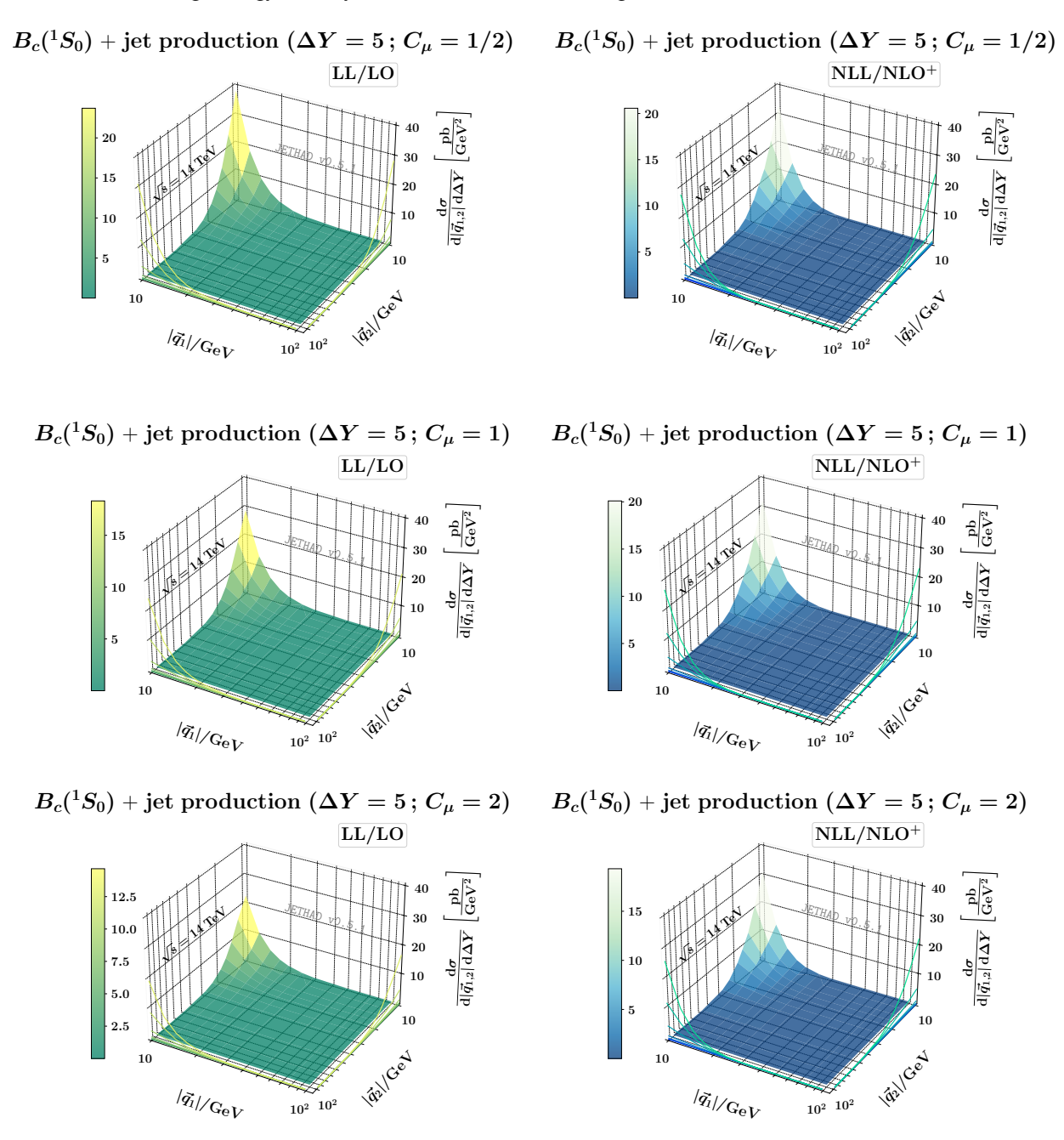


Figure 6: Doubly-differential transverse-momentum distribution for the $B_c(^1S_0)$ -plus-jet production at $\Delta Y = 5$, $\sqrt{s} = 14$ TeV, and within the LL/LO (left) and NLL/NLO⁺ (right) accuracy. The C_μ scale parameter goes from 1/2 (top) to 2 (bottom).

distributions (right panels) instead generally oscillate around $C_{\mu}=1$, which turns out to work as a critical point. This is a clear signal that our NLL/NLO⁺ doubly-differential cross sections are quite stable under MHOU analyses. Notably, no distribution comes with a peak, which might however be present in the low-TM range (excluded from our study), where TM-resummation effects would dominate. The information contained in the core of our 3D figures is supplemented by 2D slice projections highlighting the behavior of our observables at $|\vec{q}_1|=0$ and at $|\vec{q}_2|=0$. What emerges from the inspection of these 2D contour plots at low or intermediate transverse momentum is a smaller

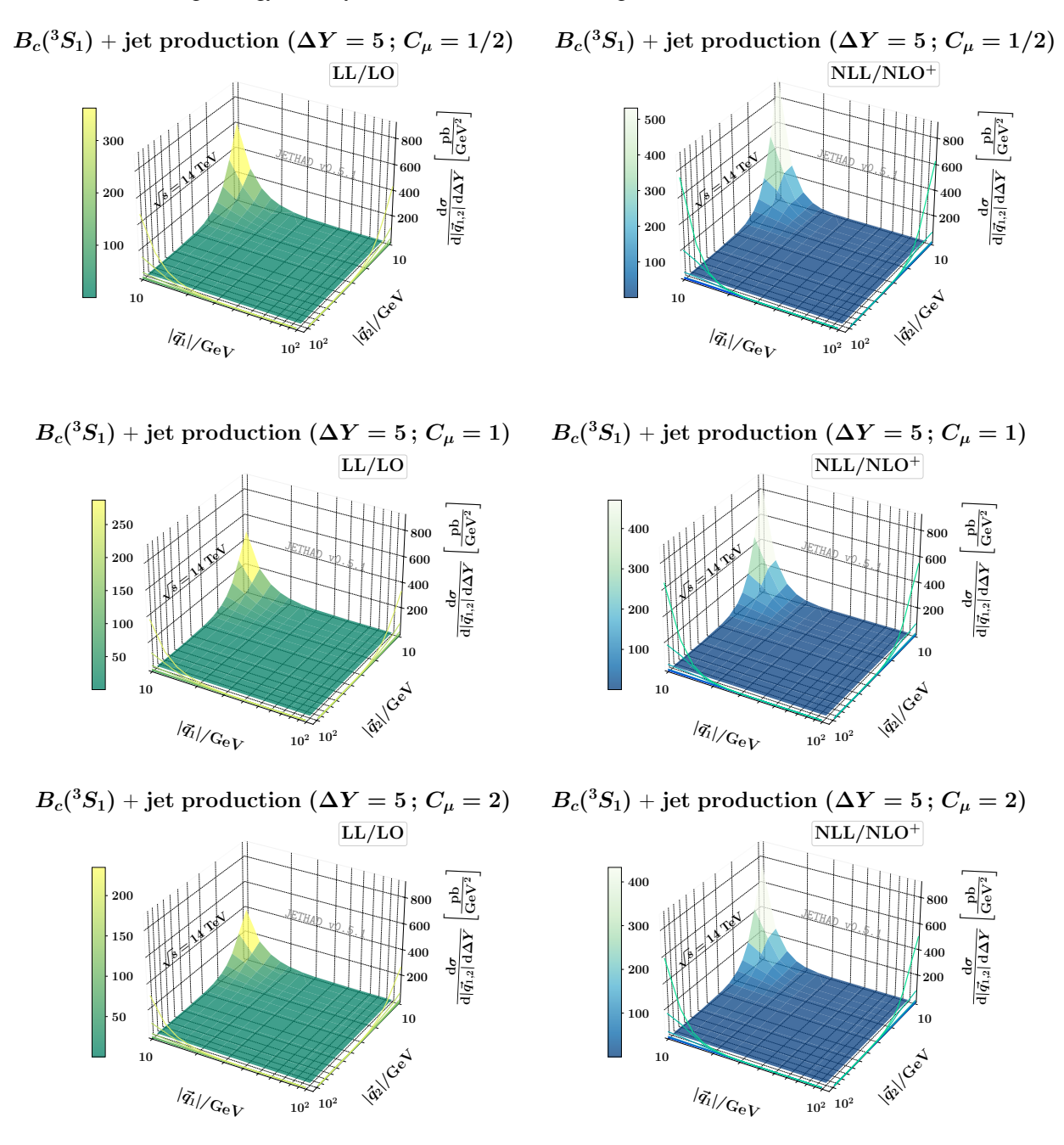


Figure 7: Doubly-differential transverse-momentum distribution for the $B_c(^1S_0)$ -plus-jet production at $\Delta Y = 5$, $\sqrt{s} = 14$ TeV, and within the LL/LO (left) and NLL/NLO⁺ (right) accuracy. The C_μ scale parameter goes from 1/2 (top) to 2 (bottom).

statistics in the $|\vec{q}_1| > |\vec{q}_2|$ range than in the opposite case. This happens because cross sections are globally smaller when a bottomed hadron is produced rather than a light-flavored jet [84, 165].

Finally, numeric checks on our transverse-momentum distributions have shown a noncharmed versus charmed B-meson production-rate hierarchy analogous to the one found in the case of rapidity-interval distributions (see

Section 3.3). B_c production rates are almost always three orders of magnitude smaller than \mathcal{H}_b ones, whereas rates of the B_c^* resonance range from 10^{-2} to 1/60 times the ones of \mathcal{H}_b hadrons.

4. Summary and Outlooks

We considered the semi-inclusive production of a forward noncharmed or charmed *b*-hadron in association with a backward noncharmed *b*-hadron or a jet in high-energy regimes that can be accessed at current LHC analyses and its forthcoming Hi-Lumi upgrade. We depicted the production of bottom-flavored hadrons by means of a VFNS collinear-fragmentation approach, whose validity is justified by the large transverse-momentum regime matter of our analysis.

Singly heavy-flavored particles, namely inclusive states consisting of B mesons and Λ_b baryons, were described via the KKSS07 [56, 58] NLO FFs based on a fit to global data and assuming a three-parameter power-like initial-scale parametrization for b and \bar{b} fragmentation channels [225]. As for charmed B mesons, i.e. $B_c \equiv B_c(^1S_0)$ states and $B_c^* \equiv B_c(^3S_1)$ resonances, we adopted a more sophisticated strategy. First, we modeled the initial-scale input for the fragmentation of heavy quarks (charm, bottom, and their antiparticles) and gluons to observed hadrons by means of corresponding NLO calculations within the NRQCD effective theory [226, 227]. Then, we plugged these inputs into the APFEL(++) DGLAP evolution code [231–233] to generate phenomenology-ready VFNS FF grids in LHAPDF format [222], which we named ZCFW22 NLO functions [84]. These novel FF sets will play a role in future phenomenological applications lying outside the semi-hard regime. They also will serve as a support basis to shed light on the intersection corner between the collinear factorization and the NRQCD formalism.

By relying upon a traditional as well as an extended MHOU scan on our hybrid-factorization setup, we hunted for clues of stabilization of the high-energy resummation under next-to-leading logarithmic corrections. We provided strong evidence that these effects are present and they allow for a fair description of high-energy distributions, differential in the rapidity interval and in the final-state transverse momenta. As a bonus, we highlighted that the predicted production-rate hierarchy between noncharmed b-hadrons and charmed $B_c(^1S_0)$ mesons is in line with recent LHCb estimates. In particular, the production rate of B_c states is three orders of magnitude lower than the \mathcal{H}_b one. This served as a simultaneous benchmark for both the hybrid factorization and the NRQCD fragmentation applied to charmed B mesons at our reference transverse masses (see Section 3.2).

Our analysis on bottom-flavor collinear fragmentation stands as a step forward in the study of heavy-flavored emissions within the NLL/NLO⁽⁺⁾ accuracy, originally started from the analytic calculation of singly off-shell emission functions depicting the production of heavy-quark pairs in the moderate-to-low transverse-momentum regime [136, 138, 163]. It also represents a fair contact point with phenomenology of bottom-flavor production in the high-energy sector. The extension of this study to wider kinematic ranges, like the ones typical of new-generation colliding machines [335–354], as well as possible contact points with heavy-flavor fragmentation studies in the TMD formalism [355–361], is underway.

As a prospect, we plan to investigate bottom-flavor emissions in the moderate transverse-momentum sector, namely at the intersection line between the VFNS and the FFNS scheme, and possibly set the stage for a matching between the two descriptions. Here, high-energy tags of charmed *B* mesons will bring novelty to the plan. In that case, indeed, the VFNS versus FFNS dichotomy translates into a short-distance versus fragmentation dichotomy. This calls for a further enhancement of our ZCFW22-based treatment, which currently relies upon NRQCD-modeled calculations for initial-scale inputs, but will serve in the medium-term future as a "launch pad" for extractions through fits to new data to be collected at the Hi-Lumi LHC. In this respect, neural-network strategies already employed to extract collinear FFs for lighter hadron species will be an asset [238, 239, 362–365]. As mentioned in Section 2.4, a proper determination of FF uncertainties with possible inclusion of MHOU effects, not yet encoded in our ZCFW22 sets, is needed. It might take inspiration from the MCscales approach [366] (for close-in-spirit studies on proton and pion PDFs, see Refs. [367–370] and Ref. [371]).

The fair stability exhibited by our NLL/NLO⁺ distributions motivates our interest in proposing the hybrid factorization as useful tool to enhance and extend the standard collinear description. To reach the precision level, our NLL/NLO⁺ hybrid approach needs to evolve into a *multi-lateral* formalism where different resummation mechanisms are at work. As a first steps, links with the soft-gluon [279, 280, 372, 373] and the jet-radius [374–378]⁴ resummations

⁴In Ref. [161] it was shown that high-energy angular multiplicities become more and more sensitive to jet-radius variations as the final-state azimuthal-angle distance grows.

should be found. Possible common grounds with studies on jet angularities [379–381] also represent an intriguing perspective.

Then, the resummation of energy logarithms from BFKL could improve the description of DGLAP-evolved bottom-flavor FFs, its effect becoming sizable already at moderate values of final-state hadron longitudinal fraction [382]. Another engaging development would be exploring the validity of the use of a ZM-VFNS with higher HFMPs in the context of heavy-meson fragmentation [21]. Finally, the striking evidence of intrinsic charm quarks in the proton [383], now corroborated by quite recent studies on its valence distribution [384], traces the path towards searches for imprints of the possible existence of an intrinsic bottom component. In this respect, any progress in widening the horizons of our knowledge of bottom physics is needed. We believe that studies aimed at shedding light on the bottom-flavor collinear fragmentation go along these directions.

Acknowledgements

The author would like to express his gratitude to colleagues of the **Heavy Flavours at High pT Workshop 2023** (Higgs Centre for Theoretical Physics, University of Edinburgh) and the **Milan Christmas Meeting 2023** (University of Milan) for the welcoming atmosphere and for insightful discussions. The author is grateful to Alessandro Papa for a critical reading of the manuscript, useful suggestions, and encouragement. This work is supported by the Atracción de Talento Grant n. 2022-T1/TIC-24176 of the Comunidad Autónoma de Madrid, Spain.

Appendix A: NLO b-hadron emission function

In this Appendix we provide the expression of the NLO correction for the emission function of a forward *b*-hadron tagged at large transverse momentum (see Ref. [126] for technical details). We write

$$\hat{\mathcal{E}}_{B}(n,v,|\vec{q}_{B}|,x_{B}) = \frac{1}{\pi} \sqrt{\frac{C_{F}}{C_{A}}} \left(|\vec{q}_{B}|^{2} \right)^{iv-\frac{1}{2}} \int_{x_{B}}^{1} \frac{\mathrm{d}x}{x} \int_{\frac{x_{B}}{x}}^{1} \frac{\mathrm{d}\tau}{\tau} \left(\frac{x\tau}{x_{B}} \right)^{2iv-1} \\
\times \left[\frac{C_{A}}{C_{F}} f_{g}(x) D_{g}^{B} \left(\frac{x_{B}}{x\tau} \right) C_{gg}(x,\tau) + \sum_{i=q\bar{q}} f_{i}(x) D_{i}^{B} \left(\frac{x_{B}}{x\tau} \right) C_{qq}(x,\tau) \right. \\
\times \left. D_{g}^{B} \left(\frac{x_{B}}{x\tau} \right) \sum_{i=\bar{q}} f_{i}(x) C_{qg}(x,\tau) + \frac{C_{A}}{C_{F}} f_{g}(x) \sum_{i=\bar{q}} D_{i}^{B} \left(\frac{x_{B}}{x\tau} \right) C_{gq}(x,\tau) \right] , \tag{23}$$

with

$$C_{gg}(x,\tau) = P_{gg}(\tau) \left(1 + \tau^{-2\gamma}\right) \ln\left(\frac{|\vec{q}_{B}|^{2} x^{2} \tau^{2}}{\mu_{F}^{2} x_{B}^{2}}\right) - \frac{\beta_{0}}{2} \ln\left(\frac{|\vec{q}_{B}|^{2} x^{2} \tau^{2}}{\mu_{R}^{2} x_{B}^{2}}\right) + \delta(1 - \tau) \left[C_{A} \ln\left(\frac{s_{0} x^{2}}{|\vec{q}_{B}|^{2} x_{B}^{2}}\right) \chi(n,\gamma) - C_{A} \left(\frac{67}{18} - \frac{\pi^{2}}{2}\right) + \frac{5}{9} n_{f} + \frac{C_{A}}{2} \left(\psi'\left(1 + \gamma + \frac{n}{2}\right) - \psi'\left(\frac{n}{2} - \gamma\right) - \chi^{2}(n,\gamma)\right)\right] + C_{A} \left(\frac{1}{\tau} + \frac{1}{(1 - \tau)_{+}} - 2 + \tau \bar{\tau}\right) \times \left(\chi(n,\gamma)(1 + \tau^{-2\gamma}) - 2(1 + 2\tau^{-2\gamma}) \ln \tau + \frac{\bar{\tau}^{2}}{\tau^{2}} I_{2}\right) + 2 C_{A} (1 + \tau^{-2\gamma}) \left(\left(\frac{1}{\tau} - 2 + \tau \bar{\tau}\right) \ln \bar{\tau} + \left(\frac{\ln(1 - \tau)}{1 - \tau}\right)_{+}\right),$$

$$C_{gq}(x,\tau) = P_{qg}(\tau) \left(\frac{C_F}{C_A} + \tau^{-2\gamma} \right) \ln \left(\frac{|\vec{q}_B|^2 x^2 \tau^2}{\mu_F^2 x_B^2} \right)$$
 (25)

$$+ 2\,\tau\bar{\tau}\,T_R\,\left(\frac{C_F}{C_A} + \tau^{-2\gamma}\right) +\,P_{qg}(\tau)\,\left(\frac{C_F}{C_A}\,\chi(n,\gamma) + 2\tau^{-2\gamma}\,\ln\frac{\bar{\tau}}{\tau} + \frac{\bar{\tau}}{\tau}\mathcal{I}_3\right)\,,$$

$$C_{qg}\left(x,\tau\right) = P_{gq}(\tau) \left(\frac{C_A}{C_F} + \tau^{-2\gamma}\right) \ln\left(\frac{|\vec{q}_B|^2 x^2 \tau^2}{\mu_F^2 x_B^2}\right) \tag{26}$$

$$+\tau\left(C_F\tau^{-2\gamma}+C_A\right)+\,\frac{1+\bar\tau^2}{\tau}\left[C_F\tau^{-2\gamma}(\chi(n,\gamma)-2\ln\tau)+2C_A\ln\frac{\bar\tau}{\tau}+\frac{\bar\tau}{\tau}\mathcal{I}_1\right]\,,$$

and

$$C_{qq}(x,\tau) = P_{qq}(\tau) \left(1 + \tau^{-2\gamma} \right) \ln \left(\frac{|\vec{q}_{B}|^{2} x^{2} \tau^{2}}{\mu_{F}^{2} x_{B}^{2}} \right) - \frac{\beta_{0}}{2} \ln \left(\frac{|\vec{q}_{B}|^{2} x^{2} \tau^{2}}{\mu_{F}^{2} x_{B}^{2}} \right)$$

$$+ \delta(1 - \tau) \left[C_{A} \ln \left(\frac{s_{0} x_{B}^{2}}{|\vec{q}_{B}|^{2} x^{2}} \right) \chi(n,\gamma) + C_{A} \left(\frac{85}{18} + \frac{\pi^{2}}{2} \right) - \frac{5}{9} n_{f} - 8 C_{F} \right]$$

$$+ \frac{C_{A}}{2} \left(\psi' \left(1 + \gamma + \frac{n}{2} \right) - \psi' \left(\frac{n}{2} - \gamma \right) - \chi^{2}(n,\gamma) \right) + C_{F} \bar{\tau} \left(1 + \tau^{-2\gamma} \right)$$

$$+ \left(1 + \tau^{2} \right) \left[C_{A} (1 + \tau^{-2\gamma}) \frac{\chi(n,\gamma)}{2(1 - \tau)_{+}} + \left(C_{A} - 2 C_{F} (1 + \tau^{-2\gamma}) \right) \frac{\ln \tau}{1 - \tau} \right]$$

$$+ \left(C_{F} - \frac{C_{A}}{2} \right) \left(1 + \tau^{2} \right) \left[2(1 + \tau^{-2\gamma}) \left(\frac{\ln(1 - \tau)}{1 - \tau} \right) + \frac{\bar{\tau}}{\tau^{2}} \mathcal{I}_{2} \right] ,$$

In our expressions s_0 is an energy scale that genuinely appears within the BFKL approach. We fix $s_0 \equiv \mu_C$. Then we define $\bar{\tau} = 1 - \tau$ and $\gamma = i\nu - \frac{1}{2}$. The LO DGLAP $P_{ij}(\tau)$ splitting functions are

$$P_{gq}(y) = C_F \frac{1 + (1 - y)^2}{y},$$

$$P_{qg}(y) = T_R \left[y^2 + (1 - y)^2 \right],$$

$$P_{qq}(y) = C_F \left(\frac{1 + y^2}{1 - y} \right)_+ = C_F \left[\frac{1 + y^2}{(1 - y)_+} + \frac{3}{2} \delta(1 - y) \right],$$

$$P_{gg}(y) = 2C_A \left[\frac{1}{(1 - y)_+} + \frac{1}{y} - 2 + y(1 - y) \right] + \left(\frac{11}{6} C_A - \frac{n_f}{3} \right) \delta(1 - y).$$
(28)

The $\mathcal{I}_{2,1,3}$ functions read

$$\mathcal{I}_{2} = \frac{\tau^{2}}{\bar{\tau}^{2}} \left[\tau \left(\frac{2F_{1}(1, 1 + \gamma - \frac{n}{2}, 2 + \gamma - \frac{n}{2}, \tau)}{\frac{n}{2} - \gamma - 1} - \frac{2F_{1}(1, 1 + \gamma + \frac{n}{2}, 2 + \gamma + \frac{n}{2}, \tau)}{\frac{n}{2} + \gamma + 1} \right) + \tau^{-2\gamma} \left(\frac{2F_{1}(1, -\gamma - \frac{n}{2}, 1 - \gamma - \frac{n}{2}, \tau)}{\frac{n}{2} + \gamma} - \frac{2F_{1}(1, -\gamma + \frac{n}{2}, 1 - \gamma + \frac{n}{2}, \tau)}{\frac{n}{2} - \gamma} \right) + (1 + \tau^{-2\gamma}) \left(\chi(n, \gamma) - 2\ln\bar{\tau} \right) + 2\ln\tau \right] ,$$
(29)

$$I_{1} = \frac{\bar{\tau}}{2\tau} I_{2} + \frac{\tau}{\bar{\tau}} \left[\ln \tau + \frac{1 - \tau^{-2\gamma}}{2} \left(\chi(n, \gamma) - 2 \ln \bar{\tau} \right) \right] , \tag{30}$$

and

$$I_{3} = \frac{\bar{\tau}}{2\tau} I_{2} - \frac{\tau}{\bar{\tau}} \left[\ln \tau + \frac{1 - \tau^{-2\gamma}}{2} \left(\chi(n, \gamma) - 2 \ln \bar{\tau} \right) \right] , \qquad (31)$$

with $_2F_1$ being the standard hypergeometric function.

The plus prescription entering Eqs. (24) and (27) comes out as

$$\int_{a}^{1} dx \frac{f(x)}{(1-x)_{+}} = \int_{a}^{1} dx \frac{f(x) - f(1)}{(1-x)} - \int_{0}^{a} dx \frac{f(1)}{(1-x)},$$
(32)

where f(x) is a test function regularly behaved when y approaches one.

Appendix B: NLO light-jet emission function

We present here the NLO correction to the emission function for a forward light-flavored jet emission in the small-cone selection (see Refs. [129, 213] for technical details)

$$\hat{\mathcal{E}}_{J}(n, \nu, |\vec{q}_{J}|, x_{J}) = \frac{1}{\pi} \sqrt{\frac{C_{F}}{C_{A}}} \left(|\vec{q}_{J}|^{2} \right)^{l\nu-1/2} \int_{x_{J}}^{1} \frac{d\tau}{\tau} \tau^{-\bar{q}_{z}(\mu_{R})\chi(n,\nu)}$$

$$\times \left\{ \sum_{J=q,\bar{q}} f_{J} \left(\frac{x_{J}}{\tau} \right) \left[\left(P_{qq}(\tau) + \frac{C_{A}}{C_{F}} P_{gq}(\tau) \right) \ln \frac{|\vec{q}_{J}|^{2}}{\mu_{F}^{2}} \right. \right.$$

$$\left. - 2\tau^{-2\gamma} \ln \frac{r}{\max(\tau, \bar{\tau})} \left\{ P_{qq}(\tau) + P_{gq}(\tau) \right\} - \frac{\beta_{0}}{2} \ln \frac{|\vec{q}_{J}|^{2}}{\mu_{R}^{2}} \delta(1 - \tau) \right.$$

$$\left. + C_{A}\delta(1 - \tau) \left[\chi(n, \gamma) \ln \frac{s_{0}}{|\vec{q}_{J}|^{2}} + \frac{85}{18} \right.$$

$$\left. + \frac{\pi^{2}}{2} + \frac{1}{2} \left(\psi' \left(1 + \gamma + \frac{n}{2} \right) - \psi' \left(\frac{n}{2} - \gamma \right) - \chi^{2}(n, \gamma) \right) \right] \right.$$

$$\left. + (1 + \tau^{2}) \left\{ C_{A} \left[\frac{(1 + \tau^{-2\gamma}) \chi(n, \gamma)}{2(1 - \tau)_{+}} - \tau^{-2\gamma} \left(\frac{\ln(1 - \tau)}{1 - \tau} \right)_{+} \right] \right.$$

$$\left. + \left. \left(C_{F} - \frac{C_{A}}{2} \right) \left[\frac{\bar{\tau}}{\tau^{2}} \mathcal{I}_{2} - \frac{2 \ln \tau}{1 - \tau} + 2 \left(\frac{\ln(1 - \tau)}{1 - \tau} \right)_{+} \right] \right\} \right.$$

$$\left. + \delta(1 - \tau) \left(C_{F} \left(3 \ln 2 - \frac{\pi^{2}}{3} - \frac{9}{2} \right) - \frac{5n_{f}}{9} \right) + C_{A}\tau + C_{F}\bar{\tau} \right.$$

$$\left. + \frac{1 + \bar{\tau}^{2}}{\tau} \left(C_{A} \frac{\bar{\tau}}{\tau} \mathcal{I}_{1} + 2C_{A} \ln \frac{\bar{\tau}}{\tau} + C_{F}\tau^{-2\gamma} (\chi(n, \gamma) - 2 \ln \bar{\tau}) \right) \right] \right.$$

$$\left. + f_{g} \left(\frac{x_{J}}{\tau} \right) \frac{C_{A}}{C_{F}} \left[\left(P_{gg}(\tau) + 2n_{f} \frac{C_{F}}{C_{A}} P_{qg}(\tau) \right) \ln \frac{|\vec{q}_{J}|^{2}}{\mu_{F}^{2}} \right.$$

$$\left. - 2\tau^{-2\gamma} \ln \frac{r}{\max(\tau, \bar{\tau})} \left(P_{gg}(\tau) + 2n_{f} P_{qg}(\tau) \right) - \frac{\beta_{0}}{2} \ln \frac{|\vec{q}_{J}|^{2}}{4\mu^{2}^{2}} \delta(1 - \tau) \right.$$

$$\begin{split} & + C_{A}\delta(1-\tau) \left(\chi(n,\gamma) \ln \frac{s_{0}}{|\vec{q}_{\mathcal{J}}|^{2}} + \frac{1}{12} + \frac{\pi^{2}}{6} \right. \\ & + \frac{1}{2} \left[\psi' \left(1 + \gamma + \frac{n}{2} \right) - \psi' \left(\frac{n}{2} - \gamma \right) - \chi^{2}(n,\gamma) \right] \right) \\ & + 2C_{A}(1-\tau^{-2\gamma}) \left(\left(\frac{1}{\tau} - 2 + \tau \bar{\tau} \right) \ln \bar{\tau} + \frac{\ln(1-\tau)}{1-\tau} \right) \\ & + C_{A} \left[\frac{1}{\tau} + \frac{1}{(1-\tau)_{+}} - 2 + \tau \bar{\tau} \right] \left((1+\tau^{-2\gamma})\chi(n,\gamma) - 2 \ln \tau + \frac{\bar{\tau}^{2}}{\tau^{2}} \mathcal{I}_{2} \right) \\ & + n_{f} \left[2\tau \bar{\tau} \frac{C_{F}}{C_{A}} + (\tau^{2} + \bar{\tau}^{2}) \left(\frac{C_{F}}{C_{A}} \chi(n,\gamma) + \frac{\bar{\tau}}{\tau} \mathcal{I}_{3} \right) - \frac{1}{12} \delta(1-\tau) \right] \right] \right\} \; , \end{split}$$

with r being the radius of the jet cone.

References

- [1] P. Nason, S. Dawson, R. K. Ellis, The Total Cross-Section for the Production of Heavy Quarks in Hadronic Collisions, Nucl. Phys. B 303 (1988) 607-633. doi:10.1016/0550-3213(88)90422-1.
- [2] P. Nason, S. Dawson, R. K. Ellis, The One Particle Inclusive Differential Cross-Section for Heavy Quark Production in Hadronic Collisions, Nucl. Phys. B 327 (1989) 49–92, [Erratum: Nucl.Phys.B 335, 260–260 (1990)]. doi:10.1016/0550-3213(89)90286-1.
- [3] W. Beenakker, H. Kuijf, W. L. van Neerven, J. Smith, QCD Corrections to Heavy Quark Production in p anti-p Collisions, Phys. Rev. D 40 (1989) 54–82. doi:10.1103/PhysRevD.40.54.
- [4] S. Frixione, M. L. Mangano, P. Nason, G. Ridolfi, Charm and bottom production: Theoretical results versus experimental data, Nucl. Phys. B 431 (1994) 453–483. doi:10.1016/0550-3213(94)90213-5.
- [5] S. Catani, S. Devoto, M. Grazzini, S. Kallweit, J. Mazzitelli, Bottom-quark production at hadron colliders: fully differential predictions in NNLO QCD, JHEP 03 (2021) 029. arXiv:2010.11906, doi:10.1007/JHEP03(2021)029.
- [6] J. Mazzitelli, A. Ratti, M. Wiesemann, G. Zanderighi, B-hadron production at the LHC from bottom-quark pair production at NNLO+PS, Phys. Lett. B 843 (2023) 137991. arXiv:2302.01645, doi:10.1016/j.physletb.2023.137991.
- [7] S. Alekhin, J. Blumlein, S. Klein, S. Moch, The 3, 4, and 5-flavor NNLO Parton from Deep-Inelastic-Scattering Data and at Hadron Colliders, Phys. Rev. D 81 (2010) 014032. arXiv:0908.2766, doi:10.1103/PhysRevD.81.014032.
- [8] B. Mele, P. Nason, The Fragmentation function for heavy quarks in QCD, Nucl. Phys. B 361 (1991) 626–644, [Erratum: Nucl.Phys.B 921, 841–842 (2017)]. doi:10.1016/0550-3213(91)90597-Q.
- [9] M. Cacciari, M. Greco, Large p_T hadroproduction of heavy quarks, Nucl. Phys. B 421 (1994) 530-544. arXiv:hep-ph/9311260, doi:10.1016/0550-3213(94)90515-0.
- [10] M. Buza, Y. Matiounine, J. Smith, W. L. van Neerven, Charm electroproduction viewed in the variable flavor number scheme versus fixed order perturbation theory, Eur. Phys. J. C 1 (1998) 301–320. arXiv:hep-ph/9612398, doi:10.1007/BF01245820.
- [11] J. Binnewies, B. A. Kniehl, G. Kramer, Predictions for D*+- photoproduction at HERA with new fragmentation functions from LEP-1, Phys. Rev. D 58 (1998) 014014. arXiv:hep-ph/9712482, doi:10.1103/PhysRevD.58.014014.
- [12] I. Bierenbaum, J. Blumlein, S. Klein, Mellin Moments of the O(alpha**3(s)) Heavy Flavor Contributions to unpolarized Deep-Inelastic Scattering at Q**2 >> m**2 and Anomalous Dimensions, Nucl. Phys. B 820 (2009) 417-482. arXiv:0904.3563, doi:10.1016/j.nuclphysb.2009.06.005.
- [13] I. Helenius, H. Paukkunen, B-meson hadroproduction in the SACOT- m_T scheme, JHEP 07 (2023) 054. arXiv:2303.17864, doi: 10.1007/JHEP07 (2023) 054.
- [14] A. Ghira, S. Marzani, G. Ridolfi, A consistent resummation of mass and soft logarithms in processes with heavy flavours, JHEP 11 (2023) 120. arXiv:2309.06139, doi:10.1007/JHEP11(2023)120.
- [15] M. Krämer, F. I. Olness, D. E. Soper, Treatment of heavy quarks in deeply inelastic scattering, Phys. Rev. D 62 (2000) 096007. arXiv: hep-ph/0003035, doi:10.1103/PhysRevD.62.096007.
- [16] S. Forte, E. Laenen, P. Nason, J. Rojo, Heavy quarks in deep-inelastic scattering, Nucl. Phys. B 834 (2010) 116–162. arXiv:1001.2312, doi:10.1016/j.nuclphysb.2010.03.014.
- [17] J. Blümlein, A. De Freitas, C. Schneider, K. Schönwald, The Variable Flavor Number Scheme at Next-to-Leading Order, Phys. Lett. B 782 (2018) 362–366. arXiv:1804.03129, doi:10.1016/j.physletb.2018.05.054.
- [18] M. A. G. Aivazis, J. C. Collins, F. I. Olness, W.-K. Tung, Leptoproduction of heavy quarks. 2. A Unified QCD formulation of charged and neutral current processes from fixed target to collider energies, Phys. Rev. D 50 (1994) 3102–3118. arXiv:hep-ph/9312319, doi:10.1103/PhysRevD.50.3102.
- [19] R. S. Thorne, R. G. Roberts, An Ordered analysis of heavy flavor production in deep inelastic scattering, Phys. Rev. D 57 (1998) 6871–6898. arXiv:hep-ph/9709442, doi:10.1103/PhysRevD.57.6871.
- [20] J. Gao, L. Harland-Lang, J. Rojo, The Structure of the Proton in the LHC Precision Era, Phys. Rept. 742 (2018) 1-121. arXiv:1709.04922, doi:10.1016/j.physrep.2018.03.002.
- [21] V. Bertone, A. Glazov, A. Mitov, A. Papanastasiou, M. Ubiali, Heavy-flavor parton distributions without heavy-flavor matching prescriptions, JHEP 04 (2018) 046. arXiv:1711.03355, doi:10.1007/JHEP04(2018) 046.

- [22] M. L. Czakon, T. Generet, A. Mitov, R. Poncelet, B-hadron production in NNLO QCD: application to LHC tr events with leptonic decays, JHEP 10 (2021) 216. arXiv:2102.08267, doi:10.1007/JHEP10(2021)216.
- [23] M. Czakon, T. Generet, A. Mitov, R. Poncelet, NNLO B-fragmentation fits and their application to $t\bar{t}$ production and decay at the LHC, JHEP 03 (2023) 251. arXiv:2210.06078, doi:10.1007/JHEP03(2023)251.
- [24] L. Buonocore, P. Nason, F. Tramontano, Heavy quark radiation in NLO+PS POWHEG generators, Eur. Phys. J. C 78 (2) (2018) 151. arXiv:1711.06281, doi:10.1140/epjc/s10052-018-5638-y.
- [25] F. Maltoni, G. Ridolfi, M. Ubiali, b-initiated processes at the LHC: a reappraisal, JHEP 07 (2012) 022, [Erratum: JHEP 04, 095 (2013)]. arXiv:1203.6393, doi:10.1007/JHEP04(2013)095.
- [26] E. Bagnaschi, F. Maltoni, A. Vicini, M. Zaro, Lepton-pair production in association with a bb pair and the determination of the W boson mass, JHEP 07 (2018) 101. arXiv:1803.04336, doi:10.1007/JHEP07 (2018) 101.
- [27] M. Lim, F. Maltoni, G. Ridolfi, M. Ubiali, Anatomy of double heavy-quark initiated processes, JHEP 09 (2016) 132. arXiv:1605.09411, doi:10.1007/JHEP09 (2016) 132.
- [28] R. Gauld, A. Gehrmann-De Ridder, E. W. N. Glover, A. Huss, I. Majer, Associated production of a Higgs boson decaying into bottom quarks and a weak vector boson decaying leptonically at NNLO in QCD, JHEP 10 (2019) 002. arXiv:1907.05836, doi:10.1007/JHEP10(2019) 002.
- [29] L. Barze, G. Montagna, P. Nason, O. Nicrosini, F. Piccinini, Implementation of electroweak corrections in the POWHEG BOX: single W production, JHEP 04 (2012) 037. arXiv:1202.0465, doi:10.1007/JHEP04(2012)037.
- [30] M. Cacciari, M. Greco, P. Nason, The p_T spectrum in heavy-flavour hadroproduction., JHEP 05 (1998) 007. arXiv:hep-ph/9803400, doi:10.1088/1126-6708/1998/05/007.
- [31] M. Cacciari, S. Frixione, N. Houdeau, M. L. Mangano, P. Nason, G. Ridolfi, Theoretical predictions for charm and bottom production at the LHC, JHEP 10 (2012) 137. arXiv:1205.6344, doi:10.1007/JHEP10(2012)137.
- [32] S. Forte, D. Napoletano, M. Ubiali, Higgs production in bottom-quark fusion in a matched scheme, Phys. Lett. B 751 (2015) 331–337. arXiv:1508.01529, doi:10.1016/j.physletb.2015.10.051.
- [33] S. Forte, D. Napoletano, M. Ubiali, Higgs production in bottom-quark fusion: matching beyond leading order, Phys. Lett. B 763 (2016) 190-196. arXiv:1607.00389, doi:10.1016/j.physletb.2016.10.040.
- [34] S. Forte, D. Napoletano, M. Ubiali, Z boson production in bottom-quark fusion: a study of b-mass effects beyond leading order, Eur. Phys. J. C 78 (11) (2018) 932. arXiv:1803.10248, doi:10.1140/epjc/s10052-018-6414-8.
- [35] R. Frederix, S. Frixione, V. Hirschi, F. Maltoni, R. Pittau, P. Torrielli, W and Z/γ * boson production in association with a bottom-antibottom pair, JHEP 09 (2011) 061. arXiv:1106.6019, doi:10.1007/JHEP09 (2011) 061.
- [36] M. Wiesemann, R. Frederix, S. Frixione, V. Hirschi, F. Maltoni, P. Torrielli, Higgs production in association with bottom quarks, JHEP 02 (2015) 132. arXiv:1409.5301, doi:10.1007/JHEP02(2015)132.
- [37] M. Bonvini, A. S. Papanastasiou, F. J. Tackmann, Resummation and matching of b-quark mass effects in $b\bar{b}H$ production, JHEP 11 (2015) 196. arXiv:1508.03288, doi:10.1007/JHEP11(2015)196.
- [38] M. Bonvini, A. S. Papanastasiou, F. J. Tackmann, Matched predictions for the $b\bar{b}H$ cross section at the 13 TeV LHC, JHEP 10 (2016) 053. arXiv:1605.01733, doi:10.1007/JHEP10 (2016) 053.
- [39] G. Ridolfi, M. Ubiali, M. Zaro, A fragmentation-based study of heavy quark production, JHEP 01 (2020) 196. arXiv:1911.01975, doi:10.1007/JHEP01(2020)196.
- [40] F. Maltoni, G. Ridolfi, M. Ubiali, M. Zaro, Resummation effects in the bottom-quark fragmentation function, JHEP 10 (2022) 027. arXiv:2207.10038, doi:10.1007/JHEP10(2022)027.
- [41] D. Gaggero, A. Ghira, S. Marzani, G. Ridolfi, Soft logarithms in processes with heavy quarks, JHEP 09 (2022) 058. arXiv:2207.13567, doi:10.1007/JHEP09(2022)058.
- [42] L. Bonino, M. Cacciari, G. Stagnitto, Heavy Flavoured Meson Fragmentation Functions in e^+e^- annihilation up to NNLO + NNLL, in: 57th Rencontres de Moriond on QCD and High Energy Interactions, 2023. arXiv:2306.02953.
- [43] L. Bonino, M. Cacciari, G. Stagnitto, Heavy Quark Fragmentation in e^+e^- Collisions to NNLO+NNLL Accuracy in Perturbative QCDarXiv:2312.12519.
- [44] G. Bevilacqua, M. Czakon, C. G. Papadopoulos, R. Pittau, M. Worek, Assault on the NLO Wishlist: pp —> t anti-t b anti-b, JHEP 09 (2009) 109. arXiv:0907.4723, doi:10.1088/1126-6708/2009/09/109.
- [45] F. Cascioli, P. Maierhöfer, N. Moretti, S. Pozzorini, F. Siegert, NLO matching for $t\bar{t}b\bar{b}$ production with massive *b*-quarks, Phys. Lett. B 734 (2014) 210–214. arXiv:1309.5912, doi:10.1016/j.physletb.2014.05.040.
- [46] M. V. Garzelli, A. Kardos, Z. Trócsányi, Hadroproduction of tīb̄b̄ final states at LHC: predictions at NLO accuracy matched with Parton Shower, JHEP 03 (2015) 083. arXiv:1408.0266, doi:10.1007/JHEP03(2015)083.
- [47] G. Bevilacqua, M. V. Garzelli, A. Kardos, $t\bar{t}b\bar{b}$ hadroproduction with massive bottom quarks with PowHelarXiv: 1709.06915.
- [48] G. Bevilacqua, H.-Y. Bi, H. B. Hartanto, M. Kraus, M. Lupattelli, M. Worek, tt⁻bb⁻ at the LHC: On the size of off-shell effects and prompt b-jet identification, Phys. Rev. D 107 (1) (2023) 014028. arXiv:2202.11186, doi:10.1103/PhysRevD.107.014028.
- [49] G. Chachamis, M. Deak, G. Rodrigo, Heavy quark impact factor in kT-factorization, JHEP 12 (2013) 066. arXiv:1310.6611, doi: 10.1007/JHEP12(2013)066.
- [50] G. Chachamis, M. Deak, M. Hentschinski, G. Rodrigo, A. Sabio Vera, Single bottom quark production in k₁-factorisation, JHEP 09 (2015) 123. arXiv:1507.05778, doi:10.1007/JHEP09(2015)123.
- [51] A. V. Karpishkov, M. A. Nefedov, V. A. Saleev, A. V. Shipilova, B-meson production at Tevatron and the LHC in the Regge limit of quantum chromodynamics, Phys. Atom. Nucl. 79 (2) (2016) 275–277. doi:10.1134/S1063778816020095.
- [52] A. V. Karpishkov, M. A. Nefedov, V. A. Saleev, $B\bar{B}$ angular correlations at the LHC in parton Reggeization approach merged with higher-order matrix elements, Phys. Rev. D 96 (9) (2017) 096019. arXiv:1707.04068, doi:10.1103/PhysRevD.96.096019.

- [53] R. Maciuła, A. Szczurek, G. Slipek, Kinematical correlations of dielectrons from semileptonic decays of heavy mesons and Drell-Yan processes at BNL RHIC, Phys. Rev. D 83 (2011) 054014. arXiv:1011.4207, doi:10.1103/PhysRevD.83.054014.
- [54] R. Maciuła, A. Szczurek, Double-parton scattering effects in D^0B^+ and B^+B^+ meson-meson pair production in proton-proton collisions at the LHC, Phys. Rev. D 97 (9) (2018) 094010. arXiv:1803.01198, doi:10.1103/PhysRevD.97.094010.
- [55] J. Binnewies, B. A. Kniehl, G. Kramer, Inclusive B meson production in e⁺e⁻ and p\(\bar{p}\) collisions, Phys. Rev. D 58 (1998) 034016.
 arXiv:hep-ph/9802231, doi:10.1103/PhysRevD.58.034016.
- [56] B. A. Kniehl, G. Kramer, I. Schienbein, H. Spiesberger, Finite-mass effects on inclusive B meson hadroproduction, Phys. Rev. D 77 (2008) 014011. arXiv:0705.4392, doi:10.1103/PhysRevD.77.014011.
- [57] B. A. Kniehl, G. Kramer, I. Schienbein, H. Spiesberger, Inclusive B-Meson Production at the LHC in the GM-VFN Scheme, Phys. Rev. D 84 (2011) 094026. arXiv:1109.2472, doi:10.1103/PhysRevD.84.094026.
- [58] G. Kramer, H. Spiesberger, b-hadron production in the general-mass variable-flavour-number scheme and LHC data, Phys. Rev. D 98 (11) (2018) 114010. arXiv:1809.04297, doi:10.1103/PhysRevD.98.114010.
- [59] Y. Amhis, et al., Averages of b-hadron, c-hadron, and τ-lepton properties as of summer 2016, Eur. Phys. J. C 77 (12) (2017) 895. arXiv:1612.07233, doi:10.1140/epjc/s10052-017-5058-4.
- [60] G. Kramer, H. Spiesberger, Λ_b^0 -baryon production in pp collisions in the general-mass variable-flavour-number scheme and comparison with CMS and LHCb data, Chin. Phys. C 42 (8) (2018) 083102. arXiv:1803.11103, doi:10.1088/1674-1137/42/8/083102.
- [61] R. Alonso, B. Grinstein, J. Martin Camalich, Lifetime of B_c^- Constrains Explanations for Anomalies in $B \to D^{(*)} \tau \nu$, Phys. Rev. Lett. 118 (8) (2017) 081802. arXiv:1611.06676, doi:10.1103/PhysRevLett.118.081802.
- [62] J. Aebischer, B. Grinstein, A novel determination of the Bc lifetime, Phys. Lett. B 834 (2022) 137435. arXiv:2108.10285, doi: 10.1016/j.physletb.2022.137435.
- [63] J. Aebischer, B. Grinstein, Standard Model prediction of the B_c lifetime, JHEP 07 (2021) 130. arXiv:2105.02988, doi:10.1007/ JHEP07(2021)130.
- [64] P. G. Ortega, J. Segovia, D. R. Entem, F. Fernandez, Spectroscopy of B_c mesons and the possibility of finding exotic B_c -like structures, Eur. Phys. J. C 80 (3) (2020) 223. arXiv:2001.08093, doi:10.1140/epjc/s10052-020-7764-6.
- [65] F. Abe, et al., Observation of the B_c meson in $p\bar{p}$ collisions at $\sqrt{s}=1.8$ TeV, Phys. Rev. Lett. 81 (1998) 2432–2437. arXiv: hep-ex/9805034, doi:10.1103/PhysRevLett.81.2432.
- [66] G. Aad, et al., Observation of an Excited B_c^{\pm} Meson State with the ATLAS Detector, Phys. Rev. Lett. 113 (21) (2014) 212004. arXiv: 1407.1032, doi:10.1103/PhysRevLett.113.212004.
- [67] A. A. Karyasov, A. P. Martynenko, F. A. Martynenko, Relativistic corrections to the pair B_c-meson production in e⁺e⁻ annihilation, Nucl. Phys. B 911 (2016) 36–51. arXiv:1604.07633, doi:10.1016/j.nuclphysb.2016.07.034.
- [68] Q.-L. Liao, Y. Deng, Y. Yu, G.-C. Wang, G.-Y. Xie, Heavy *P*-wave quarkonium production via Higgs decays, Phys. Rev. D 98 (3) (2018) 036014. arXiv:1807.11918, doi:10.1103/PhysRevD.98.036014.
- [69] J. Jiang, C.-F. Qiao, B_c Production in Higgs Boson Decays, Phys. Rev. D 93 (5) (2016) 054031. arXiv:1512.01327, doi:10.1103/PhysRevD.93.054031.
- [70] R. Aaij, et al., Precision measurement of CP violation in $B_s^0 \rightarrow J/\psi K^+K^-$ decays, Phys. Rev. Lett. 114 (4) (2015) 041801. arXiv: 1411.3104, doi:10.1103/PhysRevLett.114.041801.
- [71] R. Aaij, et al., Measurement of the *b*-quark production cross-section in 7 and 13 TeV *pp* collisions, Phys. Rev. Lett. 118 (5) (2017) 052002, [Erratum: Phys.Rev.Lett. 119, 169901 (2017)]. arXiv:1612.05140, doi:10.1103/PhysRevLett.118.052002.
- [72] W. E. Caswell, G. P. Lepage, Effective Lagrangians for Bound State Problems in QED, QCD, and Other Field Theories, Phys. Lett. B 167 (1986) 437–442. doi:10.1016/0370-2693(86)91297-9.
- [73] B. A. Thacker, G. P. Lepage, Heavy quark bound states in lattice QCD, Phys. Rev. D 43 (1991) 196–208. doi:10.1103/PhysRevD.43.196.
- [74] G. T. Bodwin, E. Braaten, G. P. Lepage, Rigorous QCD analysis of inclusive annihilation and production of heavy quarkonium, Phys. Rev. D 51 (1995) 1125–1171, [Erratum: Phys.Rev.D 55, 5853 (1997)]. arXiv:hep-ph/9407339, doi:10.1103/PhysRevD.55.5853.
- [75] M. Cacciari, M. Greco, J/ψ production via fragmentation at the Tevatron, Phys. Rev. Lett. 73 (1994) 1586–1589. arXiv:hep-ph/9405241, doi:10.1103/PhysRevLett.73.1586.
- [76] D. P. Roy, K. Sridhar, Fragmentation contribution to quarkonium production in hadron collision, Phys. Lett. B 339 (1994) 141–147. arXiv:hep-ph/9406386, doi:10.1016/0370-2693(94)91146-0.
- [77] M. Cacciari, M. Greco, M. L. Mangano, A. Petrelli, Charmonium production at the Tevatron, Phys. Lett. B 356 (1995) 553-560. arXiv: hep-ph/9505379, doi:10.1016/0370-2693(95)00868-L.
- [78] M. Cacciari, M. Krämer, Color octet contributions to J/ψ photoproduction, Phys. Rev. Lett. 76 (1996) 4128–4131. arXiv:hep-ph/9601276, doi:10.1103/PhysRevLett.76.4128.
- [79] J.-P. Lansberg, New Observables in Inclusive Production of Quarkonia, Phys. Rept. 889 (2020) 1-106. arXiv:1903.09185, doi: 10.1016/j.physrep.2020.08.007.
- [80] K. Kolodziej, A. Leike, R. Ruckl, Production of B(c) mesons in hadronic collisions, Phys. Lett. B 355 (1995) 337–344. arXiv:hep-ph/9505298, doi:10.1016/0370-2693(95)00710-3.
- [81] P. Artoisenet, J. P. Lansberg, F. Maltoni, Hadroproduction of J/ψ and Υ in association with a heavy-quark pair, Phys. Lett. B 653 (2007) 60–66. arXiv:hep-ph/0703129, doi:10.1016/j.physletb.2007.04.031.
- [82] X.-C. Zheng, C.-H. Chang, T.-F. Feng, X.-G. Wu, QCD NLO fragmentation functions for c or b⁻ quark to Bc or Bc* meson and their application, Phys. Rev. D 100 (3) (2019) 034004. arXiv:1901.03477, doi:10.1103/PhysRevD.100.034004.
- [83] X.-C. Zheng, C.-H. Chang, X.-G. Wu, Fragmentation functions for gluon into B_c or B^{*}_c meson, JHEP 05 (2022) 036. arXiv:2112.10520, doi:10.1007/JHEP05 (2022) 036.
- [84] F. G. Celiberto, The high-energy spectrum of QCD from inclusive emissions of charmed B-mesons, Phys. Lett. B 835 (2022) 137554. arXiv:2206.09413, doi:10.1016/j.physletb.2022.137554.

- [85] F. G. Celiberto, M. Fucilla, Diffractive semi-hard production of a J/ψ or a Υ from single-parton fragmentation plus a jet in hybrid factorization, Eur. Phys. J. C 82 (10) (2022) 929. arXiv:2202.12227, doi:10.1140/epjc/s10052-022-10818-8.
- [86] F. G. Celiberto, Vector quarkonia at the LHC with JETHAD: A high-energy viewpoint, Universe 9 (7) (2023) 324. arXiv:2305.14295, doi:10.3390/universe9070324.
- [87] D. Colferai, F. Schwennsen, L. Szymanowski, S. Wallon, Mueller Navelet jets at LHC complete NLL BFKL calculation, JHEP 12 (2010) 026. arXiv:1002.1365, doi:10.1007/JHEP12(2010)026.
- [88] F. G. Celiberto, Hunting BFKL in semi-hard reactions at the LHC, Eur. Phys. J. C 81 (8) (2021) 691. arXiv:2008.07378, doi: 10.1140/epjc/s10052-021-09384-2.
- [89] F. G. Celiberto, D. Yu. Ivanov, M. M. A. Mohammed, A. Papa, High-energy resummed distributions for the inclusive Higgs-plus-jet production at the LHC, Eur. Phys. J. C 81 (4) (2021) 293. arXiv:2008.00501, doi:10.1140/epjc/s10052-021-09063-2.
- [90] A. D. Bolognino, F. G. Celiberto, M. Fucilla, D. Yu. Ivanov, A. Papa, Inclusive production of a heavy-light dijet system in hybrid high-energy and collinear factorization, Phys. Rev. D 103 (9) (2021) 094004. arXiv:2103.07396, doi:10.1103/PhysRevD.103.094004.
- [91] F. G. Celiberto, High-energy emissions of light mesons plus heavy flavor at the LHC and the Forward Physics Facility, Phys. Rev. D 105 (11) (2022) 114008. arXiv: 2204.06497, doi:10.1103/PhysRevD.105.114008.
- [92] M. Deak, F. Hautmann, H. Jung, K. Kutak, Forward Jet Production at the Large Hadron Collider, JHEP 09 (2009) 121. arXiv:0908.0538, doi:10.1088/1126-6708/2009/09/121.
- [93] M. Deak, A. van Hameren, H. Jung, A. Kusina, K. Kutak, M. Serino, Calculation of the Z+jet cross section including transverse momenta of initial partons, Phys. Rev. D 99 (9) (2019) 094011. arXiv:1809.03854, doi:10.1103/PhysRevD.99.094011.
- [94] A. van Hameren, L. Motyka, G. Ziarko, Hybrid k_T -factorization and impact factors at NLO, JHEP 11 (2022) 103. arXiv:2205.09585, doi:10.1007/JHEP11(2022)103.
- [95] M. Bonvini, S. Marzani, Double resummation for Higgs production, Phys. Rev. Lett. 120 (20) (2018) 202003. arXiv:1802.07758, doi:10.1103/PhysRevLett.120.202003.
- [96] F. Silvetti, M. Bonvini, Differential heavy quark pair production at small x, Eur. Phys. J. C 83 (4) (2023) 267. arXiv:2211.10142, doi:10.1140/epjc/s10052-023-11326-z.
- [97] M. Bonvini, S. Marzani, T. Peraro, Small-x resummation from HELL, Eur. Phys. J. C 76 (11) (2016) 597. arXiv:1607.02153, doi: 10.1140/epjc/s10052-016-4445-6.
- [98] M. Bonvini, S. Marzani, C. Muselli, Towards parton distribution functions with small-x resummation: HELL 2.0, JHEP 12 (2017) 117. arXiv:1708.07510, doi:10.1007/JHEP12(2017)117.
- [99] M. Bonvini, Small-x phenomenology at the LHC and beyond: HELL 3.0 and the case of the Higgs cross section, Eur. Phys. J. C 78 (10) (2018) 834. arXiv:1805.08785, doi:10.1140/epjc/s10052-018-6315-x.
- [100] R. D. Ball, S. Forte, Summation of leading logarithms at small x, Phys. Lett. B 351 (1995) 313-324. arXiv:hep-ph/9501231, doi:10.1016/0370-2693(95)00395-2.
- [101] R. D. Ball, S. Forte, Asymptotically free partons at high-energy, Phys. Lett. B 405 (1997) 317-326. arXiv:hep-ph/9703417, doi: 10.1016/S0370-2693(97)00625-4.
- [102] G. Altarelli, R. D. Ball, S. Forte, Factorization and resummation of small x scaling violations with running coupling, Nucl. Phys. B 621 (2002) 359–387. arXiv:hep-ph/0109178, doi:10.1016/S0550-3213(01)00563-6.
- [103] G. Altarelli, R. D. Ball, S. Forte, An Anomalous dimension for small x evolution, Nucl. Phys. B 674 (2003) 459-483. arXiv:hep-ph/0306156, doi:10.1016/j.nuclphysb.2003.09.040.
- [104] G. Altarelli, R. D. Ball, S. Forte, Perturbatively stable resummed small x evolution kernels, Nucl. Phys. B 742 (2006) 1-40. arXiv: hep-ph/0512237, doi:10.1016/j.nuclphysb.2006.01.046.
- [105] G. Altarelli, R. D. Ball, S. Forte, Small x Resummation with Quarks: Deep-Inelastic Scattering, Nucl. Phys. B 799 (2008) 199–240. arXiv:0802.0032, doi:10.1016/j.nuclphysb.2008.03.003.
- [106] S. Catani, M. Ciafaloni, F. Hautmann, GLUON CONTRIBUTIONS TO SMALL x HEAVY FLAVOR PRODUCTION, Phys. Lett. B 242 (1990) 97–102. doi:10.1016/0370-2693(90)91601-7.
- [107] S. Catani, M. Ciafaloni, F. Hautmann, High-energy factorization and small x heavy flavor production, Nucl. Phys. B 366 (1991) 135–188. doi:10.1016/0550-3213(91)90055-3.
- [108] J. C. Collins, R. Ellis, Heavy quark production in very high-energy hadron collisions, Nucl. Phys. B 360 (1991) 3–30. doi:10.1016/0550-3213(91)90288-9.
- [109] S. Catani, F. Hautmann, High-energy factorization and small x deep inelastic scattering beyond leading order, Nucl. Phys. B 427 (1994) 475–524. arXiv:hep-ph/9405388, doi:10.1016/0550-3213(94)90636-X.
- [110] R. D. Ball, Resummation of Hadroproduction Cross-sections at High Energy, Nucl. Phys. B 796 (2008) 137-183. arXiv:0708.1277, doi:10.1016/j.nuclphysb.2007.12.014.
- [111] F. Caola, S. Forte, S. Marzani, Small x resummation of rapidity distributions: The Case of Higgs production, Nucl. Phys. B 846 (2011) 167–211. arXiv:1010.2743, doi:10.1016/j.nuclphysb.2011.01.001.
- [112] F. G. Celiberto, Stabilizing BFKL via Heavy-flavor and NRQCD Fragmentation, Acta Phys. Polon. Supp. 16 (5) (2023) 41. arXiv: 2211.11780, doi:10.5506/APhysPolBSupp.16.5-A41.
- [113] F. G. Celiberto, High-energy resummation in semi-hard processes at the LHC, Ph.D. thesis, Università della Calabria and INFN-Cosenza (2017). arXiv:1707.04315.
- [114] A. D. Bolognino, From semi-hard processes to the unintegrated gluon distribution: a phenomenological path in the high-energy framework, Ph.D. thesis, Calabria U. (2021). arXiv:2109.03033.
- [115] V. S. Fadin, E. Kuraev, L. Lipatov, On the Pomeranchuk Singularity in Asymptotically Free Theories, Phys. Lett. B 60 (1975) 50–52. doi:10.1016/0370-2693(75)90524-9.
- [116] E. Kuraev, L. Lipatov, V. S. Fadin, The Pomeranchuk Singularity in Nonabelian Gauge Theories, Sov. Phys. JETP 45 (1977) 199-204.

- [117] I. Balitsky, L. Lipatov, The Pomeranchuk Singularity in Quantum Chromodynamics, Sov. J. Nucl. Phys. 28 (1978) 822–829.
- [118] F. Caola, A. Chakraborty, G. Gambuti, A. von Manteuffel, L. Tancredi, Three-Loop Gluon Scattering in QCD and the Gluon Regge Trajectory, Phys. Rev. Lett. 128 (21) (2022) 212001. arXiv:2112.11097, doi:10.1103/PhysRevLett.128.212001.
- [119] G. Falcioni, E. Gardi, N. Maher, C. Milloy, L. Vernazza, Disentangling the Regge Cut and Regge Pole in Perturbative QCD, Phys. Rev. Lett. 128 (13) (2022) 132001. arXiv:2112.11098, doi:10.1103/PhysRevLett.128.132001.
- [120] V. Del Duca, R. Marzucca, B. Verbeek, The gluon Regge trajectory at three loops from planar Yang-Mills theory, JHEP 01 (2022) 149. arXiv:2111.14265, doi:10.1007/JHEP01(2022)149.
- [121] E. P. Byrne, V. Del Duca, L. J. Dixon, E. Gardi, J. M. Smillie, One-loop central-emission vertex for two gluons in $\mathcal{N}=4$ super Yang-Mills theory, JHEP 08 (2022) 271. arXiv:2204.12459, doi:10.1007/JHEP08(2022)271.
- [122] E. P. Byrne, One-loop five-parton amplitudes in the NMRK limitarXiv:2312.15051.
- [123] V. S. Fadin, M. Fucilla, A. Papa, One-loop Lipatov vertex in QCD with higher ε-accuracy, JHEP 04 (2023) 137. arXiv:2302.09868, doi:10.1007/JHEP04(2023) 137.
- [124] V. S. Fadin, R. Fiore, M. I. Kotsky, A. Papa, The Gluon impact factors, Phys. Rev. D 61 (2000) 094005. arXiv:hep-ph/9908264, doi:10.1103/PhysRevD.61.094005.
- [125] V. S. Fadin, R. Fiore, M. I. Kotsky, A. Papa, The Quark impact factors, Phys. Rev. D 61 (2000) 094006. arXiv:hep-ph/9908265, doi:10.1103/PhysRevD.61.094006.
- [126] D. Yu. Ivanov, A. Papa, Inclusive production of a pair of hadrons separated by a large interval of rapidity in proton collisions, JHEP 07 (2012) 045. arXiv:1205.6068, doi:10.1007/JHEP07 (2012) 045.
- [127] J. Bartels, D. Colferai, G. P. Vacca, The NLO jet vertex for Mueller-Navelet and forward jets: The Quark part, Eur. Phys. J. C 24 (2002) 83–99. arXiv:hep-ph/0112283, doi:10.1007/s100520200919.
- [128] D. Yu. Ivanov, A. Papa, The next-to-leading order forward jet vertex in the small-cone approximation, JHEP 05 (2012) 086. arXiv: 1202.1082, doi:10.1007/JHEP05(2012)086.
- [129] D. Colferai, A. Niccoli, The NLO jet vertex in the small-cone approximation for kt and cone algorithms, JHEP 04 (2015) 071. arXiv: 1501.07442, doi:10.1007/JHEP04(2015)071.
- [130] M. Hentschinski, K. Kutak, A. van Hameren, Forward Higgs production within high energy factorization in the heavy quark limit at next-to-leading order accuracy, Eur. Phys. J. C 81 (2) (2021) 112, [Erratum: Eur. Phys. J. C 81, 262 (2021)]. arXiv:2011.03193, doi:10.1140/epjc/s10052-021-08902-6.
- [131] F. G. Celiberto, M. Fucilla, D. Yu. Ivanov, M. M. A. Mohammed, A. Papa, The next-to-leading order Higgs impact factor in the infinite top-mass limit, JHEP 08 (2022) 092. arXiv:2205.02681, doi:10.1007/JHEP08(2022)092.
- [132] L. Motyka, M. Sadzikowski, T. Stebel, Twist expansion of Drell-Yan structure functions in color dipole approach, JHEP 05 (2015) 087. arXiv:1412.4675, doi:10.1007/JHEP05(2015)087.
- [133] D. Brzeminski, L. Motyka, M. Sadzikowski, T. Stebel, Twist decomposition of Drell-Yan structure functions: phenomenological implications, JHEP 01 (2017) 005. arXiv:1611.04449, doi:10.1007/JHEP01(2017)005.
- [134] L. Motyka, M. Sadzikowski, T. Stebel, Lam-Tung relation breaking in Z⁰ hadroproduction as a probe of parton transverse momentum, Phys. Rev. D95 (11) (2017) 114025. arXiv:1609.04300, doi:10.1103/PhysRevD.95.114025.
- [135] F. G. Celiberto, D. Gordo Gómez, A. Sabio Vera, Forward Drell-Yan production at the LHC in the BFKL formalism with collinear corrections, Phys. Lett. B786 (2018) 201–206. arXiv:1808.09511, doi:10.1016/j.physletb.2018.09.045.
- [136] F. G. Celiberto, D. Yu. Ivanov, B. Murdaca, A. Papa, High-energy resummation in heavy-quark pair photoproduction, Phys. Lett. B 777 (2018) 141–150. arXiv:1709.10032, doi:10.1016/j.physletb.2017.12.020.
- [137] A. D. Bolognino, F. G. Celiberto, M. Fucilla, D. Yu. Ivanov, B. Murdaca, A. Papa, Inclusive production of two rapidity-separated heavy quarks as a probe of BFKL dynamics, PoS DIS2019 (2019) 067. arXiv:1906.05940, doi:10.22323/1.352.0067.
- [138] A. D. Bolognino, F. G. Celiberto, M. Fucilla, D. Yu. Ivanov, A. Papa, High-energy resummation in heavy-quark pair hadroproduction, Eur. Phys. J. C 79 (11) (2019) 939. arXiv:1909.03068, doi:10.1140/epjc/s10052-019-7392-1.
- [139] R. Boussarie, B. Ducloué, L. Szymanowski, S. Wallon, Forward J/ψ and very backward jet inclusive production at the LHC, Phys. Rev. D 97 (1) (2018) 014008. arXiv:1709.01380, doi:10.1103/PhysRevD.97.014008.
- [140] A. H. Mueller, H. Navelet, An Inclusive Minijet Cross-Section and the Bare Pomeron in QCD, Nucl. Phys. B 282 (1987) 727–744. doi:10.1016/0550-3213(87)90705-X.
- [141] B. Ducloué, L. Szymanowski, S. Wallon, Confronting Mueller-Navelet jets in NLL BFKL with LHC experiments at 7 TeV, JHEP 05 (2013) 096. arXiv:1302.7012, doi:10.1007/JHEP05 (2013) 096.
- [142] B. Ducloué, L. Szymanowski, S. Wallon, Evidence for high-energy resummation effects in Mueller-Navelet jets at the LHC, Phys. Rev. Lett. 112 (2014) 082003. arXiv:1309.3229, doi:10.1103/PhysRevLett.112.082003.
- [143] F. Caporale, D. Yu. Ivanov, B. Murdaca, A. Papa, Mueller–Navelet jets in next-to-leading order BFKL: theory versus experiment, Eur. Phys. J. C 74 (10) (2014) 3084, [Erratum: Eur.Phys.J.C 75, 535 (2015)]. arXiv:1407.8431, doi:10.1140/epjc/s10052-015-3754-5.
- [144] F. G. Celiberto, D. Yu. Ivanov, B. Murdaca, A. Papa, Mueller-Navelet Jets at LHC: BFKL Versus High-Energy DGLAP, Eur. Phys. J. C 75 (6) (2015) 292. arXiv:1504.08233, doi:10.1140/epjc/s10052-015-3522-6.
- [145] F. G. Celiberto, D. Yu. Ivanov, B. Murdaca, A. Papa, Mueller–Navelet Jets at the LHC: Discriminating BFKL from DGLAP by Asymmetric Cuts, Acta Phys. Polon. Supp. 8 (2015) 935. arXiv:1510.01626, doi:10.5506/APhysPolBSupp.8.935.
- [146] F. G. Celiberto, D. Yu. Ivanov, B. Murdaca, A. Papa, Mueller–Navelet jets at 13 TeV LHC: dependence on dynamic constraints in the central rapidity region, Eur. Phys. J. C 76 (4) (2016) 224. arXiv:1601.07847, doi:10.1140/epjc/s10052-016-4053-5.
- [147] F. Caporale, F. G. Celiberto, G. Chachamis, D. Gordo Gómez, A. Sabio Vera, Inclusive dijet hadroproduction with a rapidity veto constraint, Nucl. Phys. B 935 (2018) 412–434. arXiv:1806.06309, doi:10.1016/j.nuclphysb.2018.09.002.
- [148] N. B. de León, G. Chachamis, A. Sabio Vera, Average minijet rapidity ratios in Mueller-Navelet jets, Eur. Phys. J. C 81 (11) (2021) 1019. arXiv:2106.11255, doi:10.1140/epjc/s10052-021-09811-4.

- [149] F. G. Celiberto, A. Papa, Mueller-Navelet jets at the LHC: Hunting data with azimuthal distributions, Phys. Rev. D 106 (11) (2022) 114004. arXiv:2207.05015, doi:10.1103/PhysRevD.106.114004.
- [150] F. G. Celiberto, D. Yu. Ivanov, B. Murdaca, A. Papa, High energy resummation in dihadron production at the LHC, Phys. Rev. D 94 (3) (2016) 034013. arXiv:1604.08013, doi:10.1103/PhysRevD.94.034013.
- [151] F. G. Celiberto, D. Yu. Ivanov, B. Murdaca, A. Papa, Dihadron production at the LHC: full next-to-leading BFKL calculation, Eur. Phys. J. C 77 (6) (2017) 382. arXiv:1701.05077, doi:10.1140/epjc/s10052-017-4949-8.
- [152] F. Caporale, F. G. Celiberto, G. Chachamis, A. Sabio Vera, Multi-Regge kinematics and azimuthal angle observables for inclusive four-jet production, Eur. Phys. J. C 76 (3) (2016) 165. arXiv:1512.03364, doi:10.1140/epjc/s10052-016-3963-6.
- [153] F. Caporale, F. G. Celiberto, G. Chachamis, D. Gordo Gómez, A. Sabio Vera, BFKL azimuthal imprints in inclusive three-jet production at 7 and 13 TeV, Nucl. Phys. B 910 (2016) 374–386. arXiv:1603.07785, doi:10.1016/j.nuclphysb.2016.07.012.
- [154] F. Caporale, F. G. Celiberto, G. Chachamis, D. Gordo Gómez, A. Sabio Vera, Inclusive Four-jet Production at 7 and 13 TeV: Azimuthal Profile in Multi-Regge Kinematics, Eur. Phys. J. C 77 (1) (2017) 5. arXiv:1606.00574, doi:10.1140/epjc/s10052-016-4557-z.
- [155] F. G. Celiberto, BFKL phenomenology: resummation of high-energy logs in semi-hard processes at LHC, Frascati Phys. Ser. 63 (2016) 43–48. arXiv:1606.07327.
- [156] F. Caporale, F. G. Celiberto, G. Chachamis, D. Gordo Gómez, A. Sabio Vera, Stability of Azimuthal-angle Observables under Higher Order Corrections in Inclusive Three-jet Production, Phys. Rev. D 95 (7) (2017) 074007. arXiv:1612.05428, doi:10.1103/PhysRevD.95. 074007.
- [157] A. D. Bolognino, F. G. Celiberto, D. Yu. Ivanov, M. M. A. Mohammed, A. Papa, Hadron-jet correlations in high-energy hadronic collisions at the LHC, Eur. Phys. J. C 78 (9) (2018) 772. arXiv:1808.05483, doi:10.1140/epjc/s10052-018-6253-7.
- [158] A. D. Bolognino, F. G. Celiberto, D. Yu. Ivanov, M. M. A. Mohammed, A. Papa, High-energy effects in forward inclusive dijet and hadron-jet production, PoS DIS2019 (2019) 049. arXiv:1906.11800, doi:10.22323/1.352.0049.
- [159] A. D. Bolognino, F. G. Celiberto, D. Yu. Ivanov, M. M. A. Mohammed, A. Papa, Inclusive hadron-jet production at the LHC, Acta Phys. Polon. Supp. 12 (4) (2019) 773. arXiv:1902.04511, doi:10.5506/APhysPolBSupp.12.773.
- [160] F. G. Celiberto, D. Yu. Ivanov, A. Papa, Diffractive production of Λ hyperons in the high-energy limit of strong interactions, Phys. Rev. D 102 (2020) 094019. arXiv:2008.10513, doi:10.1103/PhysRevD.102.094019.
- [161] F. G. Celiberto, Emergence of high-energy dynamics from cascade-baryon detections at the LHC, Eur. Phys. J. C 83 (4) (2023) 332. arXiv:2208.14577, doi:10.1140/epjc/s10052-023-11417-x.
- [162] K. Golec-Biernat, L. Motyka, T. Stebel, Forward Drell-Yan and backward jet production as a probe of the BFKL dynamics, JHEP 12 (2018) 091. arXiv:1811.04361, doi:10.1007/JHEP12(2018)091.
- [163] A. D. Bolognino, F. G. Celiberto, M. Fucilla, D. Yu. Ivanov, B. Murdaca, A. Papa, Inclusive production of two rapidity-separated heavy quarks as a probe of BFKL dynamics, PoS DIS2019 (2019) 067. arXiv:1906.05940, doi:10.22323/1.352.0067.
- [164] F. G. Celiberto, M. Fucilla, D. Yu. Ivanov, A. Papa, High-energy resummation in Λ_c baryon production, Eur. Phys. J. C 81 (8) (2021) 780. arXiv:2105.06432, doi:10.1140/epjc/s10052-021-09448-3.
- [165] F. G. Celiberto, M. Fucilla, D. Yu. Ivanov, M. M. A. Mohammed, A. Papa, Bottom-flavored inclusive emissions in the variable-flavor number scheme: A high-energy analysis, Phys. Rev. D 104 (11) (2021) 114007. arXiv:2109.11875, doi:10.1103/PhysRevD.104.114007.
- [166] A. D. Bolognino, F. G. Celiberto, M. Fucilla, D. Yu. Ivanov, M. M. A. Mohammed, A. Papa, High-energy Signals from Heavy-flavor Physics, Acta Phys. Polon. Supp. 16 (5) (2023) 17. arXiv:2211.16818, doi:10.5506/APhysPolBSupp.16.5-A17.
- [167] F. G. Celiberto, M. Fucilla, M. M. A. Mohammed, A. Papa, Ultraforward production of a charmed hadron plus a Higgs boson in unpolarized proton collisions, Phys. Rev. D 105 (11) (2022) 114056. arXiv:2205.13429, doi:10.1103/PhysRevD.105.114056.
- [168] I. Anikin, A. Besse, D. Yu. Ivanov, B. Pire, L. Szymanowski, S. Wallon, A phenomenological study of helicity amplitudes of high energy exclusive leptoproduction of the rho meson, Phys. Rev. D 84 (2011) 054004. arXiv:1105.1761, doi:10.1103/PhysRevD.84.054004.
- [169] A. Besse, L. Szymanowski, S. Wallon, Saturation effects in exclusive rhoT, rhoL meson electroproduction, JHEP 11 (2013) 062. arXiv: 1302.1766, doi:10.1007/JHEP11(2013)062.
- [170] A. D. Bolognino, F. G. Celiberto, D. Yu. Ivanov, A. Papa, Unintegrated gluon distribution from forward polarized ρ-electroproduction, Eur. Phys. J. C78 (12) (2018) 1023. arXiv:1808.02395, doi:10.1140/epjc/s10052-018-6493-6.
- [171] A. D. Bolognino, F. G. Celiberto, D. Yu. Ivanov, A. Papa, ρ-meson leptoproduction as testfield for the unintegrated gluon distribution in the proton, Frascati Phys. Ser. 67 (2018) 76–82. arXiv:1808.02958.
- [172] A. D. Bolognino, F. G. Celiberto, D. Yu. Ivanov, A. Papa, Leptoproduction of ρ-mesons as discriminator for the unintegrated gluon distribution in the proton, Acta Phys. Polon. Supp. 12 (4) (2019) 891. arXiv:1902.04520, doi:10.5506/APhysPolBSupp.12.891.
- [173] A. D. Bolognino, A. Szczurek, W. Schaefer, Exclusive production of ϕ meson in the $\gamma^* p \to \phi p$ reaction at large photon virtualities within k_T -factorization approach, Phys. Rev. D 101 (5) (2020) 054041. arXiv:1912.06507, doi:10.1103/PhysRevD.101.054041.
- [174] F. G. Celiberto, Unraveling the Unintegrated Gluon Distribution in the Proton via ρ-Meson Leptoproduction, Nuovo Cim. C42 (2019) 220. arXiv:1912.11313, doi:10.1393/ncc/i2019-19220-9.
- [175] A. Łuszczak, M. Łuszczak, W. Schäfer, Unintegrated gluon distributions from the color dipole cross section in the BGK saturation model, Phys. Lett. B 835 (2022) 137582. arXiv:2210.02877, doi:10.1016/j.physletb.2022.137582.
- [176] A. D. Bolognino, F. G. Celiberto, D. Yu. Ivanov, A. Papa, W. Schäfer, A. Szczurek, Exclusive production of ρ-mesons in high-energy factorization at HERA and EIC, Eur. Phys. J. C 81 (10) (2021) 846. arXiv:2107.13415, doi:10.1140/epjc/s10052-021-09593-9.
- [177] A. D. Bolognino, F. G. Celiberto, D. Yu. Ivanov, A. Papa, Exclusive emissions of rho-mesons and the unintegrated gluon distribution, SciPost Phys. Proc. 8 (2022) 089. arXiv:2107.12725, doi:10.21468/SciPostPhysProc.8.089.
- [178] A. D. Bolognino, F. G. Celiberto, M. Fucilla, D. Yu. Ivanov, A. Papa, W. Schäfer, A. Szczurek, Hadron structure at small-x via unintegrated gluon densities, Rev. Mex. Fis. Suppl. 3 (3) (2022) 0308109. arXiv:2202.02513, doi:10.31349/SuplRevMexFis.3.0308109.
- [179] F. G. Celiberto, Phenomenology of the hadronic structure at small-x, 2022. arXiv:2202.04207.

- [180] A. D. Bolognino, F. G. Celiberto, D. Yu.. Ivanov, A. Papa, W. Schäfer, A. Szczurek, Exclusive emissions of polarized ρ mesons at the EIC and the proton content at low x, in: 29th International Workshop on Deep-Inelastic Scattering and Related Subjects, 2022. arXiv: 2207.05726, doi:10.5281/zenodo.7112750.
- [181] I. Bautista, A. Fernandez Tellez, M. Hentschinski, BFKL evolution and the growth with energy of exclusive J/ψ and Y photoproduction cross sections, Phys. Rev. D 94 (5) (2016) 054002. arXiv:1607.05203, doi:10.1103/PhysRevD.94.054002.
- [182] A. Arroyo Garcia, M. Hentschinski, K. Kutak, QCD evolution based evidence for the onset of gluon saturation in exclusive photo-production of vector mesons. Phys. Lett. B 795 (2019) 569–575. arXiv:1904.04394, doi:10.1016/j.physletb.2019.06.061.
- [183] M. Hentschinski, E. Padrón Molina, Exclusive J/Ψ and $\Psi(2s)$ photo-production as a probe of QCD low x evolution equations, Phys. Rev. D 103 (7) (2021) 074008. arXiv:2011.02640, doi:10.1103/PhysRevD.103.074008.
- [184] R. D. Ball, V. Bertone, M. Bonvini, S. Marzani, J. Rojo, L. Rottoli, Parton distributions with small-x resummation: evidence for BFKL dynamics in HERA data, Eur. Phys. J. C78 (4) (2018) 321. arXiv:1710.05935, doi:10.1140/epjc/s10052-018-5774-4.
- [185] H. Abdolmaleki, et al., Impact of low-x resummation on QCD analysis of HERA data, Eur. Phys. J. C 78 (8) (2018) 621. arXiv:1802.00064, doi:10.1140/epjc/s10052-018-6090-8.
- [186] M. Bonvini, F. Giuli, A new simple PDF parametrization: improved description of the HERA data, Eur. Phys. J. Plus 134 (10) (2019) 531. arXiv:1902.11125, doi:10.1140/epjp/i2019-12872-x.
- [187] A. Bacchetta, F. G. Celiberto, M. Radici, P. Taels, Transverse-momentum-dependent gluon distribution functions in a spectator model, Eur. Phys. J. C 80 (8) (2020) 733. arXiv:2005.02288, doi:10.1140/epjc/s10052-020-8327-6.
- [188] A. Bacchetta, F. G. Celiberto, M. Radici, T-odd gluon distribution functions in a spectator modelarXiv: 2402.17556.
- [189] F. G. Celiberto, 3D tomography of the nucleon: transverse-momentum-dependent gluon distributions, Nuovo Cim. C44 (2021) 36. arXiv: 2101.04630, doi:10.1393/ncc/i2021-21036-3.
- [190] A. Bacchetta, F. G. Celiberto, M. Radici, P. Taels, A spectator-model way to transverse-momentum-dependent gluon distribution functions, SciPost Phys. Proc. 8 (2022) 040. arXiv:2107.13446, doi:10.21468/SciPostPhysProc.8.040.
- [191] A. Bacchetta, F. G. Celiberto, M. Radici, Toward twist-2 *T*-odd transverse-momentum-dependent gluon distributions: the *f*-type Sivers function, PoS EPS-HEP2021 (2022) 376. arXiv:2111.01686, doi:10.22323/1.398.0376.
- [192] A. Bacchetta, F. G. Celiberto, M. Radici, Toward twist-2 *T*-odd transverse-momentum-dependent gluon distributions: the *f*-type linearity function, PoS PANIC2021 (2022) 378. arXiv:2111.03567, doi:10.22323/1.380.0378.
- [193] A. Bacchetta, F. G. Celiberto, M. Radici, Towards Leading-twist T-odd TMD Gluon Distributions, JPS Conf. Proc. 37 (2022) 020124. arXiv:2201.10508, doi:10.7566/JPSCP.37.020124.
- [194] A. Bacchetta, F. G. Celiberto, M. Radici, Unveiling the proton structure via transverse-momentum-dependent gluon distributions, Rev. Mex. Fis. Suppl. 3 (3) (2022) 0308108. arXiv:2206.07815, doi:10.31349/SuplRevMexFis.3.0308108.
- [195] A. Bacchetta, F. G. Celiberto, M. Radici, A. Signori, Phenomenology of gluon TMDs from η_{b,c} production, in: 29th International Workshop on Deep-Inelastic Scattering and Related Subjects, 2022. arXiv:2208.06252, doi:10.5281/zenodo.7085045.
- [196] F. G. Celiberto, A Journey into the Proton Structure: Progresses and Challenges, Universe 8 (12) (2022) 661. arXiv:2210.08322, doi:10.3390/universe8120661.
- [197] A. Bacchetta, F. G. Celiberto, M. Radici, Spectator-model studies for spin-dependent gluon TMD PDFs at the LHC and EIC, PoS EPS-HEP2023 (2024) 247. arXiv:2310.19916, doi:10.22323/1.449.0247.
- [198] M. Hentschinski, Transverse momentum dependent gluon distribution within high energy factorization at next-to-leading order, Phys. Rev. D 104 (5) (2021) 054014. arXiv:2107.06203, doi:10.1103/PhysRevD.104.054014.
- [199] G. R. Boroun, Dipole cross section from the unintegrated gluon distribution at small x, Phys. Rev. D 108 (3) (2023) 034025. arXiv: 2301.01083, doi:10.1103/PhysRevD.108.034025.
- [200] G. R. Boroun, The unintegrated gluon distribution from the GBW and BGK models, Eur. Phys. J. A 60 (3) (2024) 48. arXiv:2309.04832, doi:10.1140/epja/s10050-024-01255-0.
- [201] S. J. Brodsky, F. Hautmann, D. E. Soper, Probing the QCD pomeron in e+ e- collisions, Phys. Rev. Lett. 78 (1997) 803-806, [Erratum: Phys.Rev.Lett. 79, 3544 (1997)]. arXiv:hep-ph/9610260, doi:10.1103/PhysRevLett.78.803.
- [202] S. J. Brodsky, V. S. Fadin, V. T. Kim, L. N. Lipatov, G. B. Pivovarov, High-energy QCD asymptotics of photon-photon collisions, JETP Lett. 76 (2002) 249–252. arXiv:hep-ph/0207297, doi:10.1134/1.1520615.
- [203] F. Caporale, D. Yu. Ivanov, B. Murdaca, A. Papa, Brodsky-Lepage-Mackenzie optimal renormalization scale setting for semihard processes, Phys. Rev. D 91 (11) (2015) 114009. arXiv:1504.06471, doi:10.1103/PhysRevD.91.114009.
- [204] M. M. A. Mohammed, Hunting stabilization effects of the high-energy resummation at the LHC, Ph.D. thesis, Università della Calabria and INFN-Cosenza (4 2022). arXiv: 2204.11606.
- [205] F. G. Celiberto, A. Papa, The high-energy QCD dynamics from Higgs-plus-jet correlations at the FCCarXiv: 2305.00962.
- [206] F. G. Celiberto, L. Delle Rose, M. Fucilla, G. Gatto, A. Papa, High-energy resummed Higgs-plus-jet distributions at NLL/NLO* with POWHEG+JETHAD, in: 57th Rencontres de Moriond on QCD and High Energy Interactions, 2023. arXiv:2305.05052.
- [207] F. G. Celiberto, L. Delle Rose, M. Fucilla, G. Gatto, A. Papa, NLL/NLO⁻ studies on Higgs-plus-jet production with POWHEG+JETHAD, PoS RADCOR2023 (2024) 069. arXiv:2309.11573, doi:10.22323/1.432.0069.
- [208] F. G. Celiberto, L. Delle Rose, M. Fucilla, G. Gatto, A. Papa, Towards high-energy Higgs+jet distributions at NLL matched to NLO, PoS EPS-HEP2023 (2024) 390. arXiv:2310.16967, doi:10.22323/1.449.0390.
- [209] F. G. Celiberto, M. Fucilla, M. M. A. Mohammed, D. Yu. Ivanov, A. Papa, High-energy resummation in Higgs production at the next-to-leading order, PoS RADCOR2023 (2024) 091. arXiv:2309.07570, doi:10.22323/1.432.0091.
- [210] F. G. Celiberto, A. Papa, A high-energy QCD portal to exotic matter: Heavy-light tetraquarks at the HL-LHC, Phys. Lett. B 848 (2024) 138406. arXiv:2308.00809, doi:10.1016/j.physletb.2023.138406.
- [211] D. Binosi, J. Collins, C. Kaufhold, L. Theussl, JaxoDraw: A Graphical user interface for drawing Feynman diagrams. Version 2.0 release notes, Comput. Phys. Commun. 180 (2009) 1709–1715. arXiv:0811.4113, doi:10.1016/j.cpc.2009.02.020.

- [212] W. A. Bardeen, A. J. Buras, D. W. Duke, T. Muta, Deep-inelastic scattering beyond the leading order in asymptotically free gauge theories, Phys. Rev. D 18 (1978) 3998–4017. doi:10.1103/PhysRevD.18.3998.
- [213] F. Caporale, D. Yu. Ivanov, B. Murdaca, A. Papa, Mueller-Navelet small-cone jets at LHC in next-to-leading BFKL, Nucl. Phys. B 877 (2013) 73–94. arXiv:1211.7225, doi:10.1016/j.nuclphysb.2013.09.013.
- [214] A. V. Kotikov, L. N. Lipatov, NLO corrections to the BFKL equation in QCD and in supersymmetric gauge theories, Nucl. Phys. B 582 (2000) 19-43. arXiv:hep-ph/0004008, doi:10.1016/S0550-3213(00)00329-1.
- [215] M. Furman, Study of a Nonleading {QCD} Correction to Hadron Calorimeter Reactions, Nucl. Phys. B 197 (1982) 413–445. doi: 10.1016/0550-3213(82)90452-7.
- [216] F. Aversa, P. Chiappetta, M. Greco, J. P. Guillet, QCD Corrections to Parton-Parton Scattering Processes, Nucl. Phys. B 327 (1989) 105. doi:10.1016/0550-3213(89)90288-5.
- [217] S. Alioli, P. Nason, C. Oleari, E. Re, A general framework for implementing NLO calculations in shower Monte Carlo programs: the POWHEG BOX, JHEP 06 (2010) 043. arXiv:1002.2581, doi:10.1007/JHEP06 (2010) 043.
- [218] J. M. Campbell, R. K. Ellis, R. Frederix, P. Nason, C. Oleari, C. Williams, NLO Higgs Boson Production Plus One and Two Jets Using the POWHEG BOX, MadGraph4 and MCFM, JHEP 07 (2012) 092. arXiv:1202.5475, doi:10.1007/JHEP07(2012)092.
- [219] K. Hamilton, P. Nason, C. Oleari, G. Zanderighi, Merging H/W/Z + 0 and 1 jet at NLO with no merging scale: a path to parton shower + NNLO matching, JHEP 05 (2013) 082. arXiv:1212.4504, doi:10.1007/JHEP05 (2013) 082.
- [220] R. D. Ball, et al., An open-source machine learning framework for global analyses of parton distributions, Eur. Phys. J. C 81 (10) (2021) 958. arXiv:2109.02671.
- [221] R. D. Ball, et al., The path to proton structure at 1% accuracy, Eur. Phys. J. C 82 (5) (2022) 428. arXiv: 2109.02653, doi:10.1140/epjc/s10052-022-10328-7.
- [222] A. Buckley, J. Ferrando, S. Lloyd, K. Nordström, B. Page, M. Rüfenacht, M. Schönherr, G. Watt, LHAPDF6: parton density access in the LHC precision era, Eur. Phys. J. C 75 (2015) 132. arXiv:1412.7420, doi:10.1140/epjc/s10052-015-3318-8.
- [223] S. Forte, L. Garrido, J. I. Latorre, A. Piccione, Neural network parametrization of deep inelastic structure functions, JHEP 05 (2002) 062. arXiv:hep-ph/0204232, doi:10.1088/1126-6708/2002/05/062.
- [224] R. D. Ball, S. Forte, R. Stegeman, Correlation and combination of sets of parton distributions, Eur. Phys. J. C 81 (11) (2021) 1046. arXiv:2110.08274, doi:10.1140/epjc/s10052-021-09863-6.
- [225] V. G. Kartvelishvili, A. K. Likhoded, Structure Functions and Leptonic Widths of Heavy Mesons, Yad. Fiz. 42 (1985) 1306–1308.
- [226] F. Feng, Y. Jia, D. Yang, Gluon fragmentation into Bc(*) in NRQCD factorization, Phys. Rev. D 106 (5) (2022) 054030. arXiv:2112.15569, doi:10.1103/PhysRevD.106.054030.
- [227] F. Feng, Y. Jia, Next-to-leading-order QCD corrections to gluon fragmentation into quarkonia*, Chin. Phys. C 47 (3) (2023) 033103. arXiv:1810.04138, doi:10.1088/1674-1137/aca1aa.
- [228] A. Vogt, Efficient evolution of unpolarized and polarized parton distributions with QCD-PEGASUS, Comput. Phys. Commun. 170 (2005) 65–92. arXiv:hep-ph/0408244, doi:10.1016/j.cpc.2005.03.103.
- [229] G. P. Salam, J. Rojo, A Higher Order Perturbative Parton Evolution Toolkit (HOPPET), Comput. Phys. Commun. 180 (2009) 120–156. arXiv:0804.3755, doi:10.1016/j.cpc.2008.08.010.
- [230] M. Botje, QCDNUM: Fast QCD Evolution and Convolution, Comput. Phys. Commun. 182 (2011) 490-532. arXiv:1005.1481, doi: 10.1016/j.cpc.2010.10.020.
- [231] V. Bertone, S. Carrazza, J. Rojo, APFEL: A PDF Evolution Library with QED corrections, Comput. Phys. Commun. 185 (2014) 1647–1668. arXiv:1310.1394, doi:10.1016/j.cpc.2014.03.007.
- [232] S. Carrazza, A. Ferrara, D. Palazzo, J. Rojo, APFEL Web: a web-based application for the graphical visualization of parton distribution functions, J. Phys. G 42 (5) (2015) 057001. arXiv:1410.5456, doi:10.1088/0954-3899/42/5/057001.
- [233] V. Bertone, APFEL++: A new PDF evolution library in C++, PoS DIS2017 (2018) 201. arXiv:1708.00911, doi:10.22323/1.297.0201.
- [234] A. Candido, F. Hekhorn, G. Magni, EKO: evolution kernel operators, Eur. Phys. J. C 82 (10) (2022) 976. arXiv:2202.02338, doi: 10.1140/epjc/s10052-022-10878-w.
- [235] F. Hekhorn, G. Magni, DGLAP evolution of parton distributions at approximate N³LOarXiv: 2306.15294.
- [236] G. Curci, W. Furmanski, R. Petronzio, Evolution of Parton Densities Beyond Leading Order: The Nonsinglet Case, Nucl. Phys. B 175 (1980) 27–92. doi:10.1016/0550-3213(80)90003-6.
- [237] W. Furmanski, R. Petronzio, Singlet Parton Densities Beyond Leading Order, Phys. Lett. B 97 (1980) 437–442. doi:10.1016/0370-2693(80)90636-X.
- [238] V. Bertone, S. Carrazza, N. P. Hartland, E. R. Nocera, J. Rojo, A determination of the fragmentation functions of pions, kaons, and protons with faithful uncertainties, Eur. Phys. J. C 77 (8) (2017) 516. arXiv:1706.07049, doi:10.1140/epjc/s10052-017-5088-y.
- [239] V. Bertone, N. P. Hartland, E. R. Nocera, J. Rojo, L. Rottoli, Charged hadron fragmentation functions from collider data, Eur. Phys. J. C 78 (8) (2018) 651. arXiv:1807.03310, doi:10.1140/epjc/s10052-018-6130-4.
- [240] B. A. Kniehl, G. Kramer, I. Schienbein, H. Spiesberger, Inclusive D*+- production in p anti-p collisions with massive charm quarks, Phys. Rev. D 71 (2005) 014018. arXiv:hep-ph/0410289, doi:10.1103/PhysRevD.71.014018.
- [241] B. A. Kniehl, G. Kramer, D0, D+, D+(s), and Lambda+(c) fragmentation functions from CERN LEP1, Phys. Rev. D 71 (2005) 094013. arXiv:hep-ph/0504058, doi:10.1103/PhysRevD.71.094013.
- [242] B. A. Kniehl, G. Kramer, Charmed-hadron fragmentation functions from CERN LEP1 revisited, Phys. Rev. D 74 (2006) 037502. arXiv: hep-ph/0607306, doi:10.1103/PhysRevD.74.037502.
- [243] T. Kneesch, B. A. Kniehl, G. Kramer, I. Schienbein, Charmed-meson fragmentation functions with finite-mass corrections, Nucl. Phys. B 799 (2008) 34–59. arXiv:0712.0481, doi:10.1016/j.nuclphysb.2008.02.015.

- [244] G. Corcella, G. Ferrera, Charm-quark fragmentation with an effective coupling constant, JHEP 12 (2007) 029. arXiv:0706.2357, doi:10.1088/1126-6708/2007/12/029.
- [245] D. P. Anderle, T. Kaufmann, M. Stratmann, F. Ringer, I. Vitev, Using hadron-in-jet data in a global analysis of *D** fragmentation functions, Phys. Rev. D 96 (3) (2017) 034028. arXiv:1706.09857, doi:10.1103/PhysRevD.96.034028.
- [246] M. Salajegheh, S. M. Moosavi Nejad, M. Soleymaninia, H. Khanpour, S. Atashbar Tehrani, NNLO charmed-meson fragmentation functions and their uncertainties in the presence of meson mass corrections, Eur. Phys. J. C 79 (12) (2019) 999. arXiv:1904.09832, doi: 10.1140/epjc/s10052-019-7521-x.
- [247] M. Salajegheh, S. M. Moosavi Nejad, M. Delpasand, Determination of D_s^+ meson fragmentation functions through two different approaches, Phys. Rev. D 100 (11) (2019) 114031. doi:10.1103/PhysRevD.100.114031.
- [248] M. Soleymaninia, H. Khanpour, S. M. Moosavi Nejad, First determination of *D*+*-meson fragmentation functions and their uncertainties at next-to-next-to-leading order, Phys. Rev. D 97 (7) (2018) 074014. arXiv:1711.11344, doi:10.1103/PhysRevD.97.074014.
- [249] B. A. Kniehl, G. Kramer, I. Schienbein, H. Spiesberger, A[±]_c production in pp collisions with a new fragmentation function, Phys. Rev. D 101 (11) (2020) 114021. arXiv:2004.04213, doi:10.1103/PhysRevD.101.114021.
- [250] M. Delpasand, S. M. Moosavi Nejad, M. Soleymaninia, Λ⁺ fragmentation functions from pQCD approach and the Suzuki model, Phys. Rev. D 101 (11) (2020) 114022. arXiv:2006.07602, doi:10.1103/PhysRevD.101.114022.
- [251] B. A. Kniehl, G. Kramer, I. Schienbein, H. Spiesberger, Finite-mass effects on inclusive B meson hadroproduction, Phys. Rev. D 77 (2008) 014011. arXiv:0705.4392, doi:10.1103/PhysRevD.77.014011.
- [252] B. A. Kniehl, G. Kramer, S. M. Moosavi Nejad, Bottom-Flavored Hadrons from Top-Quark Decay at Next-to-Leading order in the General-Mass Variable-Flavor-Number Scheme, Nucl. Phys. B 862 (2012) 720–736. arXiv:1205.2528, doi:10.1016/j.nuclphysb.2012.05.008
- [253] M. Salajegheh, S. M. Moosavi Nejad, H. Khanpour, B. A. Kniehl, M. Soleymaninia, *B*-hadron fragmentation functions at next-to-next-to-leading order from a global analysis of e^+e^- annihilation data, Phys. Rev. D 99 (11) (2019) 114001. arXiv:1904.08718, doi: 10.1103/PhysRevD.99.114001.
- [254] B. A. Kniehl, S. M. Moosavi Nejad, Angular analysis of bottom-flavored hadron production in semileptonic decays of polarized top quarks, Phys. Rev. D 103 (3) (2021) 034015. arXiv:2101.11521, doi:10.1103/PhysRevD.103.034015.
- [255] F. G. Celiberto, M. Fucilla, Inclusive J/ψ and Υ emissions from single-parton fragmentation in hybrid high-energy and collinear factorization, in: 29th International Workshop on Deep-Inelastic Scattering and Related Subjects, 2022. arXiv:2208.07206, doi: 10.5281/zenodo.7237044.
- [256] E. Braaten, K.-m. Cheung, T. C. Yuan, Z0 decay into charmonium via charm quark fragmentation, Phys. Rev. D 48 (1993) 4230–4235. arXiv:hep-ph/9302307, doi:10.1103/PhysRevD.48.4230.
- [257] X.-C. Zheng, C.-H. Chang, X.-G. Wu, NLO fragmentation functions of heavy quarks into heavy quarkonia, Phys. Rev. D 100 (1) (2019) 014005. arXiv:1905.09171, doi:10.1103/PhysRevD.100.014005.
- [258] E. Braaten, T. C. Yuan, Gluon fragmentation into heavy quarkonium, Phys. Rev. Lett. 71 (1993) 1673-1676. arXiv:hep-ph/9303205, doi:10.1103/PhysRevLett.71.1673.
- [259] C.-H. Chang, Y.-Q. Chen, The Production of B(c) or anti-B(c) meson associated with two heavy quark jets in Z0 boson decay, Phys. Rev. D 46 (1992) 3845, [Erratum: Phys.Rev.D 50, 6013 (1994)]. doi:10.1103/PhysRevD.46.3845.
- [260] E. Braaten, K.-m. Cheung, T. C. Yuan, Perturbative QCD fragmentation functions for B_c and B_c * production, Phys. Rev. D 48 (11) (1993) R5049. arXiv:hep-ph/9305206, doi:10.1103/PhysRevD.48.R5049.
- [261] J. P. Ma, Calculating fragmentation functions from definitions, Phys. Lett. B 332 (1994) 398-404. arXiv:hep-ph/9401249, doi: 10.1016/0370-2693(94)91271-8.
- [262] F. G. Celiberto, Exotic tetraquarks at the HL-LHC with JETHAD: A high-energy viewpointarXiv: 2403.15639.
- [263] M. Suzuki, Spin Property of Heavy Hadron in Heavy Quark Fragmentation: A Simple Model, Phys. Rev. D 33 (1986) 676. doi: 10.1103/PhysRevD.33.676.
- [264] S. M. Moosavi Nejad, N. Amiri, Ground state heavy tetraquark production in heavy quark fragmentation, Phys. Rev. D 105 (3) (2022) 034001. arXiv:2110.15251, doi:10.1103/PhysRevD.105.034001.
- [265] M. Suzuki, Fragmentation of Hadrons from Heavy Quark Partons, Phys. Lett. B 71 (1977) 139–141. doi:10.1016/0370-2693(77) 90761-4.
- [266] F. Amiri, C.-R. Ji, Perturbative Quantum Chromodynamic Prediction for the Heavy Quark Fragmentation Function, Phys. Lett. B 195 (1987) 593–598. doi:10.1016/0370-2693(87)91579-6.
- [267] G. P. Lepage, S. J. Brodsky, Exclusive Processes in Perturbative Quantum Chromodynamics, Phys. Rev. D 22 (1980) 2157. doi: 10.1103/PhysRevD.22.2157.
- [268] S. J. Brodsky, C.-R. Ji, Exclusive Production of Higher Generation Hadrons and Form-factor Zeros in Quantum Chromodynamics, Phys. Rev. Lett. 55 (1985) 2257. doi:10.1103/PhysRevLett.55.2257.
- [269] G. P. Salam, A Resummation of large subleading corrections at small x, JHEP 07 (1998) 019. arXiv:hep-ph/9806482, doi:10.1088/1126-6708/1998/07/019.
- [270] M. Ciafaloni, D. Colferai, G. P. Salam, A. M. Stasto, Renormalization group improved small x Green's function, Phys. Rev. D 68 (2003) 114003. arXiv:hep-ph/0307188, doi:10.1103/PhysRevD.68.114003.
- [271] A. Sabio Vera, An 'All-poles' approximation to collinear resummations in the Regge limit of perturbative QCD, Nucl. Phys. B 722 (2005) 65–80. arXiv:hep-ph/0505128, doi:10.1016/j.nuclphysb.2005.06.003.
- [272] R. Barbieri, E. d'Emilio, G. Curci, E. Remiddi, Strong Radiative Corrections to Annihilations of Quarkonia in QCD, Nucl. Phys. B 154 (1979) 535-546. doi:10.1016/0550-3213(79)90047-6.
- [273] W. Celmaster, R. J. Gonsalves, Quantum-chromodynamics perturbation expansions in a coupling constant renormalized by momentum-space subtraction, Phys. Rev. Lett. 42 (1979) 1435–1438. doi:10.1103/PhysRevLett.42.1435.

- [274] V. Khachatryan, et al., Azimuthal decorrelation of jets widely separated in rapidity in pp collisions at √s = 7 TeV, JHEP 08 (2016) 139. arXiv:1601.06713, doi:10.1007/JHEP08 (2016) 139.
- [275] A. Mueller, B.-W. Xiao, F. Yuan, Sudakov double logarithms resummation in hard processes in the small-x saturation formalism, Phys. Rev. D 88 (11) (2013) 114010. arXiv:1308.2993, doi:10.1103/PhysRevD.88.114010.
- [276] S. Marzani, Combining Q_T and small-x resummations, Phys. Rev. D 93 (5) (2016) 054047. arXiv:1511.06039, doi:10.1103/PhysRevD.93.054047.
- [277] A. Mueller, L. Szymanowski, S. Wallon, B.-W. Xiao, F. Yuan, Sudakov Resummations in Mueller-Navelet Dijet Production, JHEP 03 (2016) 096. arXiv:1512.07127, doi:10.1007/JHEP03(2016)096.
- [278] B.-W. Xiao, F. Yuan, BFKL and Sudakov Resummation in Higgs Boson Plus Jet Production with Large Rapidity Separation, Phys. Lett. B 782 (2018) 28-33. arXiv:1801.05478, doi:10.1016/j.physletb.2018.04.070.
- [279] Y. Hatta, B.-W. Xiao, F. Yuan, J. Zhou, Anisotropy in Dijet Production in Exclusive and Inclusive Processes, Phys. Rev. Lett. 126 (14) (2021) 142001. arXiv: 2010.10774, doi:10.1103/PhysRevLett.126.142001.
- [280] Y. Hatta, B.-W. Xiao, F. Yuan, J. Zhou, Azimuthal angular asymmetry of soft gluon radiation in jet production, Phys. Rev. D 104 (5) (2021) 054037. arXiv:2106.05307, doi:10.1103/PhysRevD.104.054037.
- [281] J. R. Andersen, V. Del Duca, S. Frixione, C. R. Schmidt, W. J. Stirling, Mueller-Navelet jets at hadron colliders, JHEP 02 (2001) 007. arXiv:hep-ph/0101180, doi:10.1088/1126-6708/2001/02/007.
- [282] M. Fontannaz, J. P. Guillet, G. Heinrich, Is a large intrinsic k(T) needed to describe photon + jet photoproduction at HERA?, Eur. Phys. J. C 22 (2001) 303–315. arXiv:hep-ph/0107262, doi:10.1007/s100520100797.
- [283] B. Ducloué, L. Szymanowski, S. Wallon, Violation of energy-momentum conservation in Mueller-Navelet jets production, Phys. Lett. B 738 (2014) 311-316. arXiv:1407.6593, doi:10.1016/j.physletb.2014.09.025.
- [284] S. Chatrchyan, et al., Measurement of the Λ_b cross section and the $\bar{\Lambda}_b$ to Λ_b ratio with $J/\Psi\Lambda$ decays in pp collisions at $\sqrt{s}=7$ TeV, Phys. Lett. B 714 (2012) 136–157. arXiv:1205.0594, doi:10.1016/j.physletb.2012.05.063.
- [285] G. F. Sterman, Summation of Large Corrections to Short Distance Hadronic Cross-Sections, Nucl. Phys. B 281 (1987) 310–364. doi: 10.1016/0550-3213(87)90258-6.
- [286] S. Catani, L. Trentadue, Resummation of the QCD Perturbative Series for Hard Processes, Nucl. Phys. B 327 (1989) 323–352. doi: 10.1016/0550-3213(89)90273-3.
- [287] S. Catani, M. L. Mangano, P. Nason, L. Trentadue, The Resummation of soft gluons in hadronic collisions, Nucl. Phys. B 478 (1996) 273–310. arXiv:hep-ph/9604351, doi:10.1016/0550-3213(96)00399-9.
- [288] R. Bonciani, S. Catani, M. L. Mangano, P. Nason, Sudakov resummation of multiparton QCD cross-sections, Phys. Lett. B 575 (2003) 268–278. arXiv:hep-ph/0307035, doi:10.1016/j.physletb.2003.09.068.
- [289] D. de Florian, A. Kulesza, W. Vogelsang, Threshold resummation for high-transverse-momentum Higgs production at the LHC, JHEP 02 (2006) 047. arXiv:hep-ph/0511205, doi:10.1088/1126-6708/2006/02/047.
- [290] V. Ahrens, T. Becher, M. Neubert, L. L. Yang, Renormalization-Group Improved Prediction for Higgs Production at Hadron Colliders, Eur. Phys. J. C 62 (2009) 333–353. arXiv:0809.4283, doi:10.1140/epjc/s10052-009-1030-2.
- [291] D. de Florian, M. Grazzini, Higgs production at the LHC: updated cross sections at $\sqrt{s}=8$ TeV, Phys. Lett. B 718 (2012) 117–120. arXiv:1206.4133, doi:10.1016/j.physletb.2012.10.019.
- [292] S. Forte, G. Ridolfi, S. Rota, Threshold resummation of transverse momentum distributions beyond next-to-leading log, JHEP 08 (2021) 110. arXiv:2106.11321, doi:10.1007/JHEP08(2021)110.
- [293] A. Mukherjee, W. Vogelsang, Threshold resummation for W-boson production at RHIC, Phys. Rev. D 73 (2006) 074005. arXiv: hep-ph/0601162, doi:10.1103/PhysRevD.73.074005.
- [294] P. Bolzoni, Threshold resummation of Drell-Yan rapidity distributions, Phys. Lett. B 643 (2006) 325-330. arXiv:hep-ph/0609073, doi:10.1016/j.physletb.2006.10.064.
- [295] T. Becher, M. Neubert, Threshold resummation in momentum space from effective field theory, Phys. Rev. Lett. 97 (2006) 082001. arXiv:hep-ph/0605050, doi:10.1103/PhysRevLett.97.082001.
- [296] T. Becher, M. Neubert, G. Xu, Dynamical Threshold Enhancement and Resummation in Drell-Yan Production, JHEP 07 (2008) 030. arXiv:0710.0680, doi:10.1088/1126-6708/2008/07/030.
- [297] M. Bonvini, S. Forte, G. Ridolfi, Soft gluon resummation of Drell-Yan rapidity distributions: Theory and phenomenology, Nucl. Phys. B 847 (2011) 93–159. arXiv:1009.5691, doi:10.1016/j.nuclphysb.2011.01.023.
- [298] T. Ahmed, M. K. Mandal, N. Rana, V. Ravindran, Higgs Rapidity Distribution in $b\bar{b}$ Annihilation at Threshold in N³LO QCD, JHEP 02 (2015) 131. arXiv:1411.5301, doi:10.1007/JHEP02(2015)131.
- [299] C. Muselli, S. Forte, G. Ridolfi, Combined threshold and transverse momentum resummation for inclusive observables, JHEP 03 (2017) 106. arXiv:1701.01464.doi:10.1007/JHEP03(2017)106.
- [300] P. Banerjee, G. Das, P. K. Dhani, V. Ravindran, Threshold resummation of the rapidity distribution for Drell-Yan production at NNLO+NNLL, Phys. Rev. D 98 (5) (2018) 054018. arXiv:1805.01186, doi:10.1103/PhysRevD.98.054018.
- [301] C. Duhr, B. Mistlberger, G. Vita, Soft integrals and soft anomalous dimensions at N³LO and beyond, JHEP 09 (2022) 155. arXiv: 2205.04493, doi:10.1007/JHEP09(2022)155.
- [302] Y. Shi, L. Wang, S.-Y. Wei, B.-W. Xiao, Pursuing the Precision Study for Color Glass Condensate in Forward Hadron Productions, Phys. Rev. Lett. 128 (20) (2022) 202302. arXiv:2112.06975, doi:10.1103/PhysRevLett.128.202302.
- [303] L. Wang, L. Chen, Z. Gao, Y. Shi, S.-Y. Wei, B.-W. Xiao, Forward inclusive jet productions in pA collisions, Phys. Rev. D 107 (1) (2023) 016016. arXiv:2211.08322, doi:10.1103/PhysRevD.107.016016.
- [304] M. Bonvini, G. Marinelli, On the approaches to threshold resummation of rapidity distributions for the Drell-Yan process, Eur. Phys. J. C 83 (10) (2023) 931. arXiv:2306.03568, doi:10.1140/epjc/s10052-023-12089-3.

- [305] R. D. Ball, M. Bonvini, S. Forte, S. Marzani, G. Ridolfi, Higgs production in gluon fusion beyond NNLO, Nucl. Phys. B 874 (2013) 746–772. arXiv:1303.3590, doi:10.1016/j.nuclphysb.2013.06.012.
- [306] M. Bonvini, S. Marzani, Resummed Higgs cross section at N³LL, JHEP 09 (2014) 007. arXiv:1405.3654, doi:10.1007/JHEP09 (2014)
- [307] J. Bartels, H. Lotter, A Note on the BFKL pomeron and the 'hot spot' cross-section, Phys. Lett. B 309 (1993) 400–408. doi:10.1016/0370-2693(93)90953-F
- [308] F. Caporale, G. Chachamis, J. D. Madrigal, B. Murdaca, A. Sabio Vera, A study of the diffusion pattern in N = 4 SYM at high energies, Phys. Lett. B 724 (2013) 127–132. arXiv:1305.1474, doi:10.1016/j.physletb.2013.05.058.
- [309] D. A. Ross, A. Sabio Vera, The Effect of the Infrared Phase of the Discrete BFKL Pomeron on Transverse Momentum Diffusion, JHEP 08 (2016) 071. arXiv:1605.08265, doi:10.1007/JHEP08(2016)071.
- [310] S. Catani, D. de Florian, M. Grazzini, Universality of nonleading logarithmic contributions in transverse momentum distributions, Nucl. Phys. B 596 (2001) 299–312. arXiv:hep-ph/0008184, doi:10.1016/S0550-3213(00)00617-9.
- [311] G. Bozzi, S. Catani, D. de Florian, M. Grazzini, Transverse-momentum resummation and the spectrum of the Higgs boson at the LHC, Nucl. Phys. B 737 (2006) 73–120. arXiv:hep-ph/0508068, doi:10.1016/j.nuclphysb.2005.12.022.
- [312] G. Bozzi, S. Catani, G. Ferrera, D. de Florian, M. Grazzini, Transverse-momentum resummation: A Perturbative study of Z production at the Tevatron, Nucl. Phys. B 815 (2009) 174–197. arXiv:0812.2862, doi:10.1016/j.nuclphysb.2009.02.014.
- [313] S. Catani, M. Grazzini, QCD transverse-momentum resummation in gluon fusion processes, Nucl. Phys. B 845 (2011) 297–323. arXiv: 1011.3918, doi:10.1016/j.nuclphysb.2010.12.007.
- [314] S. Catani, M. Grazzini, Higgs Boson Production at Hadron Colliders: Hard-Collinear Coefficients at the NNLO, Eur. Phys. J. C 72 (2012) 2013, [Erratum: Eur.Phys.J.C 72, 2132 (2012)]. arXiv:1106.4652, doi:10.1140/epjc/s10052-012-2013-2.
- [315] S. Catani, L. Cieri, D. de Florian, G. Ferrera, M. Grazzini, Universality of transverse-momentum resummation and hard factors at the NNLO, Nucl. Phys. B 881 (2014) 414–443. arXiv:1311.1654, doi:10.1016/j.nuclphysb.2014.02.011.
- [316] S. Catani, D. de Florian, G. Ferrera, M. Grazzini, Vector boson production at hadron colliders: transverse-momentum resummation and leptonic decay, JHEP 12 (2015) 047. arXiv:1507.06937, doi:10.1007/JHEP12(2015)047.
- [317] C. Duhr, B. Mistlberger, G. Vita, Four-Loop Rapidity Anomalous Dimension and Event Shapes to Fourth Logarithmic Order, Phys. Rev. Lett. 129 (16) (2022) 162001. arXiv:2205.02242, doi:10.1103/PhysRevLett.129.162001.
- [318] L. Cieri, F. Coradeschi, D. de Florian, Diphoton production at hadron colliders: transverse-momentum resummation at next-to-next-to-leading logarithmic accuracy, JHEP 06 (2015) 185. arXiv:1505.03162, doi:10.1007/JHEP06(2015) 185.
- [319] S. Alioli, A. Broggio, A. Gavardi, S. Kallweit, M. A. Lim, R. Nagar, D. Napoletano, L. Rottoli, Precise predictions for photon pair production matched to parton showers in GENEVA, JHEP 04 (2021) 041. arXiv:2010.10498, doi:10.1007/JHEP04(2021)041.
- [320] T. Becher, T. Neumann, Fiducial q_T resummation of color-singlet processes at N³LL+NNLO, JHEP 03 (2021) 199. arXiv:2009.11437, doi:10.1007/JHEP03(2021)199.
- [321] T. Neumann, The diphoton q_T spectrum at N³LL' + NNLO, Eur. Phys. J. C 81 (10) (2021) 905. arXiv:2107.12478, doi:10.1140/epjc/s10052-021-09687-4.
- [322] G. Ferrera, J. Pires, Transverse-momentum resummation for Higgs boson pair production at the LHC with top-quark mass effects, JHEP 02 (2017) 139. arXiv:1609.01691, doi:10.1007/JHEP02(2017)139.
- [323] W.-L. Ju, M. Schönherr, The q_T and $\Delta \phi$ spectra in W and Z production at the LHC at N³LL'+N²LO, JHEP 10 (2021) 088. arXiv: 2106.11260, doi:10.1007/JHEP10(2021)088.
- [324] P. F. Monni, L. Rottoli, P. Torrielli, Higgs transverse momentum with a jet veto: a double-differential resummation, Phys. Rev. Lett. 124 (25) (2020) 252001. arXiv:1909.04704, doi:10.1103/PhysRevLett.124.252001.
- [325] L. Buonocore, M. Grazzini, J. Haag, L. Rottoli, Transverse-momentum resummation for boson plus jet production at hadron colliders, Eur. Phys. J. C 82 (1) (2022) 27. arXiv:2110.06913, doi:10.1140/epjc/s10052-021-09962-4.
- [326] M. Wiesemann, L. Rottoli, P. Torrielli, The Zγ transverse-momentum spectrum at NNLO+N³LL, Phys. Lett. B 809 (2020) 135718. arXiv:2006.09338, doi:10.1016/j.physletb.2020.135718.
- [327] M. A. Ebert, J. K. L. Michel, I. W. Stewart, F. J. Tackmann, Drell-Yan q_T resummation of fiducial power corrections at N³LL, JHEP 04 (2021) 102. arXiv:2006.11382, doi:10.1007/JHEP04(2021)102.
- [328] E. Re, L. Rottoli, P. Torrielli, Fiducial Higgs and Drell-Yan distributions at N³LL'+NNLO with RadISH, JHEP 09 (2021) 108. arXiv: 2104.07509, doi:10.1007/JHEP09(2021)108.
- [329] X. Chen, T. Gehrmann, E. W. N. Glover, A. Huss, P. F. Monni, E. Re, L. Rottoli, P. Torrielli, Third-Order Fiducial Predictions for Drell-Yan Production at the LHC, Phys. Rev. Lett. 128 (25) (2022) 252001. arXiv:2203.01565, doi:10.1103/PhysRevLett.128.252001.
- [330] T. Neumann, J. Campbell, Fiducial Drell-Yan production at the LHC improved by transverse-momentum resummation at N4LLp+N3LO, Phys. Rev. D 107 (1) (2023) L011506. arXiv:2207.07056, doi:10.1103/PhysRevD.107.L011506.
- [331] W. Bizon, P. F. Monni, E. Re, L. Rottoli, P. Torrielli, Momentum-space resummation for transverse observables and the Higgs p_{\perp} at N³LL+NNLO, JHEP 02 (2018) 108. arXiv:1705.09127, doi:10.1007/JHEP02(2018)108.
- [332] G. Billis, B. Dehnadi, M. A. Ebert, J. K. L. Michel, F. J. Tackmann, Higgs pT Spectrum and Total Cross Section with Fiducial Cuts at Third Resummed and Fixed Order in QCD, Phys. Rev. Lett. 127 (7) (2021) 072001. arXiv:2102.08039, doi:10.1103/PhysRevLett.127.072001.
- [333] F. Caola, W. Chen, C. Duhr, X. Liu, B. Mistlberger, F. Petriello, G. Vita, S. Weinzierl, The Path forward to N³LO, in: 2022 Snowmass Summer Study, 2022. arXiv: 2203.06730.
- [334] S. Kallweit, E. Re, L. Rottoli, M. Wiesemann, Accurate single- and double-differential resummation of colour-singlet processes with MATRIX+RADISH: W⁺W⁻ production at the LHC, JHEP 12 (2020) 147. arXiv:2004.07720, doi:10.1007/JHEP12(2020)147.
- [335] E. Chapon, et al., Prospects for quarkonium studies at the high-luminosity LHC, Prog. Part. Nucl. Phys. 122 (2022) 103906. arXiv: 2012.14161, doi:10.1016/j.ppnp.2021.103906.

- [336] L. A. Anchordoqui, et al., The Forward Physics Facility: Sites, experiments, and physics potential, Phys. Rept. 968 (2022) 1–50. arXiv: 2109.10905, doi:10.1016/j.physrep.2022.04.004.
- [337] J. L. Feng, et al., The Forward Physics Facility at the High-Luminosity LHC, J. Phys. G 50 (3) (2023) 030501. arXiv:2203.05090, doi:10.1088/1361-6471/ac865e.
- [338] M. Hentschinski, et al., White Paper on Forward Physics, BFKL, Saturation Physics and Diffraction, Acta Phys. Polon. B 54 (3) (2023) 2. arXiv:2203.08129, doi:10.5506/APhysPolB.54.3-A2.
- [339] A. Accardi, et al., Electron Ion Collider: The Next QCD Frontier: Understanding the glue that binds us all, Eur. Phys. J. A 52 (9) (2016) 268. arXiv:1212.1701, doi:10.1140/epja/i2016-16268-9.
- [340] R. Abdul Khalek, et al., Science Requirements and Detector Concepts for the Electron-Ion Collider: EIC Yellow Report, Nucl. Phys. A 1026 (2022) 122447. arXiv:2103.05419, doi:10.1016/j.nuclphysa.2022.122447.
- [341] R. Abdul Khalek, et al., Snowmass 2021 White Paper: Electron Ion Collider for High Energy Physics, in: 2022 Snowmass Summer Study, 2022. arXiv:2203.13199.
- [342] I. Adachi, et al., The International Linear Collider: Report to Snowmass 2021arXiv: 2203.07622.
- [343] A. Arbuzov, et al., On the physics potential to study the gluon content of proton and deuteron at NICA SPD, Prog. Part. Nucl. Phys. 119 (2021) 103858. arXiv:2011.15005, doi:10.1016/j.ppnp.2021.103858.
- [344] S. Amoroso, et al., Snowmass 2021 whitepaper: Proton structure at the precision frontier, Acta Phys. Polon. B 53 (12) (2022) A1. arXiv:2203.13923, doi:10.5506/APhysPolB.53.12-A1.
- [345] J. de Blas, et al., The physics case of a 3 TeV muon collider stagearXiv: 2203.07261.
- [346] C. Aimè, et al., Muon Collider Physics SummaryarXiv: 2203.07256.
- [347] N. Bartosik, et al., Simulated Detector Performance at the Muon Collider, in: 2022 Snowmass Summer Study, 2022. arXiv: 2203.07964.
- [348] C. Accettura, et al., Towards a muon collider, Eur. Phys. J. C 83 (9) (2023) 864, [Erratum: Eur.Phys.J.C 84, 36 (2024)]. arXiv:2303.08533, doi:10.1140/epjc/s10052-023-11889-x.
- [349] K. M. Black, et al., Muon Collider Forum report, JINST 19 (02) (2024) T02015. arXiv:2209.01318, doi:10.1088/1748-0221/19/02/T02015.
- [350] S. Dawson, et al., Report of the Topical Group on Higgs Physics for Snowmass 2021: The Case for Precision Higgs Physics, in: 2022 Snowmass Summer Study, 2022. arXiv: 2209.07510.
- [351] T. Bose, et al., Report of the Topical Group on Physics Beyond the Standard Model at Energy Frontier for Snowmass 2021, in: 2022 Snowmass Summer Study, 2022. arXiv: 2209.13128.
- [352] M. Begel, et al., Precision QCD, Hadronic Structure & Forward QCD, Heavy Ions: Report of Energy Frontier Topical Groups 5, 6, 7 submitted to Snowmass 2021arXiv: 2209.14872.
- [353] R. Abir, et al., The case for an EIC Theory Alliance: Theoretical Challenges of the EICarXiv: 2305.14572.
- [354] A. Accardi, et al., Strong Interaction Physics at the Luminosity Frontier with 22 GeV Electrons at Jefferson LabarXiv: 2306.09360.
- [355] M. G. Echevarria, Y. Makris, I. Scimemi, Quarkonium TMD fragmentation functions in NRQCD, JHEP 10 (2020) 164. arXiv:2007.05547, doi:10.1007/JHEP10 (2020) 164.
- [356] M. G. Echevarria, S. F. Romera, I. Scimemi, Gluon TMD fragmentation function into quarkoniumarXiv:2308.12356, doi:10.1007/ JHEP12(2023)181.
- [357] M. Copeland, S. Fleming, R. Gupta, R. Hodges, T. Mehen, Polarized TMD fragmentation functions for J/ψ productionarXiv: 2308.08605.
- [358] M. Copeland, S. Fleming, R. Gupta, R. Hodges, T. Mehen, Polarized J/ψ production in semi-inclusive DIS at large Q^2 : Comparing quark fragmentation and photon-gluon fusionarXiv:2310.13737.
- [359] R. von Kuk, J. K. L. Michel, Z. Sun, Transverse momentum distributions of heavy hadrons and polarized heavy quarks, JHEP 09 (2023) 205. arXiv:2305.15461, doi:10.1007/JHEP09 (2023) 205.
- [360] L. Dai, C. Kim, A. K. Leibovich, Heavy quark transverse momentum dependent fragmentationarXiv: 2310.19207.
- [361] Z.-B. Kang, H. Xing, F. Zhao, Y. Zhou, Polarized fragmenting jet functions in Inclusive and Exclusive Jet ProductionarXiv: 2311.00672.
- [362] E. R. Nocera, Towards a Neural Network Determination of Charged Pion Fragmentation Functions, in: 22nd International Symposium on Spin Physics, 2017. arXiv:1701.09186.
- [363] V. Bertone, S. Carrazza, E. R. Nocera, N. P. Hartland, J. Rojo, Towards a Neural Network determination of Pion Fragmentation Functions, in: Parton radiation and fragmentation from LHC to FCC-ee, 2017, pp. 19–25.
- [364] R. Abdul Khalek, V. Bertone, E. R. Nocera, Determination of unpolarized pion fragmentation functions using semi-inclusive deep-inelastic-scattering data, Phys. Rev. D 104 (3) (2021) 034007. arXiv:2105.08725, doi:10.1103/PhysRevD.104.034007.
- [365] R. Abdul Khalek, V. Bertone, A. Khoudli, E. R. Nocera, Pion and kaon fragmentation functions at next-to-next-to-leading order, Phys. Lett. B 834 (2022) 137456. arXiv:2204.10331, doi:10.1016/j.physletb.2022.137456.
- [366] Z. Kassabov, M. Ubiali, C. Voisey, Parton distributions with scale uncertainties: a Monte Carlo sampling approach, JHEP 03 (2023) 148. arXiv:2207.07616, doi:10.1007/JHEP03(2023)148.
- [367] L. A. Harland-Lang, R. S. Thorne, On the Consistent Use of Scale Variations in PDF Fits and Predictions, Eur. Phys. J. C 79 (3) (2019) 225. arXiv:1811.08434, doi:10.1140/epjc/s10052-019-6731-6.
- [368] R. D. Ball, R. L. Pearson, Correlation of theoretical uncertainties in PDF fits and theoretical uncertainties in predictions, Eur. Phys. J. C 81 (9) (2021) 830. arXiv:2105.05114, doi:10.1140/epjc/s10052-021-09602-x.
- [369] J. McGowan, T. Cridge, L. A. Harland-Lang, R. S. Thorne, Approximate N³LO parton distribution functions with theoretical uncertainties: MSHT20aN³LO PDFs, Eur. Phys. J. C 83 (3) (2023) 185, [Erratum: Eur.Phys.J.C 83, 302 (2023)]. arXiv:2207.04739, doi:10.1140/epjc/s10052-023-11236-0.
- [370] R. D. Ball, et al., Determination of the theory uncertainties from missing higher orders on NNLO parton distributions with percent accuracyarXiv:2401.10319.

- [371] B. Pasquini, S. Rodini, S. Venturini, Valence quark, sea, and gluon content of the pion from the parton distribution functions and the electromagnetic form factor, Phys. Rev. D 107 (11) (2023) 114023. arXiv:2303.01789, doi:10.1103/PhysRevD.107.114023.
- [372] P. Caucal, F. Salazar, B. Schenke, R. Venugopalan, Back-to-back inclusive dijets in DIS at small x: Sudakov suppression and gluon saturation at NLO, JHEP 11 (2022) 169. arXiv:2208.13872, doi:10.1007/JHEP11(2022)169.
- [373] P. Taels, T. Altinoluk, G. Beuf, C. Marquet, Dijet photoproduction at low x at next-to-leading order and its back-to-back limit, JHEP 10 (2022) 184. arXiv:2204.11650, doi:10.1007/JHEP10(2022)184.
- [374] M. Dasgupta, F. Dreyer, G. P. Salam, G. Soyez, Small-radius jets to all orders in QCD, JHEP 04 (2015) 039. arXiv:1411.5182, doi:10.1007/JHEP04(2015)039.
- [375] M. Dasgupta, F. A. Dreyer, G. P. Salam, G. Soyez, Inclusive jet spectrum for small-radius jets, JHEP 06 (2016) 057. arXiv:1602.01110, doi:10.1007/JHEP06(2016)057.
- [376] A. Banfi, P. F. Monni, G. P. Salam, G. Zanderighi, Higgs and Z-boson production with a jet veto, Phys. Rev. Lett. 109 (2012) 202001. arXiv:1206.4998.doi:10.1103/PhysRevLett.109.202001.
- [377] A. Banfi, F. Caola, F. A. Dreyer, P. F. Monni, G. P. Salam, G. Zanderighi, F. Dulat, Jet-vetoed Higgs cross section in gluon fusion at N³LO+NNLL with small-*R* resummation, JHEP 04 (2016) 049. arXiv:1511.02886, doi:10.1007/JHEP04 (2016) 049.
- [378] X. Liu, S.-O. Moch, F. Ringer, Threshold and jet radius joint resummation for single-inclusive jet production, Phys. Rev. Lett. 119 (21) (2017) 212001. arXiv:1708.04641, doi:10.1103/PhysRevLett.119.212001.
- [379] G. Luisoni, S. Marzani, QCD resummation for hadronic final states, J. Phys. G 42 (10) (2015) 103101. arXiv:1505.04084, doi: 10.1088/0954-3899/42/10/103101.
- [380] S. Caletti, O. Fedkevych, S. Marzani, D. Reichelt, S. Schumann, G. Soyez, V. Theeuwes, Jet angularities in Z+jet production at the LHC, JHEP 07 (2021) 076. arXiv:2104.06920, doi:10.1007/JHEP07 (2021) 076.
- [381] D. Reichelt, S. Caletti, O. Fedkevych, S. Marzani, S. Schumann, G. Soyez, Phenomenology of jet angularities at the LHC, JHEP 03 (2022) 131. arXiv:2112.09545, doi:10.1007/JHEP03(2022)131.
- [382] M. Ubiali, M. Zaro, F. G. Celiberto, Conversations at the Heavy Flavours at High pT Workshop 2023 (Higgs Centre for Theoretical Physics, University of Edinburgh).
- [383] R. D. Ball, A. Candido, J. Cruz-Martinez, S. Forte, T. Giani, F. Hekhorn, K. Kudashkin, G. Magni, J. Rojo, Evidence for intrinsic charm quarks in the proton, Nature 608 (7923) (2022) 483–487. arXiv:2208.08372, doi:10.1038/s41586-022-04998-2.
- [384] R. D. Ball, A. Candido, J. Cruz-Martinez, S. Forte, T. Giani, F. Hekhorn, G. Magni, E. R. Nocera, J. Rojo, R. Stegeman, The intrinsic charm quark valence distribution of the protonarXiv:2311.00743.